Knockout-reaction with RIB

A3F-CNSSS20, August 17th-21st, 2020

My aim is:

– to explain very basic (but important) things on proton-“induced” knockout reactions,

– to instruct how to perform DWIA calculations with a code pikoe (with thought!),

– not to demonstrate our recent activities or to go into the very details of theories.

Kazuyuki Ogata

RCNP, Osaka University

Plan of this talk (1/2)

1) Overview of (p,2p) studies (on stable nuclei)

T. Wakasa, KO, T. Noro, PPNP 96, 32 (2017); T. Noro+, PTEP 2020 (in press).

1-1. "Definition" of the KO reaction

1-2. What we can learn from PWIA analysis of KO reactions.

1-3. What we can learn from DWIA analysis of KO reactions.

2) A bit more advanced aspects of (p,2p) studies

Th. A. J. Maris, NP 9 (1958–1959) 577.

2-1. Key ingredients for spectroscopic studies

2-2. The Maris effect

2-3. Treatment of the identical particles in (p,2p)

3) Momentum distribution in inverse kinematics

KO, K. Yoshida, K. Minomo, PRC 92, 034615 (2015).

3-1. Peak shift and asymmetric shape

3-2. Phase volume (PV) and attractive distortion effects

3-3. SEASTAR, SHARAQ, and GSI data analysis with DWIA

Plan of this talk (2/2)

4) Some theoretical achievements (for future)

K. Yoshida, M. Goméz-Ramos, KO, and A. M. Moro, PRC 97, 024608 (2018).

4-1. Microscopic optical potential

4-2. Benchmark study on ^{15}C(p,pn) with DWIA, TC, and Faddeev,-AGS.

5) Divergence of the TDX in inverse kinematics

KO+, in preparation.

5-1. Two-value feature of the kinematics and divergence of PV

5-2. When occurs?

6) Some recent/ongoing KO reaction studies around RCNP/RIBF

6-1. ^{2}n correlation study via (p,pn)

6-2. α KO reactions

6-3. deuteron KO reactions

…

7) Summary

Plan of this talk (1/2)

1) Overview of (p,2p) studies (on stable nuclei)

T. Wakasa, KO, T. Noro, PPNP 96, 32 (2017); T. Noro+, PTEP 2020 (in press).

1-1. “Definition” of the KO reaction

1-2. What we can learn from PWIA analysis of KO reactions.

1-3. What we can learn from DWIA analysis of KO reactions.

2) A bit more advanced aspects of (p,2p) studies

Th. A. J. Maris, Nucl. Phys. 9 (1958–1959) 577.

2-1. Key ingredients for spectroscopic studies

2-2. The Maris effect

2-3. Treatment of the identical particles in (p,2p)

3) Momentum distribution in inverse kinematics

KO, K. Yoshida, K. Minomo, PRC 92, 034615 (2015).

3-1. Peak shift and asymmetric shape

3-2. Phase volume (PV) and attractive distortion effects

3-3. SEASTAR, SHARAQ, and GSI data analysis with DWIA

What is the knockout reaction?

Qualitatively speaking, by quasi-free scattering a process is meant in which a high energy (100–1000 MeV) particle knocks a nucleon out of a nucleus and no further violent interaction occurs between the nucleus and the incident or the two outgoing particles.

G. Jacob and Th. A. J. Maris, Rev. Mod. Phys. 38, 121 (1966).

In essence, a proton induced knockout reaction is a nuclear reaction in which an incident proton interacts with either a nucleon or a nuclear cluster in a target nucleus and knocks this entity out of the nucleus, generating a one-hole or a clusterhole state. This process, in particular the one nucleon knockout reaction, is the most dominant reaction at intermediate (200–1000 MeV) energies.

T. Wakasa, KO, T. Noro, Prog. Part. Nucl. Phys. 96, 32 (2017).

Knockout or removal?

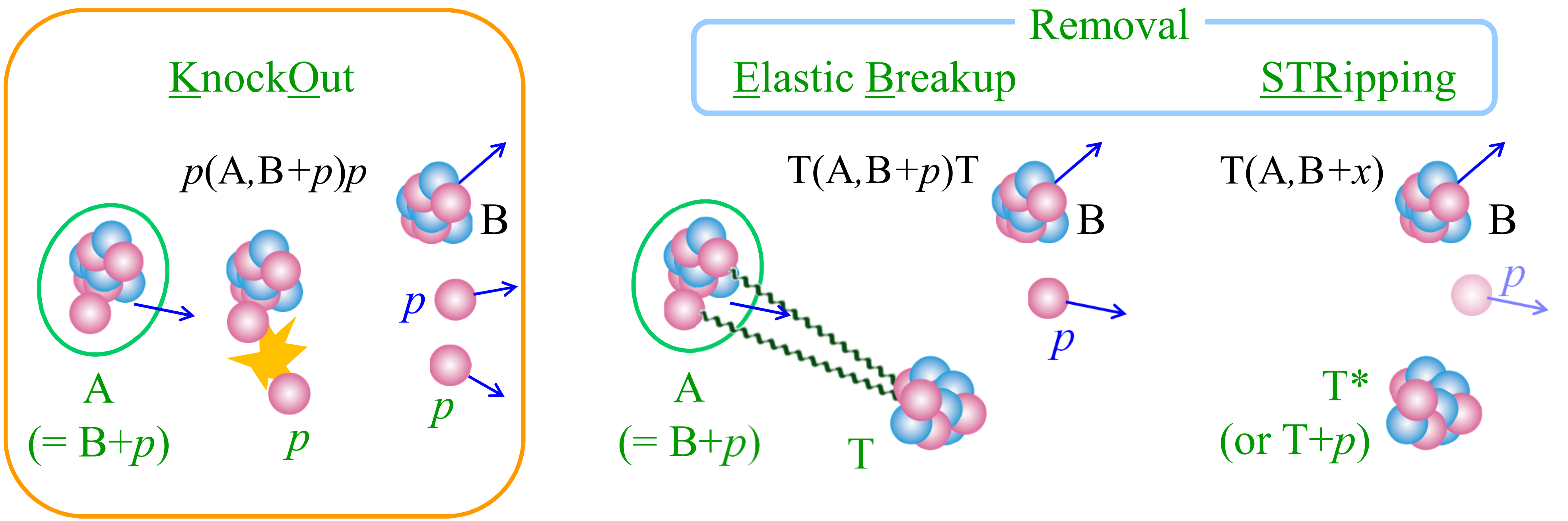

large energy-momentum transfer

small energy-momentum transfer

NOTE: At Michigan State University (MSU), nucleon removal processes have intensively been measured and studied. Some people call them "knockout" processes but those reaction mechanism is quite different from that of the knockout process.

What we can study via KO reaction?

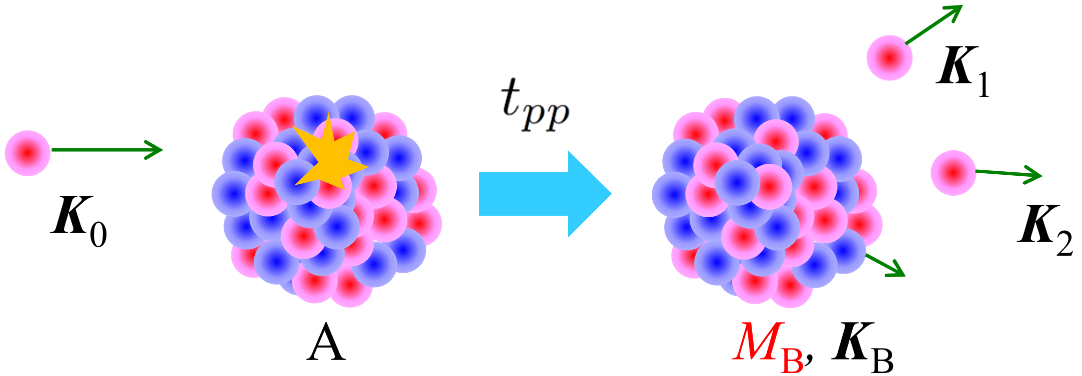

- ✓ We have 9+1 d.o.f. in the final state. Because of the energy-momentum conservation, 6 out of 10 are independent.
- ✓ If $\boldsymbol{K}_1$ and $\boldsymbol{K}_2$ are specified, all the kinematics are determined as well as M_B (internal energy of the residue B). This is called kinematically complete measurement.
- ✓ In what follows, I assume that M_B has been specified. Then, there are 5 d.o.f. left.
- ✓ In the picture of KO reactions, B behaves as a spectator. This indicates that before the KO, the nucleon had a momentum $\boldsymbol{K}_N = -\boldsymbol{K}_B$ in the nucleus A.

What we can study via KO reaction? (Con't)

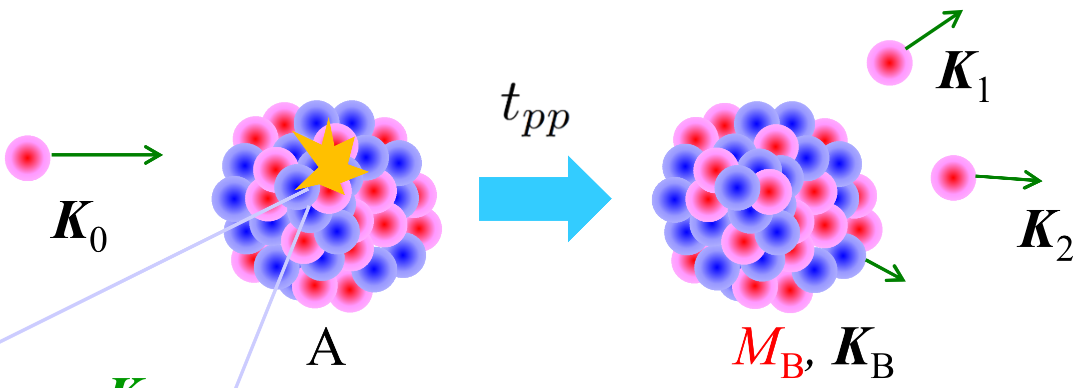

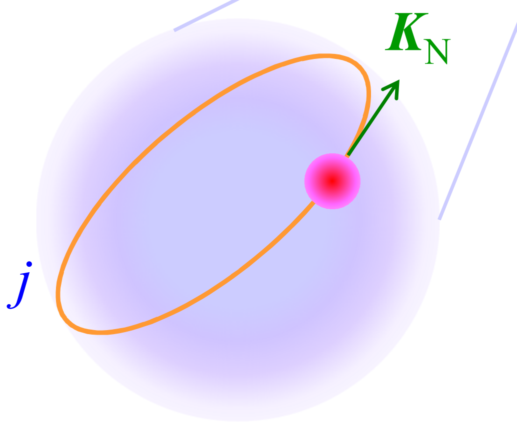

$$\boldsymbol{K}_N = -\boldsymbol{K}_B = \boldsymbol{K}_1 + \boldsymbol{K}_2 - \boldsymbol{K}_0$$

- ✓ If B is in a bound state, it has a specific J^π. Then, the s.p. orbit j of the nucleon inside A can be specified.
  (In some cases, j is not unique but the contribution of each j is incoherent so we can consider j one by one.)
- ✓ Momentum conservation and the spectator assumption for B allows a specification of $\boldsymbol{K}_N$.

By KO reactions, one may take a "snapshot" of a s.p. momentum of a nucleus.

Plane-Wave Impulse Approx^{n} (PWIA) for p2p (1/2)

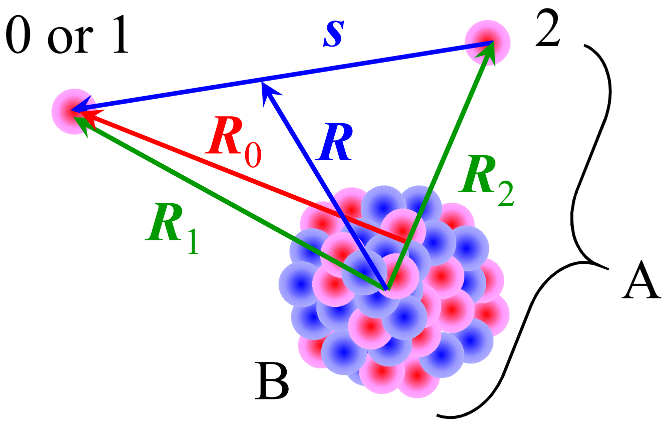

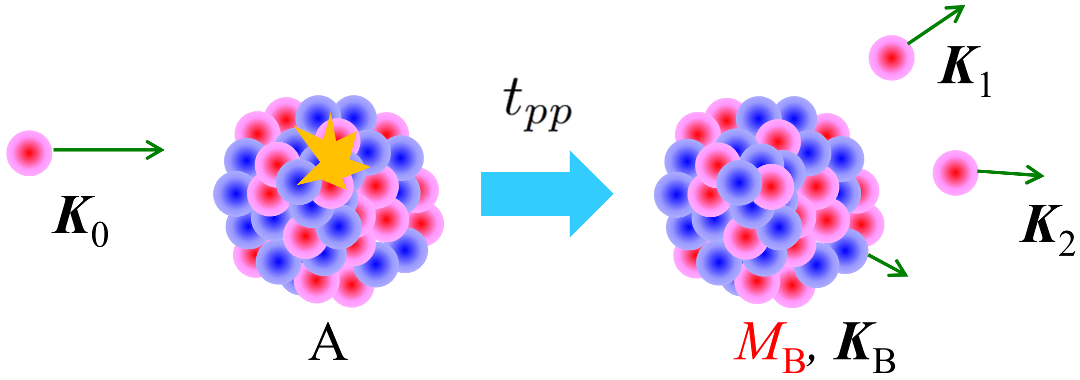

proton bound state W.Fn.

$$T^{\mathrm{PWIA}} = \left\langle e^{i\boldsymbol{K}_1\cdot\boldsymbol{R}_1} e^{i\boldsymbol{K}_2\cdot\boldsymbol{R}_2} \right| t_{pp}(s) \left| e^{i\boldsymbol{K}_0\cdot\boldsymbol{R}_0} \boxed{\varphi(\boldsymbol{R}_2)} \right\rangle$$

$$\boldsymbol{R}_1 = \boldsymbol{R} + \boldsymbol{s}/2, \quad \boldsymbol{R}_2 = \boldsymbol{R} - \boldsymbol{s}/2, \quad \boxed{\boldsymbol{R}_0 \sim \boldsymbol{R}_1}$$

just for simplicity
(in this school)

$$T^{\mathrm{PWIA}} = \int d\boldsymbol{s} d\boldsymbol{R}\, e^{-i\boldsymbol{K}_1\cdot(\boldsymbol{R}+\boldsymbol{s}/2)} e^{-i\boldsymbol{K}_2\cdot(\boldsymbol{R}-\boldsymbol{s}/2)} t_{pp}(s)\, e^{i\boldsymbol{K}_0\cdot(\boldsymbol{R}+\boldsymbol{s}/2)} \varphi(\boldsymbol{R}_2)$$

$$\varphi(\boldsymbol{R}_2) = \frac{1}{(2\pi)^3} \int d\boldsymbol{K}_N\, \tilde{\varphi}(\boldsymbol{K}_N)\, e^{i\boldsymbol{K}_N\cdot(\boldsymbol{R}-\boldsymbol{s}/2)}$$

Plane-Wave Impulse Approx$^{\mathrm{n}}$ (PWIA) for p2p (2/2)

$$T^{\mathrm{PWIA}} = \frac{1}{(2\pi)^3} \int d\boldsymbol{K}_N \, \tilde{\varphi}(\boldsymbol{K}_N) \int e^{-i\boldsymbol{K}_1 \cdot \boldsymbol{s}/2} e^{i\boldsymbol{K}_2 \cdot \boldsymbol{s}/2} t_{pp}(s) \, e^{i\boldsymbol{K}_0 \cdot \boldsymbol{s}/2} e^{-i\boldsymbol{K}_N \cdot \boldsymbol{s}/2} d\boldsymbol{s}$$

$$\times \boxed{\int e^{-i\boldsymbol{K}_1 \cdot \boldsymbol{R}} e^{-i\boldsymbol{K}_2 \cdot \boldsymbol{R}} e^{i\boldsymbol{K}_0 \cdot \boldsymbol{R}} e^{i\boldsymbol{K}_N \cdot \boldsymbol{R}} d\boldsymbol{R}} = (2\pi)^3 \, \delta(\boldsymbol{K}_0 + \boldsymbol{K}_N - \boldsymbol{K}_1 - \boldsymbol{K}_2)$$

$$\boldsymbol{\kappa} = \frac{\boldsymbol{K}_0 - (\boldsymbol{K}_1 + \boldsymbol{K}_2 - \boldsymbol{K}_0)}{2} = \frac{2\boldsymbol{K}_0 - \boldsymbol{K}_1 - \boldsymbol{K}_2}{2}, \quad \boldsymbol{\kappa}' = \frac{\boldsymbol{K}_1 - \boldsymbol{K}_2}{2}$$

Snapshot!

$$T^{\mathrm{PWIA}} = \tilde{\varphi}(\boldsymbol{K}_1 + \boldsymbol{K}_2 - \boldsymbol{K}_0) \int e^{-i\boldsymbol{\kappa}' \cdot \boldsymbol{s}} t_{pp}(s) \, e^{i\boldsymbol{\kappa} \cdot \boldsymbol{s}} d\boldsymbol{s} = \boxed{\tilde{\varphi}(\boldsymbol{K}_1 + \boldsymbol{K}_2 - \boldsymbol{K}_0)} \, \tilde{t}_{pp}(q)$$

- ✓ Momentum transfer $\boldsymbol{q}$ (usually large): $\boldsymbol{q} \equiv \boldsymbol{\kappa} - \boldsymbol{\kappa}' = \boldsymbol{K}_0 - \boldsymbol{K}_1$
- ✓ Missing momentum $\boldsymbol{Q}$ (usually intended to be small): $\boldsymbol{Q} \equiv \boldsymbol{K}_0 - \boldsymbol{K}_1 - \boldsymbol{K}_2$

  NOTE: $Q = 0$ corresponds to the recoilless condition. $= -\boldsymbol{K}_{\mathrm{B}}$

An example of PWIA calculation

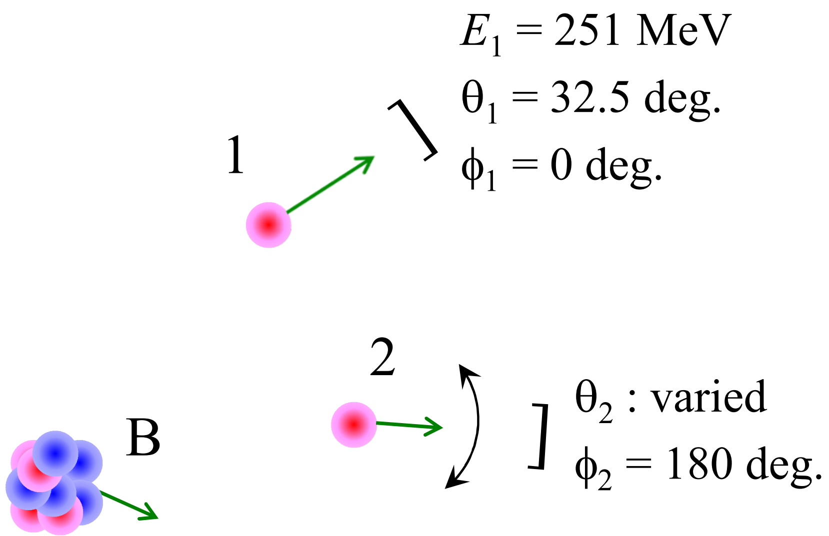

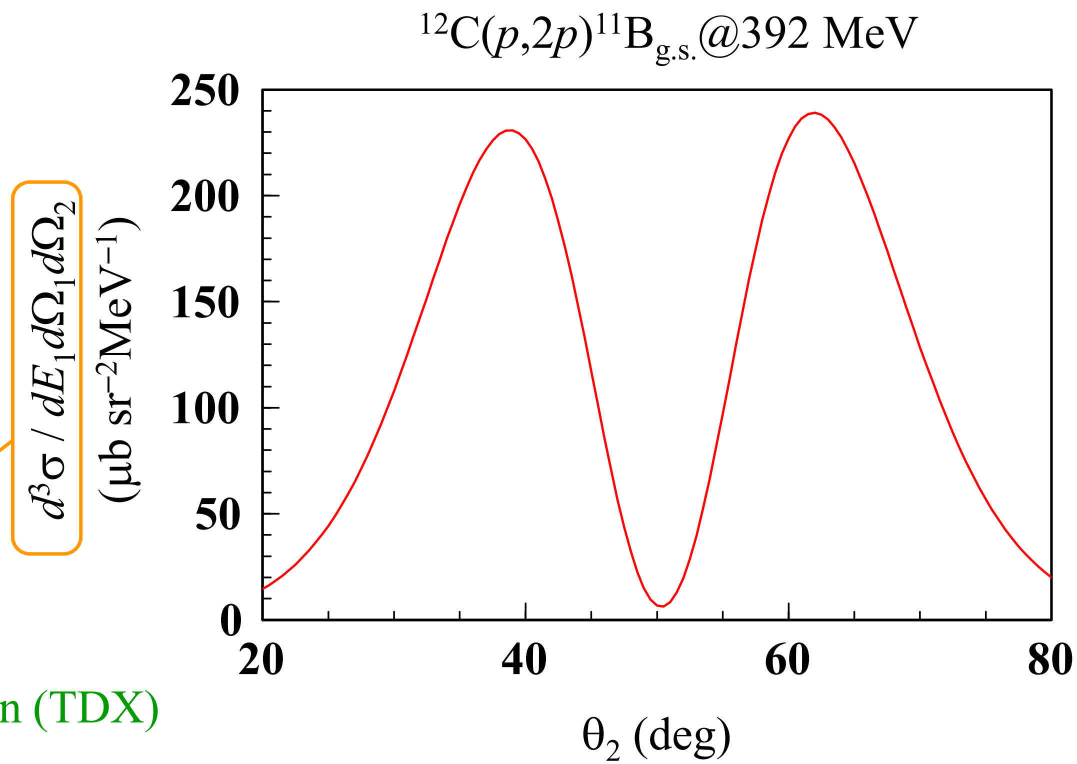

A key observable:
Triple-differential cross section (TDX)

- ✓ At θ_2 = 50 deg., K_B ~ 10.7 MeV/c, which corresponds to the recoilless condition (RLC). E_1 and θ_2 were chosen so that the RLC is achieved at a value of θ_2.

sample1.cnt

Input for pikoe (read the manual!)

You need to put FLtbl_rede.dat at the directory specified here. In this example, it must be put on the directory where pikoe1.exe (or a.out etc.) exits. You can change the path accordingly to your directory structure.

```
  **** ppN control data ****
  10:unknown ::./tbl_12Cp2p11Bgs_set1_cs_PW.dat
  11:old     ::./FLtbl_rede.dat
  06:unknown ::./12Cp2p11Bgs_set1_cs_PW.outlist
 999:
---- INPUT ----
12C(p,2p)11B_gs@392MeV set1 PWIA cs
1000 0    0    0    1                                  LIMFS IONS IFRM IMIR ICAL
1.00 1.007825 6.0  12.00                               ZP AP ZA AA
0    392.0     0                                       IKIN ELAB ICTREIN
1    15.96     1.0  1.007825  0.85      1              ISH EBIND ZSP ASP BETASP ICTRM
1.5  1.0  1.00      0                                  FJ FL SFAC NOD
0    1.35      1    0.65      1.35      1              IBMC RC ICTRC AOC RCL ICTRCL
0    8.2       1.35      1    0.65                     IBMS VOLS RS ICTRS AS
60   60   60                                           LMAX0 LMAX1 LMAX2
1    0    2.00 1    1                                  IVAR IEX FKNCUT IXUNT KUNT
0    251.0     255.0     10.0                          IVVAR VARMIN VARMAX DVAR
0    32.5      180.0     10.0                          IVTHX THXMIN THXMAX DTHX
0    0.0       40.0      10.0                          IVPHX PHXMIN PHXMAX DPHX
1    0.0       180.0     0.5                           IVTH2 TH2MIN TH2MAX DTH2
0    180.0     360.0     10.0                          IVPH2 PH2MIN PH2MAX DPH2
10   6    0    0    0    0    0                        KIB: TBL OUT TMD LG PX TR TL
3    11   1    0    1                                  IELM KIBELM IONSH KINELM IELMEDG
15.0      0.1       30   30   40   0    0              RMAX DR NG24-B,TH,PH,K1,PH1Q
0    1.00 1.00 1.00 1.00 -0.85     0    1              0: IPOT FV FW FVS FWS BET MS EDG
0    1.00 1.00 1.00 1.00 -0.85     0    1              1: IPOT FV FW FVS FWS BET MS EDG
0    1.00 1.00 1.00 1.00 -0.85     0    1              2: IPOT FV FW FVS FWS BET MS EDG
```

atomic # and mass # of ^{12}C

incident energy

proton separation energy of ^{12}C

not use the Bohr-Mottelson s.p. pot.

T_1, θ_1, ϕ_1, and ϕ_2 are fixed at 251 MeV, 32.5 deg., 0 deg., and 180 deg.

$j = 3/2$, $\ell = 1$, the S-factor is set to 1, the # of nodes is 0.

WS parameter used in ^{12}C(e,e'p) analysis

θ_2 is varied from 0 deg. to 180 deg. with the step of0.5 deg.

Distorting pots. for particles 0, 1, and 2 are switched off.

PWIA results for ^{40}Ca(p,2p)

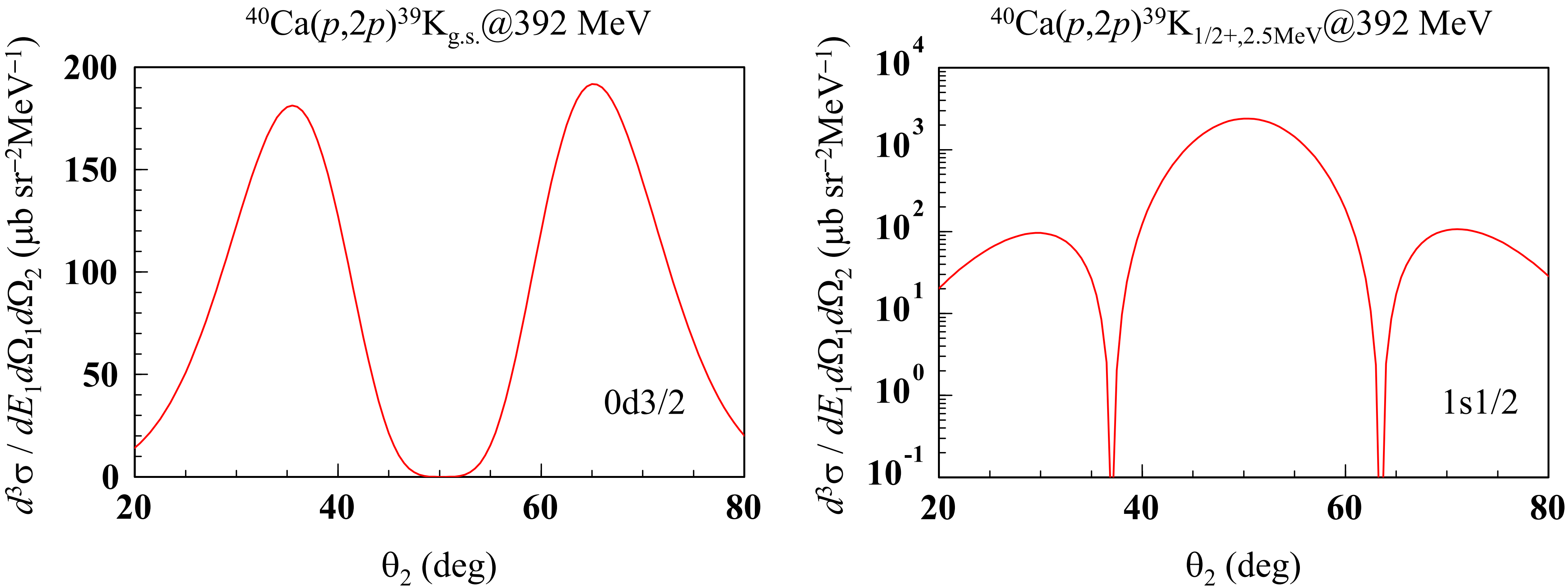

✓ The orbital angular momentum ℓ can be determined by the shape of the TDX.

HW: By preparing the input files, reproduce the results shown above. The kinematical condition for T_1, θ_1, ϕ_1, and ϕ_2 is the same as for the ^{12}C target case.

Profile of K_B

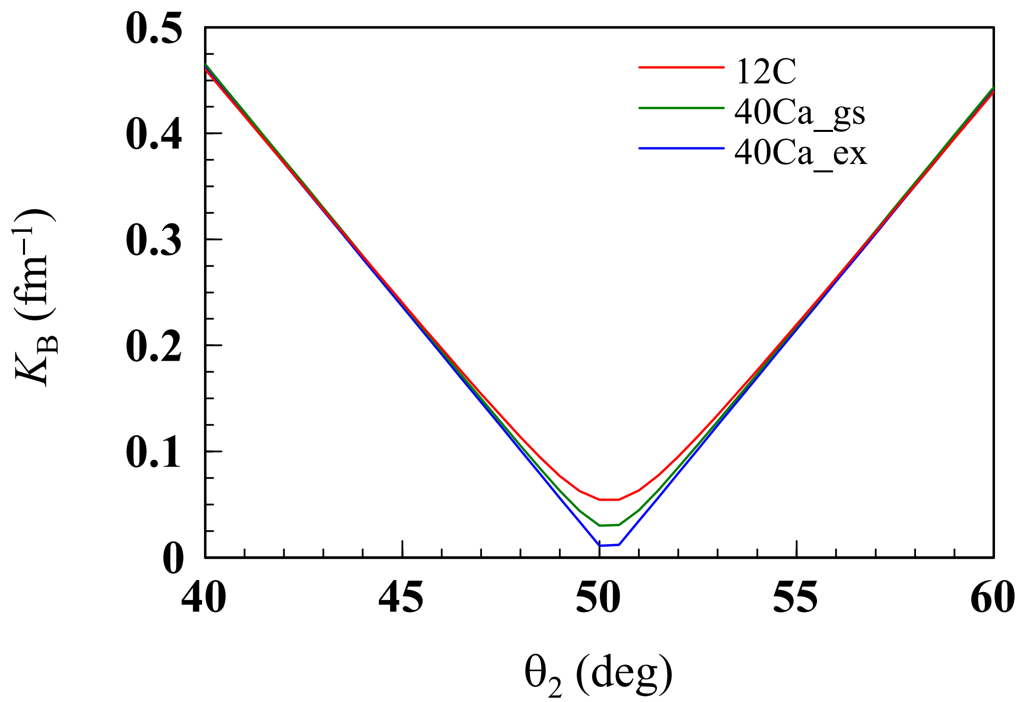

From PWIA to Distorted-Wave IA (DWIA)

$$T^{\mathrm{PWIA}} = \left\langle e^{i\boldsymbol{K}_1\cdot\boldsymbol{R}_1} e^{i\boldsymbol{K}_2\cdot\boldsymbol{R}_2} \right| t_{pp}(s) \left| e^{i\boldsymbol{K}_0\cdot\boldsymbol{R}_0} \varphi(\boldsymbol{R}_2) \right\rangle$$

$$T^{\mathrm{DWIA}} = \left\langle \chi_{\boldsymbol{K}_1}(\boldsymbol{R}_1)\, \chi_{\boldsymbol{K}_2}(\boldsymbol{R}_2) \right| t_{pp}(s) \left| \chi_{\boldsymbol{K}_0}(\boldsymbol{R}_0)\, \varphi(\boldsymbol{R}_2) \right\rangle$$

✓ The asymptotic momentum approximation (AMA) on the propagation of the DW for a short distance: $\chi_{\boldsymbol{K}_i}(\boldsymbol{R} \pm \boldsymbol{s}/2) \approx \chi_{\boldsymbol{K}_i}(\boldsymbol{R})\, e^{i\boldsymbol{K}_i\cdot\boldsymbol{s}/2}$

Factorization approx$^{\mathrm{n}}$ to the T matrix

$$T^{\mathrm{DWIA}} \approx \tilde{t}_{pp}(q) \int d\boldsymbol{R}\, \chi^{*}_{\boldsymbol{K}_1}(\boldsymbol{R})\, \chi^{*}_{\boldsymbol{K}_2}(\boldsymbol{R})\, \chi_{\boldsymbol{K}_0}(\boldsymbol{R})\, \varphi(\boldsymbol{R})$$

✓ NOTE: Some people call this the zero-range approx$^{\mathrm{n}}$ but it will be misleading. $\tilde{t}_{pp}$ does contain an integration over s. The zero-range approx$^{\mathrm{n}}$ is not adopted for t_{pp}.

Why DWIA, not DWBA?

✓ Answer: Because the transition interaction is the *NN* effective interaction in which all the ladder diagrams regarding v_{NN} are taken into account.

$$\boxed{v_{NN}(s)\,\psi(\boldsymbol{s}) = t_{NN}(s)\,e^{i\boldsymbol{\kappa}\cdot\boldsymbol{s}}}$$

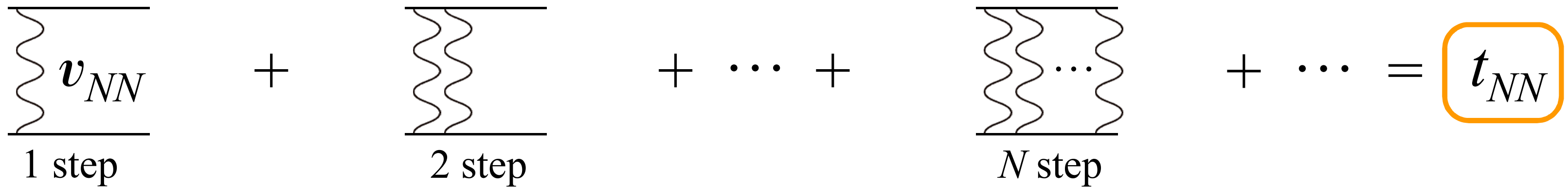

cf. Lippmann-Schwinger Eq.

$$\begin{aligned}\psi(\boldsymbol{s}) &= e^{i\boldsymbol{\kappa}\cdot\boldsymbol{s}} + \frac{1}{E_{NN} - T_{\boldsymbol{s}} + i\varepsilon} v_{NN}(s)\,\psi(\boldsymbol{s}) \\ &= e^{i\boldsymbol{\kappa}\cdot\boldsymbol{s}} + \frac{1}{E_{NN} - T_{\boldsymbol{s}} + i\varepsilon} v_{NN}(s)\left[e^{i\boldsymbol{\kappa}\cdot\boldsymbol{s}} + \frac{1}{E_{NN} - T_{\boldsymbol{s}} + i\varepsilon} v_{NN}(s)\,\psi(\boldsymbol{s})\right] = \ldots\end{aligned}$$

✓ We need an *NN* effective interaction in the many-body system but it is often replaced with t_{NN}. This is the essence of the impulse approximation, which will be valid at intermediate energies.

NN t-matrix effective interaction (in free space)

$$v_{NN}(s)\,\psi(\boldsymbol{s}) = t_{NN}(s)\,e^{i\boldsymbol{\kappa}\cdot\boldsymbol{s}}$$

Transition by a bare interaction with infinite order processes is expressed by a single step transition by an effective interaction.

- An effective interaction has no repulsive core and is easily handled.
- The wave function (of a many-body system) to be operated does not need to be very accurate.

An example of the comparison between v and t

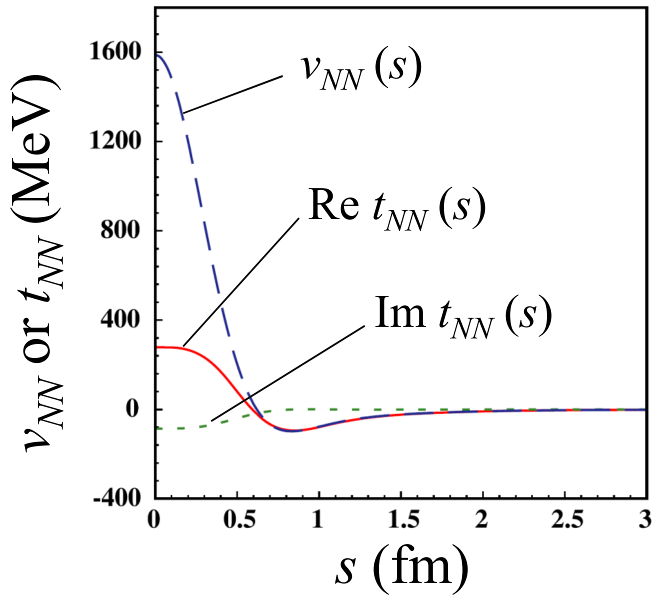

M. Yahiro, K. Minomo, KO, M. Kawai, PTP **120**, 767 (2008).

Spectroscopic study via p2p with DWIA

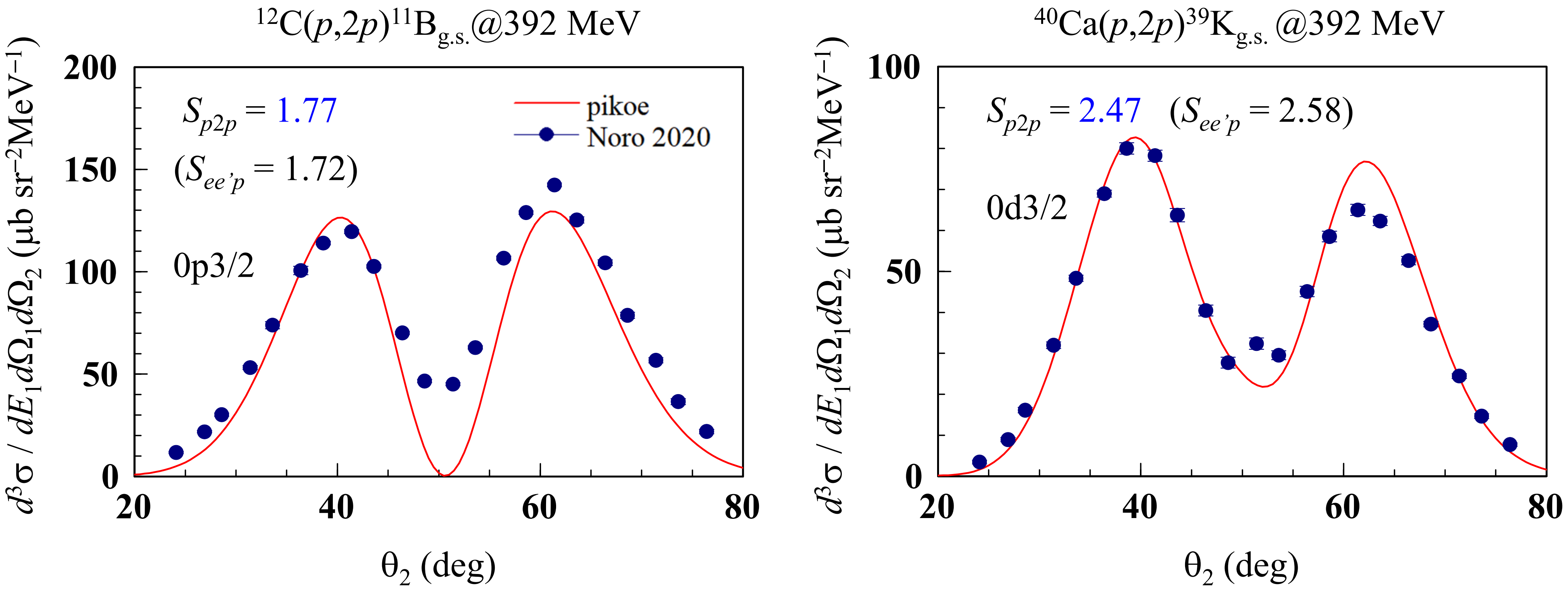

- ✓ The spectroscopic factor can be determined by the magnitude of the TDX.
- ✓ NOTE: In the PPNP review and PTEP paper, the finite solid-angle and momentum-bite (Ω-ΔP) corrections have been applied to the DWIA calculations.

Spectroscopic study via p2p with DWIA

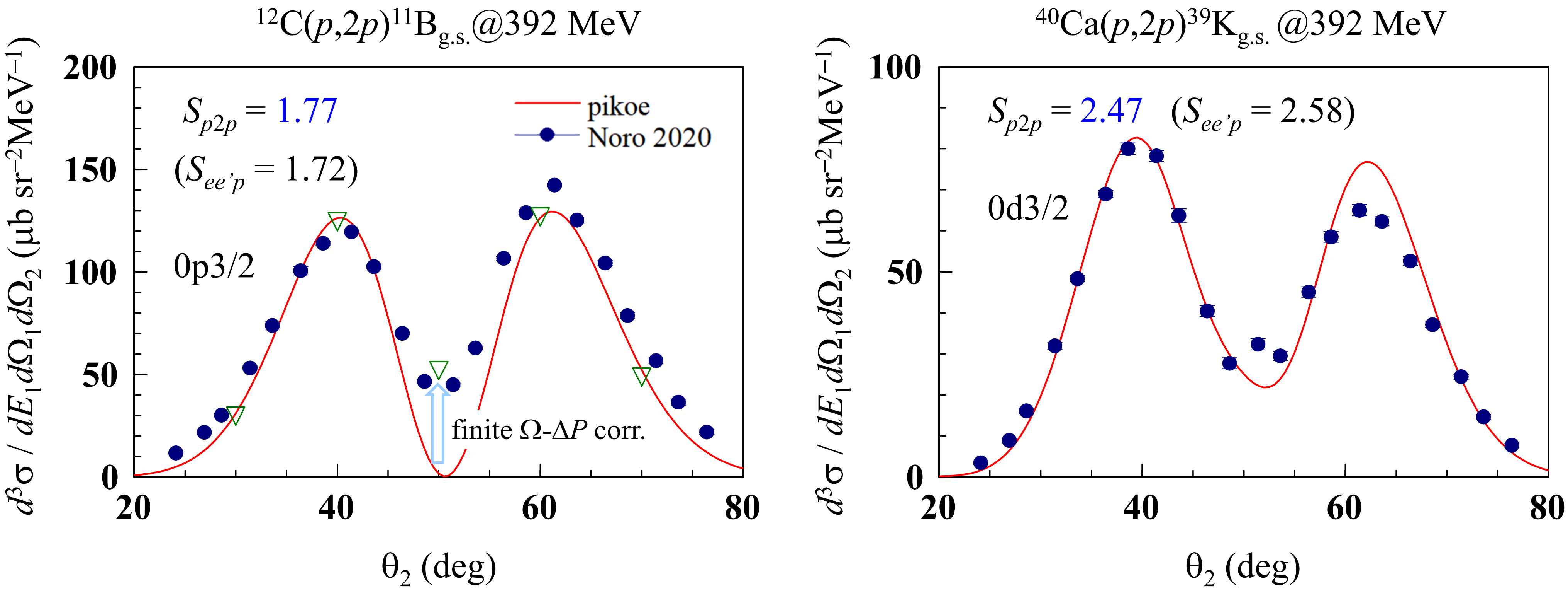

- ✓ The spectroscopic factor can be determined by the magnitude of the TDX.
- ✓ NOTE: In the PPNP review and PTEP paper, the finite solid-angle and momentum-bite (Ω-ΔP) corrections have been applied to the DWIA calculations.

sample2.cnt

Input for ^{12}C(p,2p) with DWIA

The optical potential file for particle 0 (unit # is set to 12) and that for particles 1 and 2 (unit # 13). Because the KD potential is not applicable, you need to prepare optical potentials as ext. files.

S-factor. In an actual study, it is determined to reproduce exp. data.

Distorted waves are calculated with orbital ang. mom. *L* up to 60.

Distorting pots. are given in the files of unit #s = 12, 13, and 13 for particles 0, 1, and 2.

```
  **** ppN control data ****
  10:unknown ::./tbl_12Cp2p11Bgs_set1_cs.dat
  11:old     ::./FLtbl_rede.dat
  12:old     ::./EDAD1p12C_e.dat
  13:old     ::./EDAD1p11B_e.dat
  06:unknown ::./12Cp2p11Bgs_set1_cs.outlist
 999:
---- INPUT ----
12C(p,2p)11B_gs@392MeV set1 DWIA cs
1000 0    0    0    1                             LIMFS IONS IFRM IMIR ICAL
1.00 1.007825 6.0  12.00                          ZP AP ZA AA
0    392.0     0                                  IKIN ELAB ICTREIN
1    15.96     1.0  1.007825  0.85      1         ISH EBIND ZSP ASP BETASP ICTRM
1.5  1.0  1.77      0                             FJ FL SFAC NOD
0    1.35      1    0.65      1.35      1         IBMC RC ICTRC AOC RCL ICTRCL
0    8.2       1.35      1    0.65                IBMS VOLS RS ICTRS AS
60   60   60                                      LMAX0 LMAX1 LMAX2
1    0    2.00 1    1                             IVAR IEX FKNCUT IXUNT KUNT
0    251.0     255.0     10.0                     IVVAR VARMIN VARMAX DVAR
0    32.5      180.0     10.0                     IVTHX THXMIN THXMAX DTHX
0    0.0       40.0      10.0                     IVPHX PHXMIN PHXMAX DPHX
1    0.0       180.0     0.5                      IVTH2 TH2MIN TH2MAX DTH2
0    180.0     360.0     10.0                     IVPH2 PH2MIN PH2MAX DPH2
10   6    0    0    0    0    0                   KIB: TBL OUT TMD LG PX TR TL
3    11   1    0    1                             IELM KIBELM IONSH KINELM IELMEDG
15.0      0.1       30   30   40   0    0         RMAX DR NG24-B,TH,PH,K1,PH1Q
12   1.00 1.00 1.00 1.00 -0.85     0    1         0: IPOT FV FW FVS FWS BET MS EDG
13   1.00 1.00 1.00 1.00 -0.85     0    1         1: IPOT FV FW FVS FWS BET MS EDG
13   1.00 1.00 1.00 1.00 -0.85     0    1         2: IPOT FV FW FVS FWS BET MS EDG
```

This value is negative. So the nonlocality correction function is read from the ext. files (the absolute value has no meaning in this case).

If you use KD (when it is applicable), 0.85 is recommended for these values.

Spectroscopic study via p2p with DWIA 2

T. Noro+, PTEP 2020 (in press).

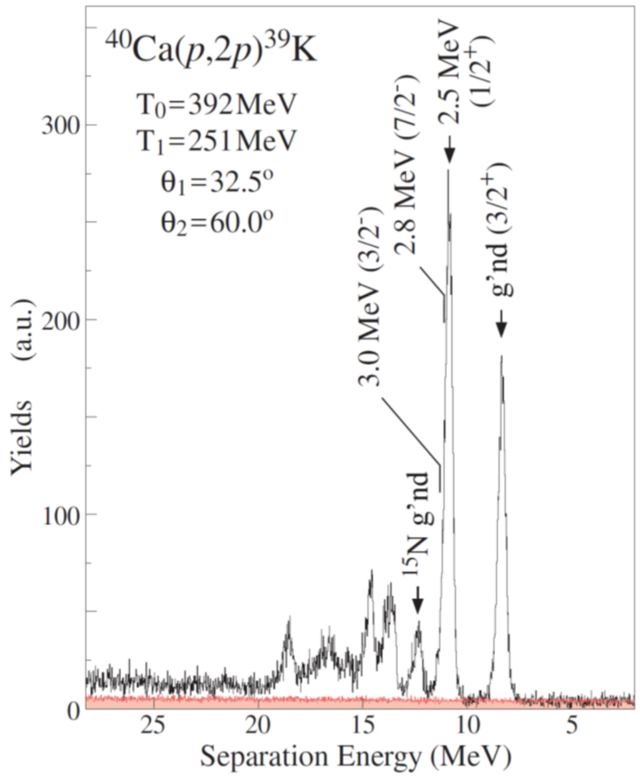

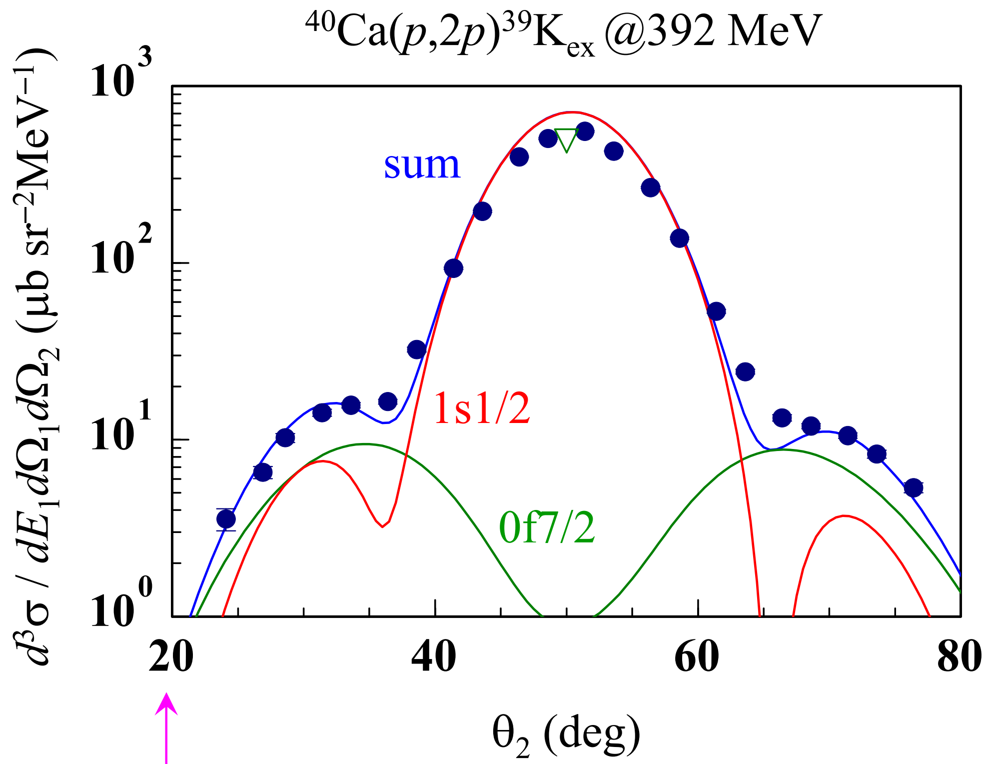

- ✓ When the states are not well separated, the multipole decomposition analysis (MDA) can be used (if ℓ are different).

$1/2^+$: $S_{p2p} = 1.03$ ($S_{ee'p} = 1.03$)

$7/2^-$: $S_{p2p} = 0.42$ ($S_{ee'p} = 0.38$)

HW: Draw this figure by yourself.

Consistency between S_{p2p} and $S_{ee'p}$

Based on data at 392 MeV taken at RCNP

T. Noro+, PTEP 2020 (in press).

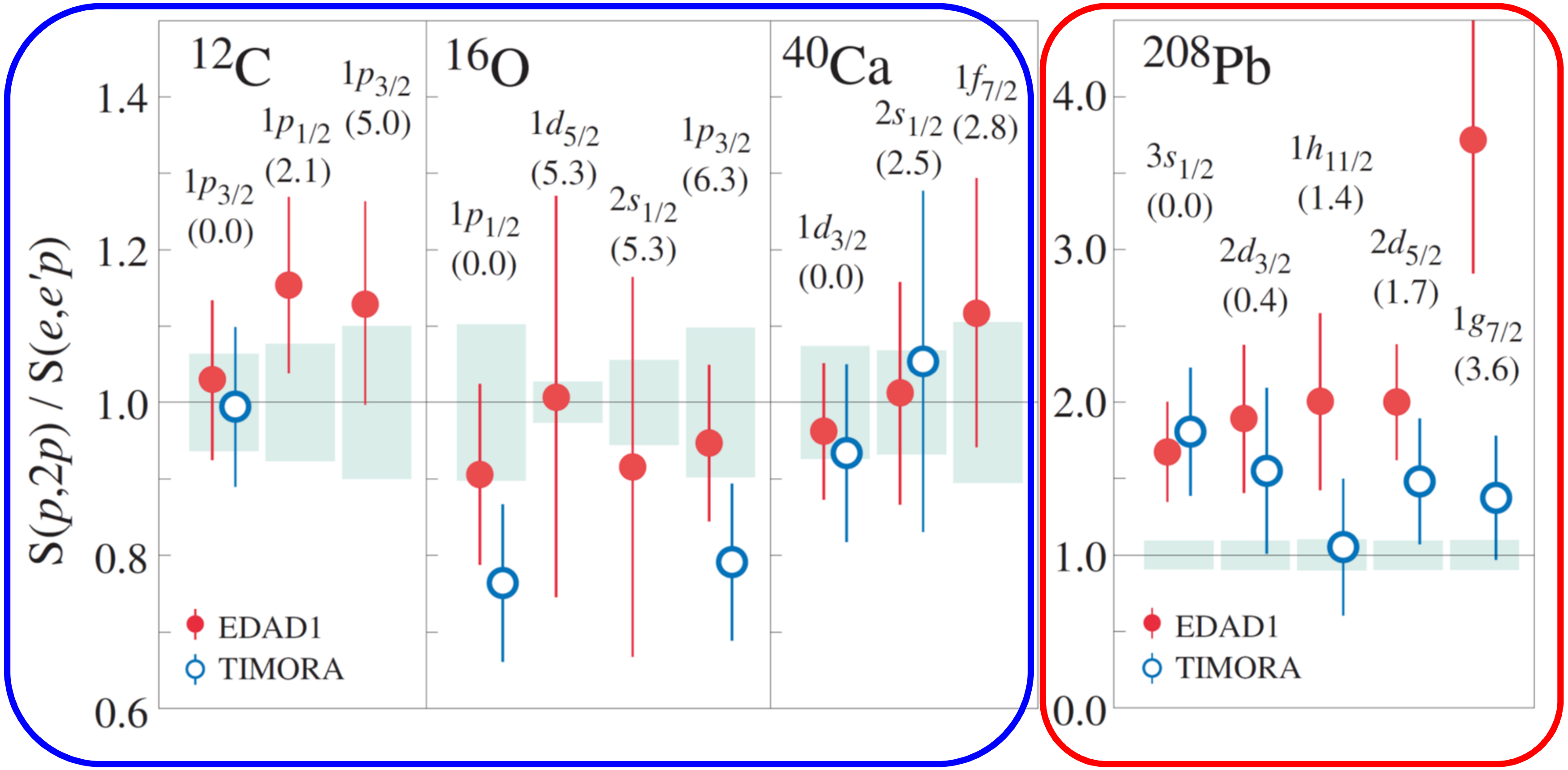

- ✓ They are consistent within uncertainties of 15–20 % except for ^{208}Pb.
- ✓ *ppN* can be applied to *n* KO and KO for unstable nuclei.

Plan of this talk (1/2)

1) Overview of (*p*,2*p*) studies (on stable nuclei)

T. Wakasa, KO, T. Noro, PPNP 96, 32 (2017); T. Noro+, PTEP 2020 (in press).

1-1. “Definition” of the KO reaction

1-2. What we can learn from PWIA analysis of KO reactions.

1-3. What we can learn from DWIA analysis of KO reactions.

2) A bit more advanced aspects of (*p*,2*p*) studies

Th. A. J. Maris, Nucl. Phys. 9 (1958–1959) 577.

2-1. Key ingredients for spectroscopic studies

2-2. The Maris effect

2-3. Treatment of the identical particles in (*p*,2*p*)

3) Momentum distribution in inverse kinematics

KO, K. Yoshida, K. Minomo, PRC 92, 034615 (2015).

3-1. Peak shift and asymmetric shape

3-2. Phase volume (PV) and attractive distortion effects

3-3. SEASTAR, SHARAQ, and GSI data analysis with DWIA

Keys to "establish" p2p as a spectroscopic tool

- ✓ Bound state W.Fn. used in the analysis of $(e,e'p)$.
  - ✓ If not available, the s.p. model of Bohr-Mottelson can be used (IBMC=IBMS=1).
- ✓ Well-constrained optical potential U_{opt}
  - ✓ The Koning-Delaroche (KD) global U_{opt} are adopted when IPOT=1. It is limited for the target mass $24 \leq A \leq 209$ and the incident energy $1\ \mathrm{keV} \leq E \leq 200\ \mathrm{MeV}$.
  - ✓ The Dirac phenomenology (Dirac PH) was employed in the PPNP review article. The EDAD1 set is applicable to nuclei from ^{12}C to ^{208}Pb for $21\ \mathrm{MeV} \leq E \leq 1040\ \mathrm{MeV}$. To use the Dirac PH, you need to prepare an external file for the potential.
- ✓ Nonlocality corrections to the bound-state W.Fn. and distorted waves (next page).
- ✓ Møller factor: the Jacobian for the *NN* *t*-matrix amplitude from the *NN* c.m. frame to the p + A c.m. frame. pikoe always takes this into account.
- ✓ Fermi motion of the nucleon in A (for $E_{\mathrm{in}} = 392$ MeV, the *NN* scattering energy varies from 95 MeV to 550 MeV). pikoe always takes this into account.

Nonlocality corrections (NLC)

- ✓ Local phenomenological N-A potentials are not constrained so as to generate a proper W.Fn in the nuclear interior region. (Its asymptotic form is OK.)
- ✓ N-A potentials are nonlocal in general. (cf. the projection operator formalism by Feshbach)

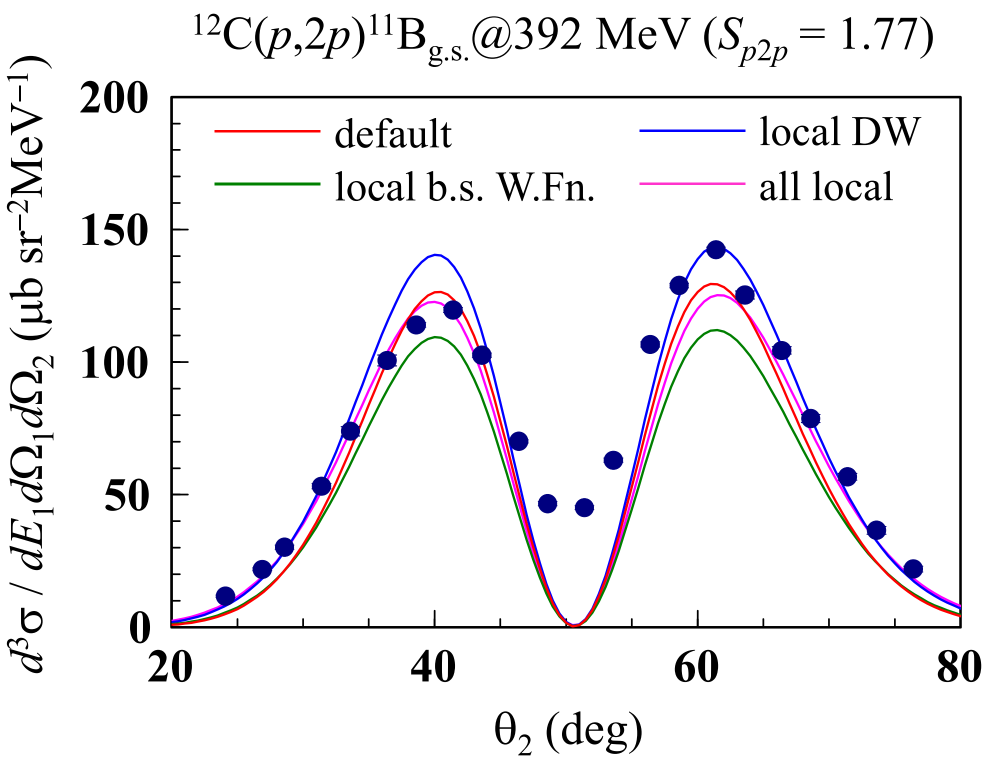

- ✓ As a phenomenological prescription, the W.Fn. is multiplied by the following Perey factor to include the nonlocality effect.

range of nonlocality (0.85 fm)

$$F_{\rm PR}(R) = \boxed{C}\left[1 - \frac{\mu}{2\hbar^2}\boxed{\beta} U(R)\right]^{-1/2}$$

renormalization factor for b.s. W.Fn.

- ✓ A similar correction can be made by using a Darwin factor in Dirac PH, though its correspondence with the Perey factor has not yet been proved.

Feshbach's projection operator formalism

✓ The entire space is divided into the P-space (to be described explicitly) and the Q-space (complement).

$$(H - E)\,\Psi = 0, \qquad \Psi = \hat{P}\Psi + \hat{Q}\Psi.$$

$$\hat{P} + \hat{Q} = 1, \quad \hat{P}^2 = \hat{P}, \quad \hat{Q}^2 = \hat{Q}, \quad \hat{P}\hat{Q} = \hat{Q}\hat{P} = 0.$$

$$\begin{cases} \left(\hat{P}H\hat{P} - E\right)\hat{P}\Psi + \hat{P}H\hat{Q}\Psi = 0, \\ \left(\hat{Q}H\hat{Q} - E\right)\hat{Q}\Psi + \hat{Q}H\hat{P}\Psi = 0. \end{cases} \Rightarrow \quad \hat{Q}\Psi = \frac{1}{E - \hat{Q}H\hat{Q} + i\eta}\hat{Q}H\hat{P}\Psi.$$

$$\boxed{\left(\hat{P}H\hat{P} + \hat{P}H\hat{Q}\frac{1}{E - \hat{Q}H\hat{Q} + i\eta}\hat{Q}H\hat{P} - E\right)\hat{P}\Psi = 0.}$$

✓ The potential to describe the P-space is complex, energy-dependent, and nonlocal.

sample2.cnt

Input for checking the NLC effect

You can switch-off the NLC for the b.s. W.Fn. by setting this value to 0.

```
  **** ppN control data ****
  10:unknown ::./tbl_12Cp2p11Bgs_set1_cs.dat
  11:old     ::./FLtbl_rede.dat
  12:old     ::./EDAD1p12C_e.dat
  13:old     ::./EDAD1p11B_e.dat
  06:unknown ::./12Cp2p11Bgs_set1_cs.outlist
 999:
---- INPUT ----
12C(p,2p)11B_gs@392MeV set1 DWIA cs
1000 0     0     0     1                              LIMFS IONS IFRM IMIR ICAL
1.00 1.007825  6.0   12.00                            ZP AP ZA AA
0    392.0       0                                    IKIN ELAB ICTREIN
1    15.96       1.0   1.007825  0.85       1         ISH EBIND ZSP ASP BETASP ICTRM
1.5  1.0   1.77        0                              FJ FL SFAC NOD
0    1.35        1     0.65      1.35       1         IBMC RC ICTRC AOC RCL ICTRCL
0    8.2         1.35       1    0.65                 IBMS VOLS RS ICTRS AS
60   60    60                                         LMAX0 LMAX1 LMAX2
1    0     2.00  1     1                              IVAR IEX FKNCUT IXUNT KUNT
0    251.0       255.0      10.0                      IVVAR VARMIN VARMAX DVAR
0    32.5        180.0      10.0                      IVTHX THXMIN THXMAX DTHX
0    0.0         40.0       10.0                      IVPHX PHXMIN PHXMAX DPHX
1    0.0         180.0      0.5                       IVTH2 TH2MIN TH2MAX DTH2
0    180.0       360.0      10.0                      IVPH2 PH2MIN PH2MAX DPH2
10   6     0     0     0    0     0                   KIB: TBL OUT TMD LG PX TR TL
3    11    1     0     1                              IELM KIBELM IONSH KINELM IELMEDG
15.0       0.1         30   30    40   0     0        RMAX DR NG24-B,TH,PH,K1,PH1Q
12   1.00  1.00  1.00  1.00 -0.85      0     1        0: IPOT FV FW FVS FWS BET MS EDG
13   1.00  1.00  1.00  1.00 -0.85      0     1        1: IPOT FV FW FVS FWS BET MS EDG
13   1.00  1.00  1.00  1.00 -0.85      0     1        2: IPOT FV FW FVS FWS BET MS EDG
```

You can switch-off the NLC for the DWs by setting these values to 0. You can also investigate the NLC effect on each particle.

HW:

Draw a figure for seeing the NLC effect on ^{40}Ca(p,2p)^{39}K$_{ex}$ at 392 MeV that is similar to the figure on the previous slide.

The Møller factor

- ✓ It is just a Jacobian but its (trivial) importance has not been recognized well in some studies (in my observation).
- ✓ Neglect of the Møller factor results in an overshooting of the TDX at high energies.

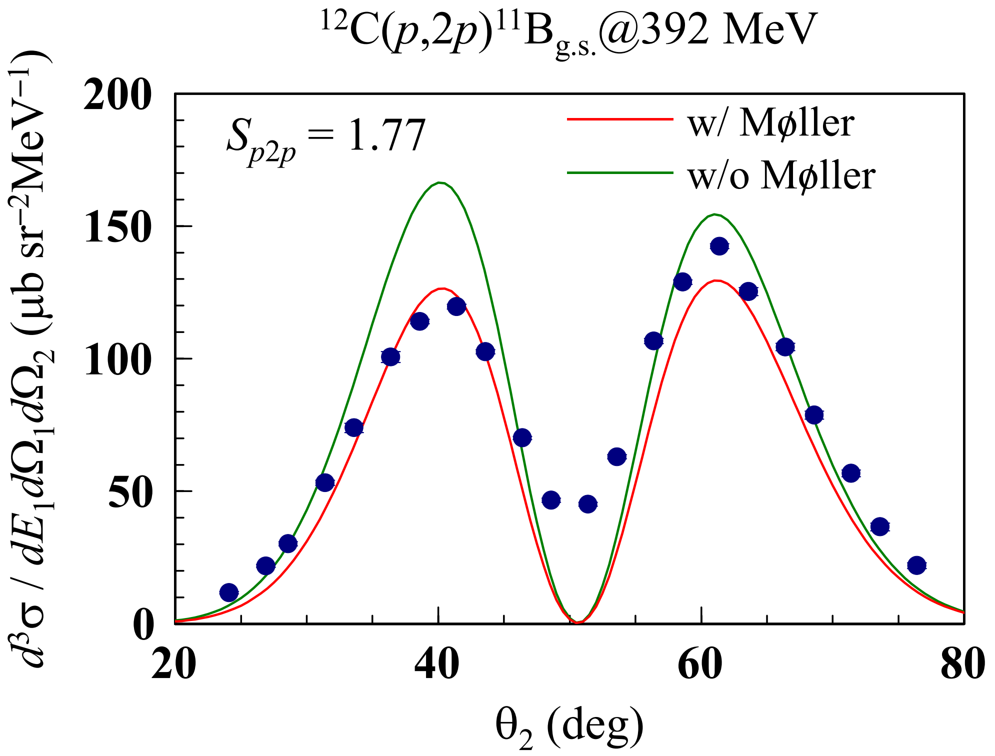

Plan of this talk (1/2)

1) Overview of (p,2p) studies (on stable nuclei)

T. Wakasa, KO, T. Noro, PPNP 96, 32 (2017); T. Noro+, PTEP 2020 (in press).

1-1. "Definition" of the KO reaction

1-2. What we can learn from PWIA analysis of KO reactions.

1-3. What we can learn from DWIA analysis of KO reactions.

2) A bit more advanced aspects of (p,2p) studies

Th. A. J. Maris, Nucl. Phys. 9 (1958–1959) 577.

2-1. Key ingredients for spectroscopic studies

2-2. The Maris effect

2-3. Treatment of the identical particles in (p,2p)

3) Momentum distribution in inverse kinematics

KO, K. Yoshida, K. Minomo, PRC 92, 034615 (2015).

3-1. Peak shift and asymmetric shape

3-2. Phase volume (PV) and attractive distortion effects

3-3. SEASTAR, SHARAQ, and GSI data analysis with DWIA

MDA for two states having the same ℓ

T. Wakasa, KO, and T. Noro, PPNP 96, 32 (2017).

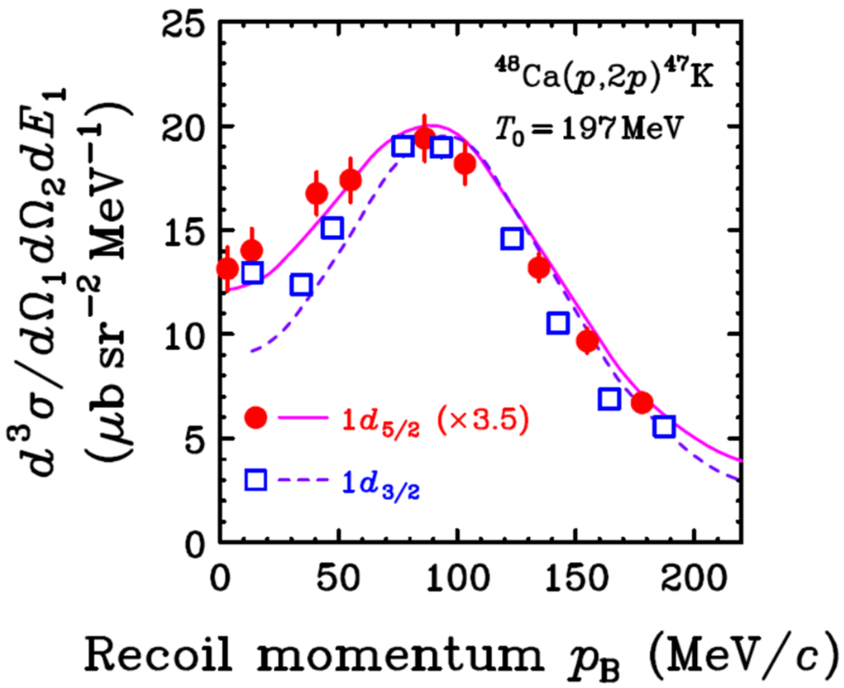

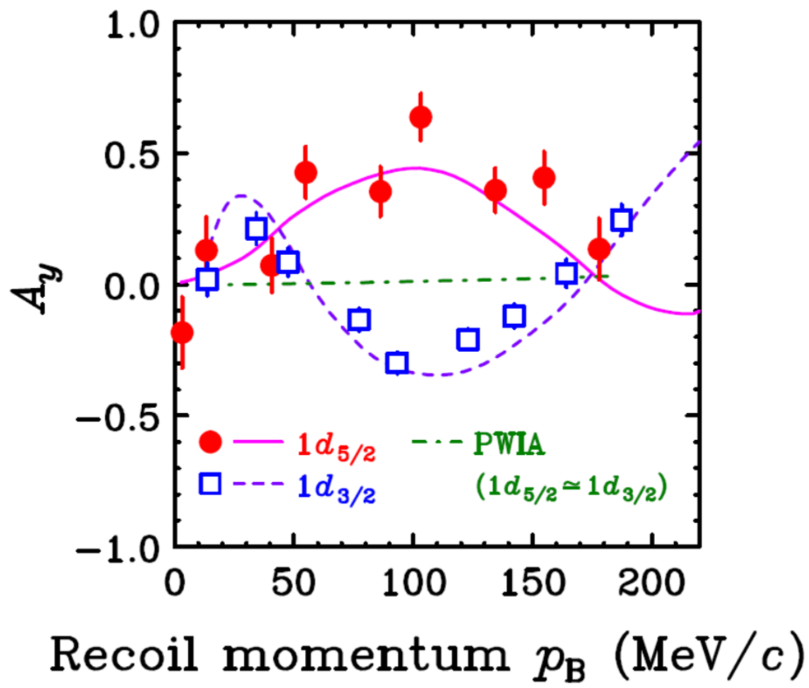

MDA fails to differentiate the two states.

The (vector) analyzing power A_y has a strong j dependence because of the Maris polarization (Maris effects).

MDA for two states having the same ℓ

T. Wakasa, KO, and T. Noro, PPNP 96, 32 (2017).

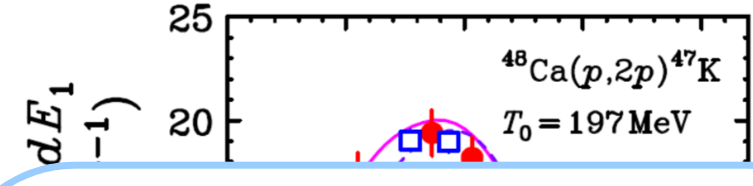

$$A_y = \frac{d\sigma(\uparrow) - d\sigma(\downarrow)}{d\sigma(\uparrow) + d\sigma(\downarrow)}$$

✓ A_y (for > 0) represents to what extent a spin-up projectile contributes the process considered.

✓ The Maris effect is useful for the j^π specification in general.

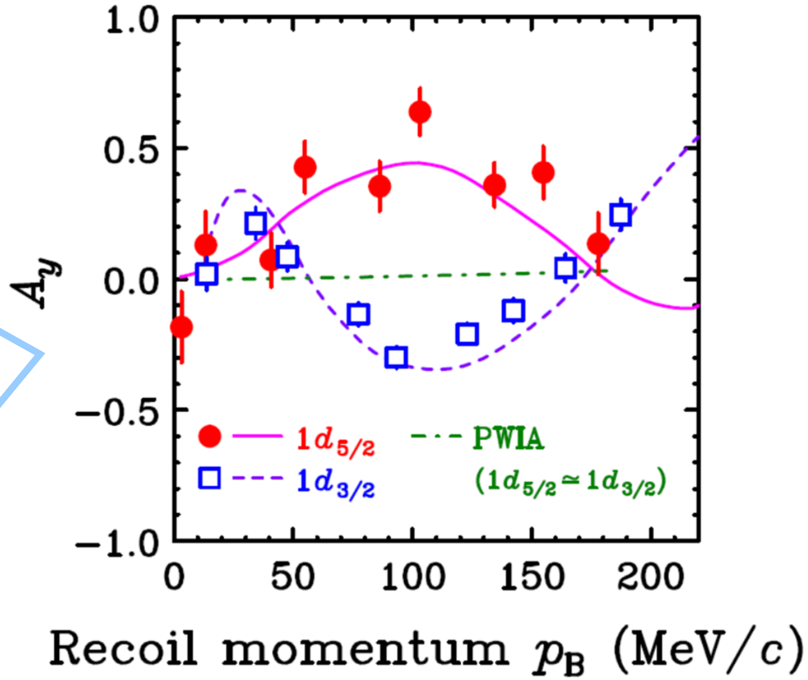

The (vector) analyzing power A_y has a strong j dependence because of the Maris polarization (Maris effects).

The Maris effect (1/2)

Th. A. J. Maris, Nucl. Phys. 9 (1958–1959) 577.

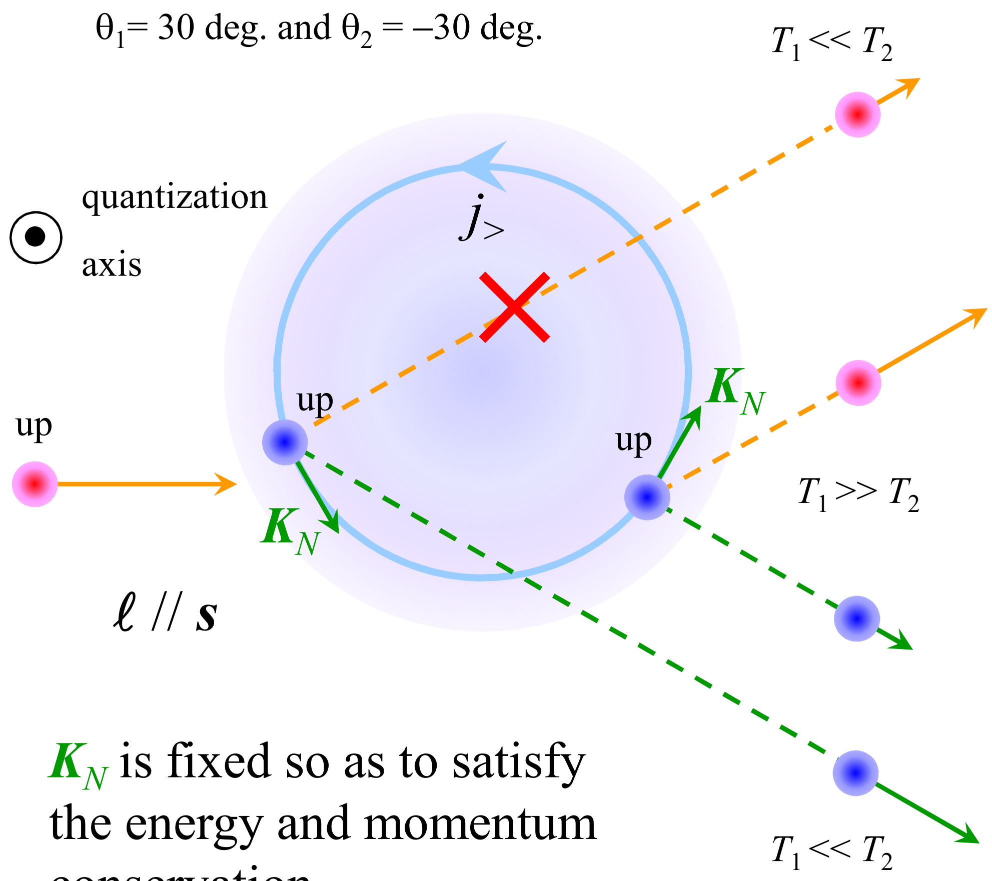

$\boldsymbol{K}_N$ is fixed so as to satisfy the energy and momentum conservation.

Assumptions

1. For *NN* collision, $\sigma_{\uparrow\uparrow}$ and $\sigma_{\downarrow\downarrow}$ dominate $\sigma_{\uparrow\downarrow}$ and $\sigma_{\downarrow\uparrow}$.
2. The mean free path for a low-energy nucleon is short.

When spin-up incident proton hits a nucleon in a $j_>$ orbit, (p,pN) events are observed only when $T_1 >> T_2$.

(This is also the case when spin-down incident proton hits a $j_<$ orbit nucleon.)

The Maris effect (2/2)

Th. A. J. Maris, Nucl. Phys. 9 (1958–1959) 577.

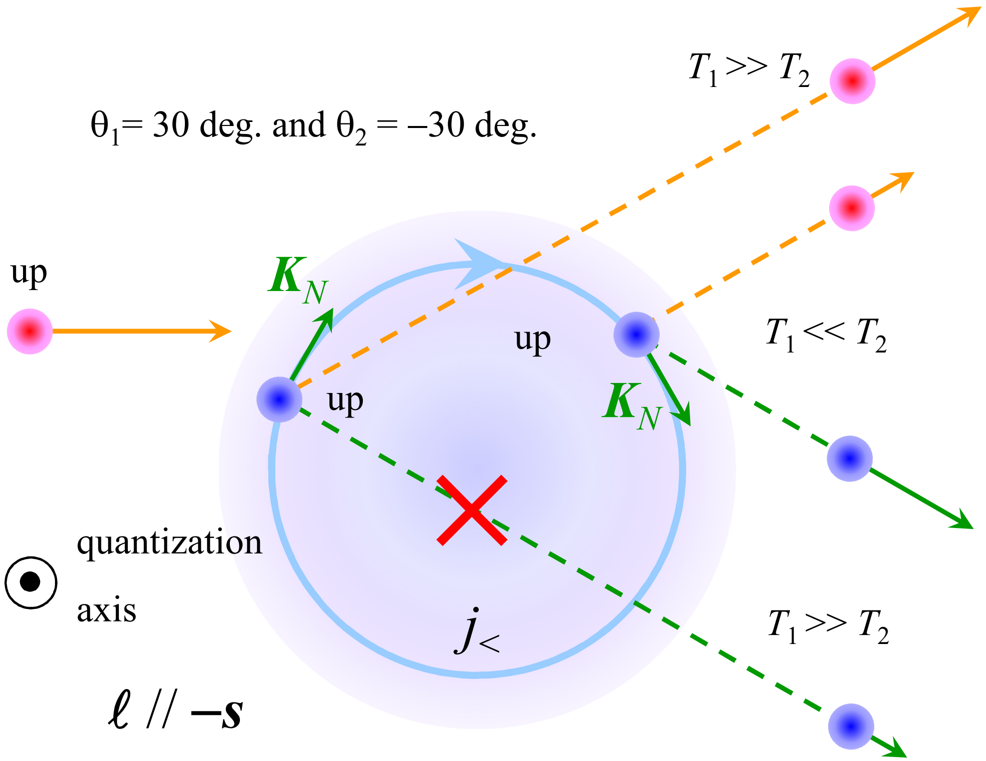

When spin-up incident proton hits a nucleon in a $j_<$ orbit, (p,pN) events are observed only when $T_2 >> T_1$.

(This is also the case when spin-down incident proton hits a $j_>$ orbit nucleon.)

A_y is positive for a $j_>$ ($j_<$) orbit with $T_1 >> T_2$ ($T_1 << T_2$).

$$A_y = \frac{d\sigma(\uparrow) - d\sigma(\downarrow)}{d\sigma(\uparrow) + d\sigma(\downarrow)}$$

MDA for two states having the same ℓ

T. Wakasa, KO, and T. Noro, PPNP 96, 32 (2017).

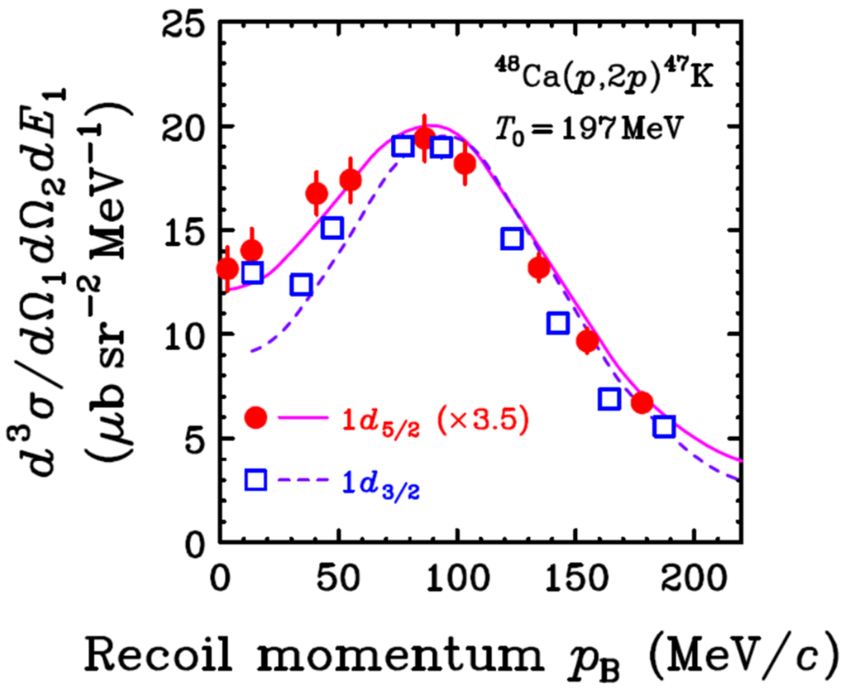

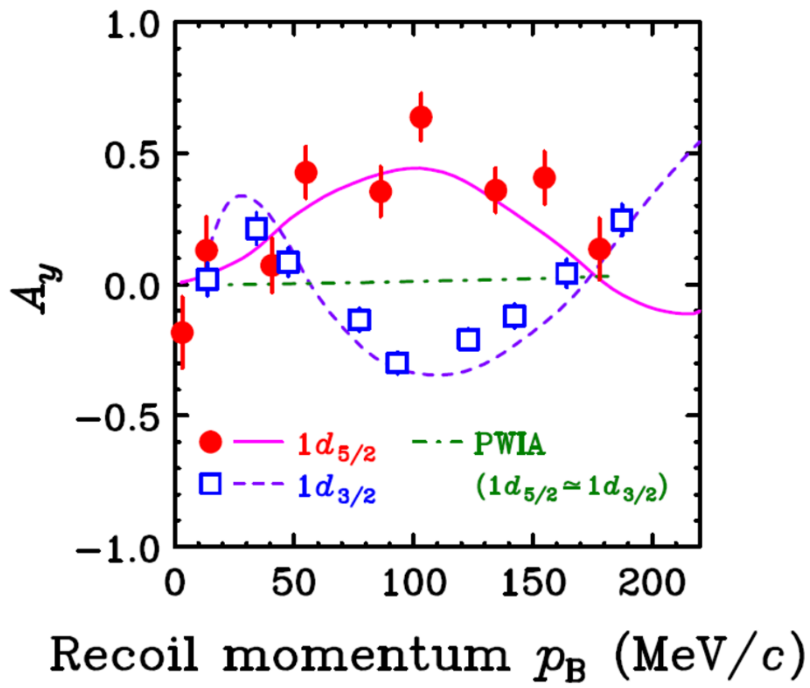

MDA fails to differentiate the two states.

The (vector) analyzing power A_y has a strong j dependence because of the Maris polarization (Maris effects).

Plan of this talk (1/2)

1) Overview of (p,2p) studies (on stable nuclei)

T. Wakasa, KO, T. Noro, PPNP 96, 32 (2017); T. Noro+, PTEP 2020 (in press).

- 1-1. "Definition" of the KO reaction
- 1-2. What we can learn from PWIA analysis of KO reactions.
- 1-3. What we can learn from DWIA analysis of KO reactions.

2) A bit more advanced aspects of (p,2p) studies

Th. A. J. Maris, Nucl. Phys. 9 (1958–1959) 577.

- 2-1. Key ingredients for spectroscopic studies
- 2-2. The Maris effect
- 2-3. Treatment of the identical particles in (p,2p)

3) Momentum distribution in inverse kinematics

KO, K. Yoshida, K. Minomo, PRC 92, 034615 (2015).

- 3-1. Peak shift and asymmetric shape
- 3-2. Phase volume (PV) and attractive distortion effects
- 3-3. SEASTAR, SHARAQ, and GSI data analysis with DWIA

The pp scattering

NOTE: An integral with no specific range means an integration over entire regions.

$$\sigma_{pp} \equiv \frac{1}{2}\int \left(\frac{d\sigma^{\text{conv}}}{d\Omega}\right) d\Omega = \int_0^{2\pi} d\phi \int_0^{\pi/2} \left(\frac{d\sigma^{\text{conv}}}{d\Omega}\right) \sin\theta d\theta$$

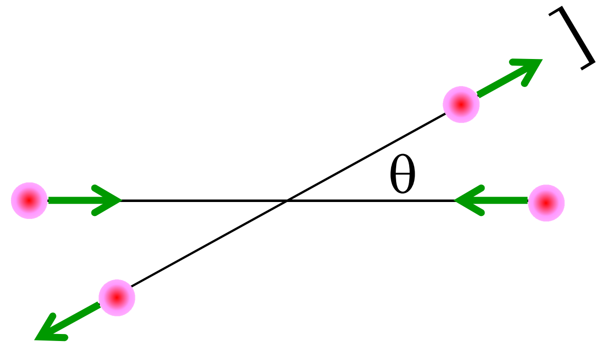

$$\frac{d\sigma^{\text{conv}}}{d\Omega} = \frac{\mu^2}{(2\pi\hbar^2)^2}\left|\left\langle \boldsymbol{\kappa}' \left| t_{NN}\left(1-\hat{P}^{\text{ex}}\right)\right| \boldsymbol{\kappa}\right\rangle\right|^2 = \boxed{\frac{d\sigma^{\text{exp}}}{d\Omega}}$$

defined by # of counts at a detector

defined by reaction probability

$$\sigma_{pp} \equiv \int \boxed{\left(\frac{d\sigma^{\text{theor}}}{d\Omega}\right)} d\Omega$$

$$\frac{d\sigma^{\text{theor}}}{d\Omega} = \frac{\mu^2}{(2\pi\hbar^2)^2}\left|\left\langle \boldsymbol{\kappa}' \left| \frac{1}{\sqrt{2}} t_{NN}\left(1-\hat{P}^{\text{ex}}\right)\right| \boldsymbol{\kappa}\right\rangle\right|^2$$

Counting rule
(classical mechanics)

Antisymmetrization of the wave function
(quantum mechanics)

pp cross section at 500 MeV

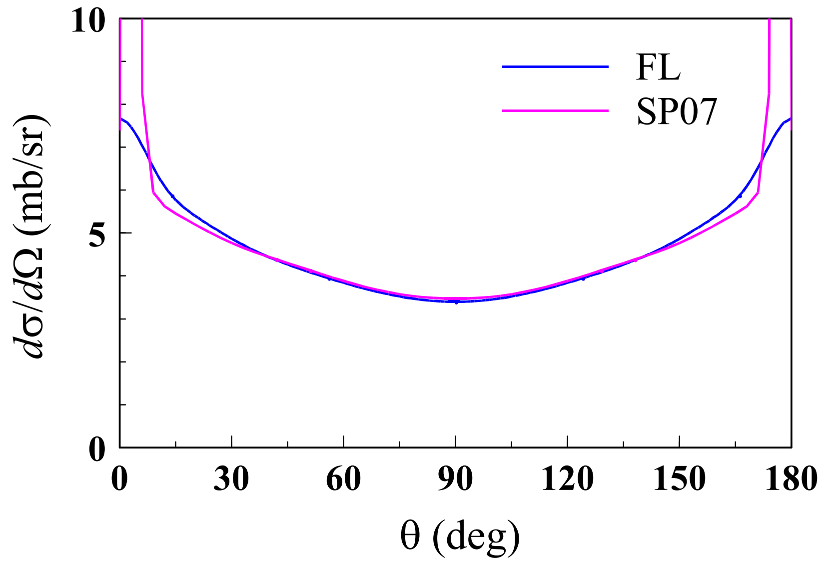

The (p,2p) process: case 1

$^{12}C(p,2p)^{11}B_{g.s.}$ at 392 MeV (RCNP data)

defined by # of counts in coincident at two detector

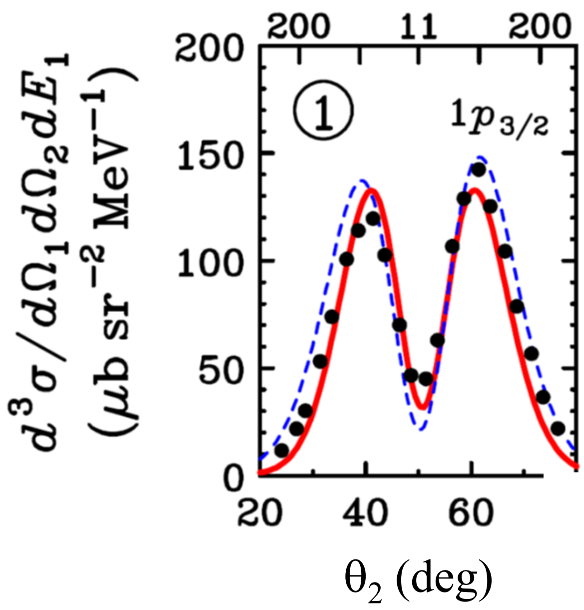

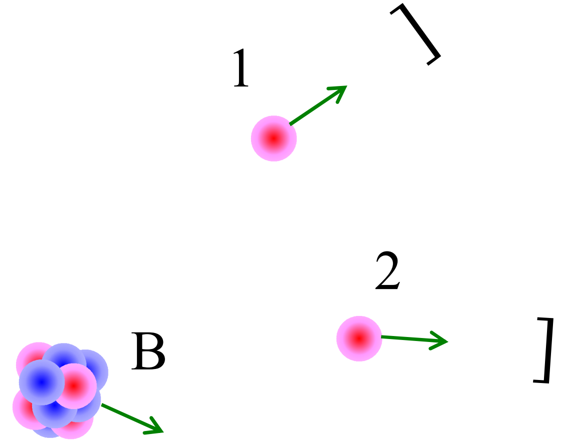

$$\frac{d^3\sigma}{dE_2 d\Omega_2 d\Omega_1}$$

$$\|$$

defined by reaction probability

$$\sigma_{p2p} = \frac{1}{2} \int \left(\frac{d^3\sigma}{dE_1 d\Omega_1 d\Omega_2} \right) dE_1 d\Omega_1 d\Omega_2$$

✓ When pikoe outputs an integrated TDX, regardless of the integration region, the value is divided by 2.

The (p,2p) process: case 2

defined by # of counts at a detector
AND reaction probability

^{12}C(p,2p)^{11}B$_{\mathrm{g.s.}}$ at 400 MeV/u (GSI data)

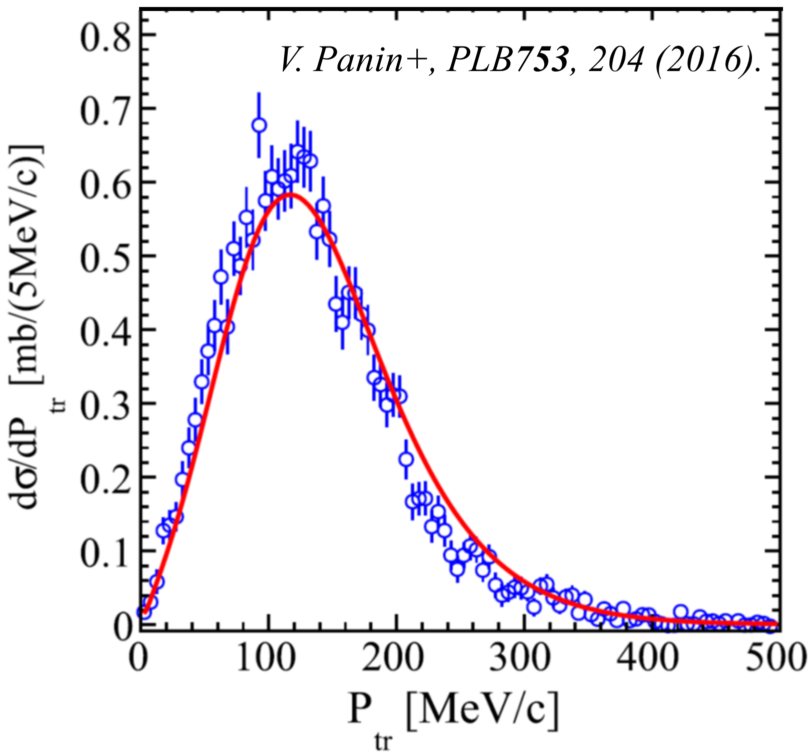

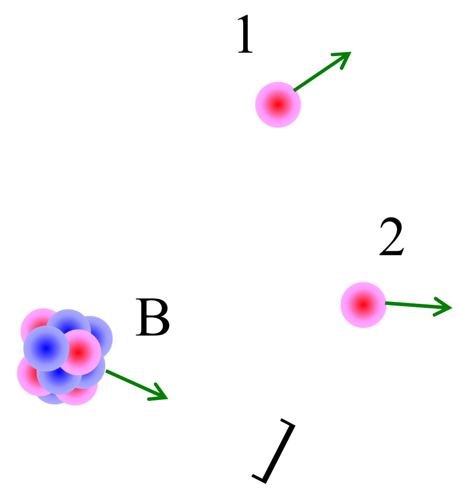

$$\frac{d^2\sigma}{d\boldsymbol{P}_{\mathrm{B}}d\Omega_1}$$

$$\|$$

$$\sigma_{p2p} = \int \left(\frac{d\sigma}{d\boldsymbol{P}_{\mathrm{B}}} \right) d\boldsymbol{P}_{\mathrm{B}} \qquad \frac{d\sigma}{d\boldsymbol{P}_{\mathrm{B}}} = \frac{1}{2} \int \left(\frac{d^2\sigma}{d\boldsymbol{P}_{\mathrm{B}}d\Omega_2} \right) d\Omega_2$$

Whether the factor 1/2 is needed depends on the definition of the observables. For the integrated (total) p2p cross sections, the division by 2 is necessary.

Plan of this talk (1/2)

1) Overview of (p,2p) studies (on stable nuclei)

T. Wakasa, KO, T. Noro, PPNP 96, 32 (2017); T. Noro+, PTEP 2020 (in press).

1-1. "Definition" of the KO reaction

1-2. What we can learn from PWIA analysis of KO reactions.

1-3. What we can learn from DWIA analysis of KO reactions.

2) A bit more advanced aspects of (p,2p) studies

Th. A. J. Maris, Nucl. Phys. 9 (1958–1959) 577.

2-1. Key ingredients for spectroscopic studies

2-2. The Maris effect

2-3. Treatment of the identical particles in (p,2p)

3) Momentum distribution in inverse kinematics

KO, K. Yoshida, K. Minomo, PRC 92, 034615 (2015).

3-1. Peak shift and asymmetric shape

3-2. Phase volume (PV) and attractive distortion effects

3-3. SEASTAR, SHARAQ, and GSI data analysis with DWIA

Spectroscopic study via p2p with DWIA 2

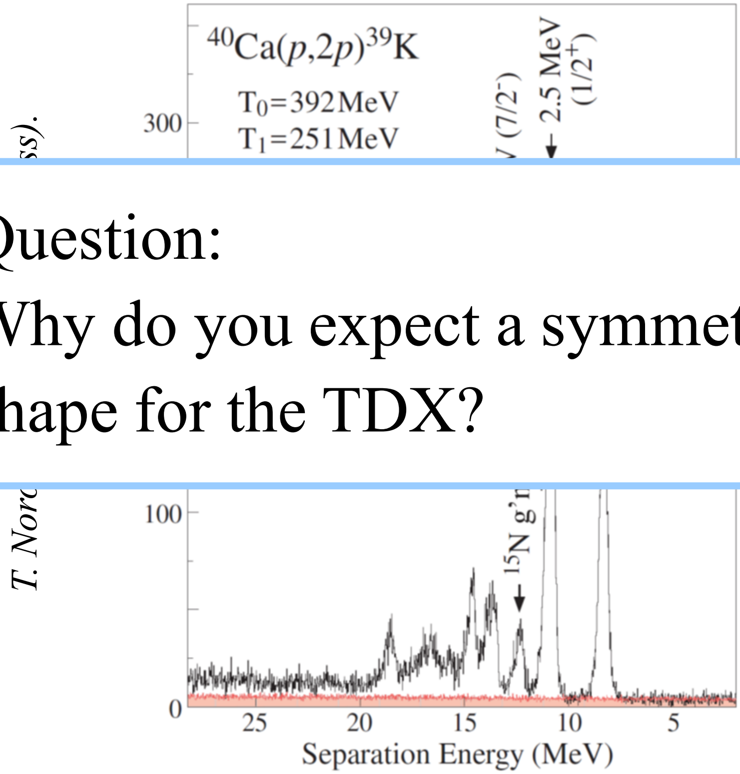

Question:
Why do you expect a symmetric shape for the TDX?

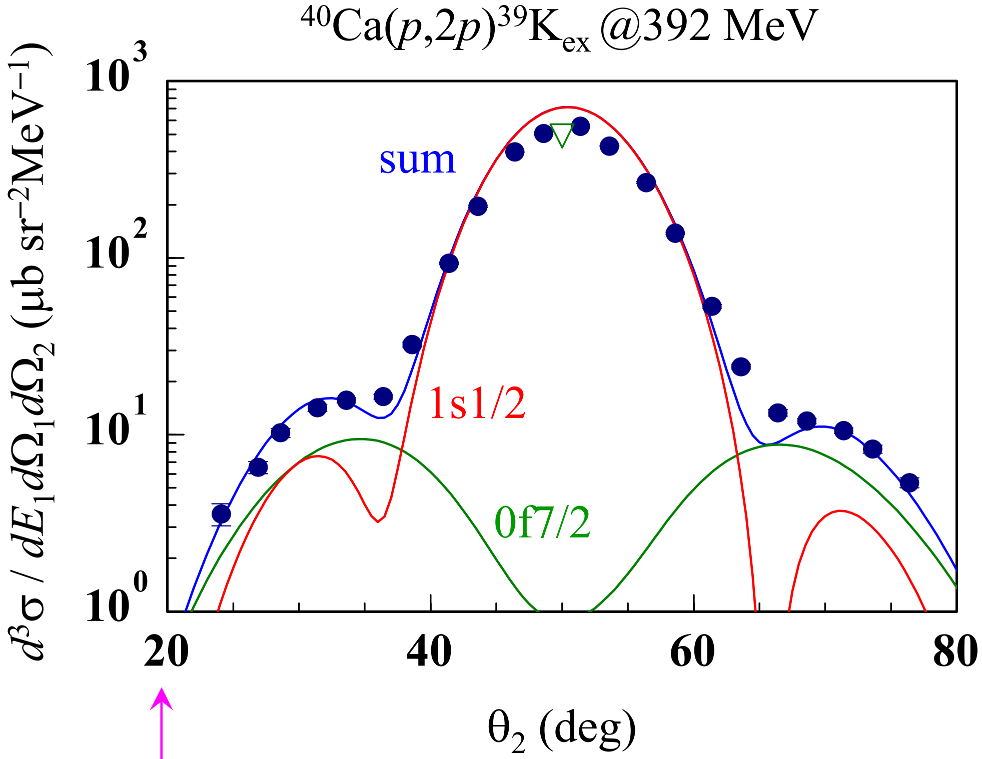

- ✓ When the states are not well separated, the multipole decomposition analysis (MDA) can be used (if ℓ are different).

1/2$^+$: S_{p2p} = 1.03 ($S_{ee'p}$ = 1.03)
7/2$^-$: S_{p2p} = 0.42 ($S_{ee'p}$ = 0.38)

HW: Draw this figure by yourself.

Symmetric or asymmetric?

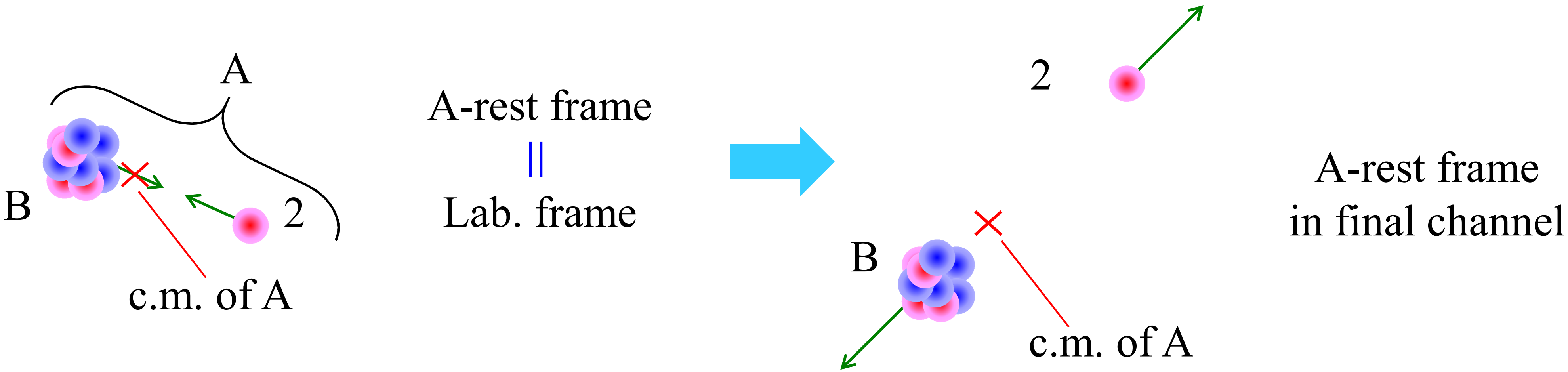

Kinematics are asymmetric so the observables. Symmetric shape is obtained <u>only when</u> the effect of the asymmetric kinematics can be neglected.

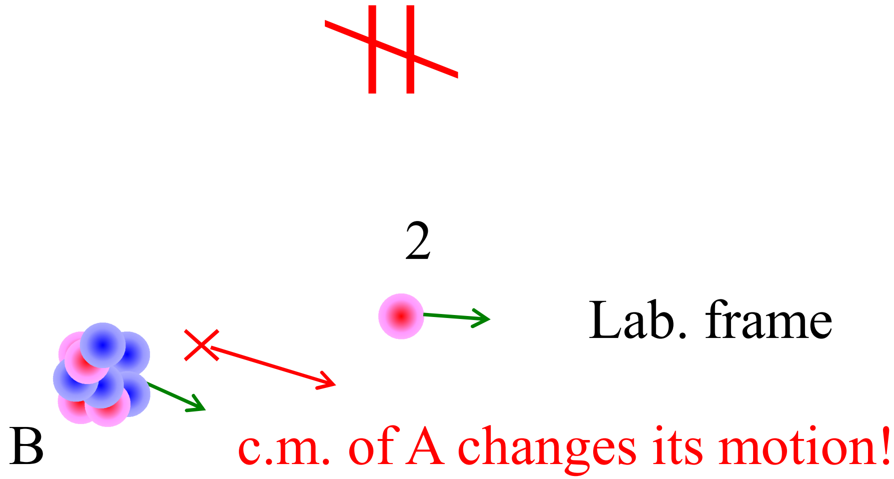

Momentum distribution (MD) of the residue B

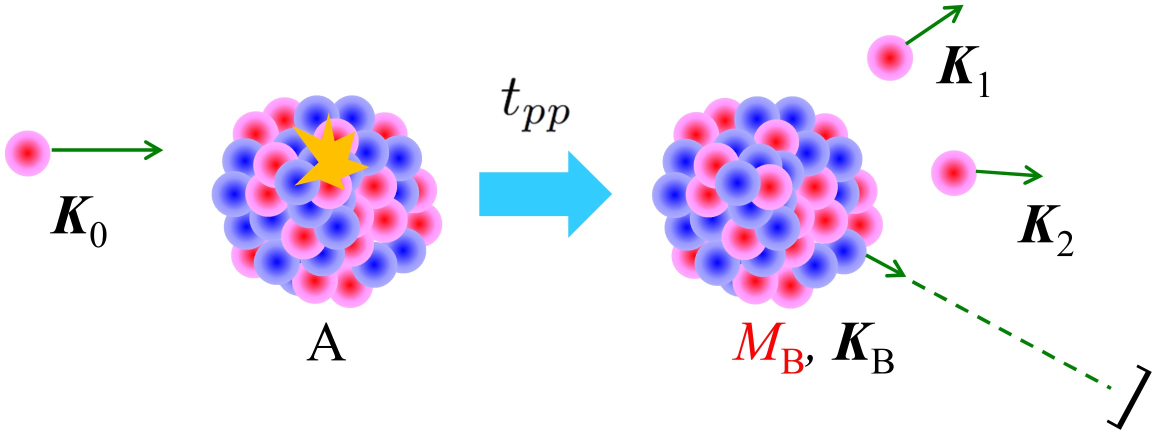

$$T^{\mathrm{PWIA}} = \tilde{\varphi}\left(\underbrace{\boldsymbol{K}_1 + \boldsymbol{K}_2 - \boldsymbol{K}_0}_{= -\boldsymbol{K}_B}\right)\tilde{t}_{pp}(q)$$

✓ $d\sigma/d\boldsymbol{K}_\mathrm{B}$, with specifying M_B, will be an ideal observable for the s.p. structure of A.

✓ It will be rather easy to measure in inverse kinematics experiments.

MD of ^{11}B of ^{12}C(p,2p)^{11}B in inverse kinematics

A-frame (A is at rest)

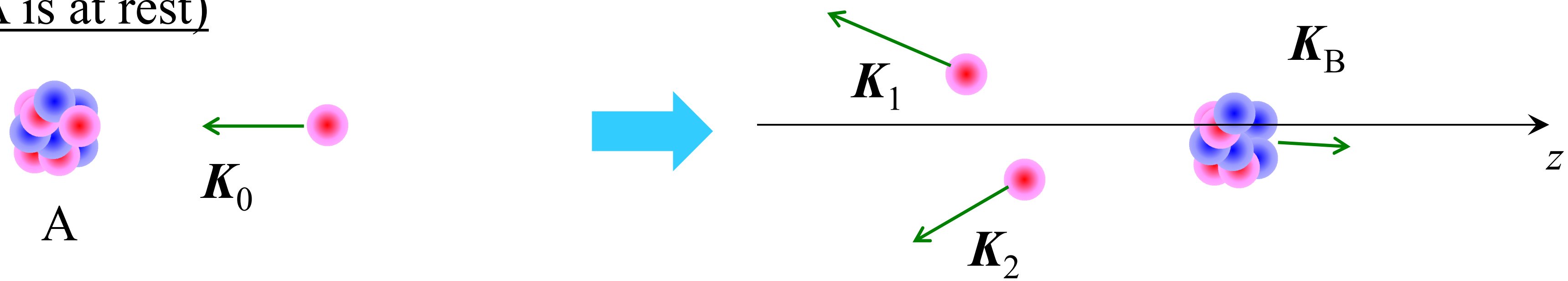

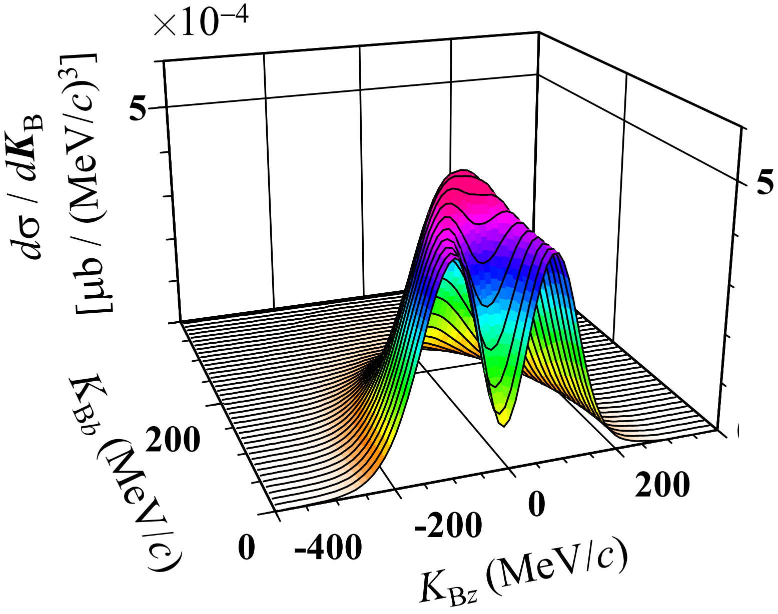

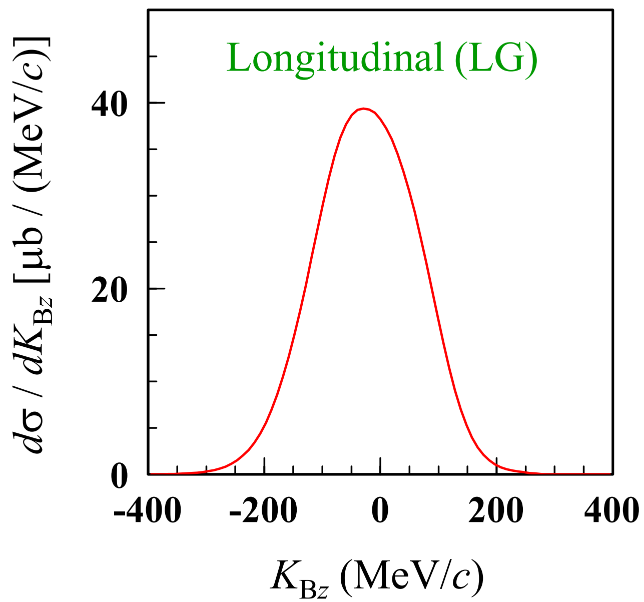

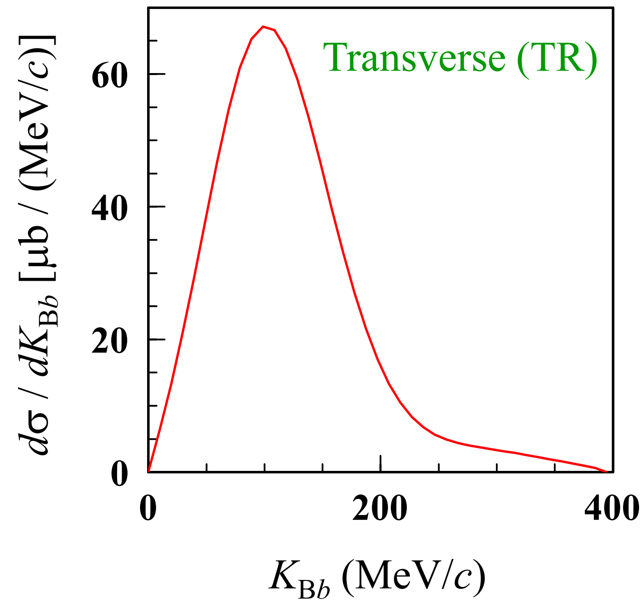

✓ The 2-dim. MD directly reflects the proton s.p. structure in ^{12}C.

Input for MD calc. of ^{12}C(p,2p) in A-frame & inv. kin.

sample3.cnt

```
  **** ppN control data ****
  10:unknown ::./tbl_12Cp2p11Bgs_MD.dat
  11:old     ::./FLtbl_rede.dat
  12:old     ::./EDAD1p12C_e.dat
  13:old     ::./EDAD1p11B_e.dat
  14:unknown ::./LG_12Cp2p11Bgs_MD.dat
  15:unknown ::./PX_12Cp2p11Bgs_MD.dat
  16:unknown ::./TR_12Cp2p11Bgs_MD.dat
  17:unknown ::./TL_12Cp2p11Bgs_MD.dat
  06:unknown ::./12Cp2p11Bgs_MD.outlist
 999:
---- INPUT ----
12C(p,2p)11B_gs@392MeV DWIA MD
1000 0    2    0    1                               LIMFS IONS IFRM IMIR ICAL
1.00 1.007825  6.0  12.00                           ZP AP ZA AA
1    392.0     0                                    IKIN ELAB ICTREIN
1    15.96     1.0  1.007825  0.85      1           ISH EBIND ZSP ASP BETASP ICTRM
1.5  1.0  1.77      0                               FJ FL SFAC NOD
0    1.35      1    0.65      1.35      1           IBMC RC ICTRC AOC RCL ICTRCL
0    8.2       1.35      1    0.65                  IBMS VOLS RS ICTRS AS
60   60   60                                        LMAX0 LMAX1 LMAX2
9    0    2.00 1    1                               IVAR IEX FKNCUT IXUNT KUNT
1    -2.0      2.0       0.05                       IVVAR VARMIN VARMAX DVAR
1    0.0       2.0       0.05                       IVTHX THXMIN THXMAX DTHX
0    0.0       40.0      10.0                       IVPHX PHXMIN PHXMAX DPHX
0    0.0       180.0     0.5                        IVTH2 TH2MIN TH2MAX DTH2
0    180.0     360.0     10.0                       IVPH2 PH2MIN PH2MAX DPH2
10   6    0    14   15   16   17                    KIB: TBL OUT TMD LG PX TR TL
3    11   1    0    1                               IELM KIBELM IONSH KINELM IELMEDG
15.0      0.1       30   30   40   15   15          RMAX DR NG24-B,TH,PH,K1,PH1Q
12   1.00 1.00 1.00 1.00 -0.85     0    1           0: IPOT FV FW FVS FWS BET MS EDG
13   1.00 1.00 1.00 1.00 -0.85     0    1           1: IPOT FV FW FVS FWS BET MS EDG
13   1.00 1.00 1.00 1.00 -0.85     0    1           2: IPOT FV FW FVS FWS BET MS EDG
```

A-frame (V-frame for inv. kin.)

inverse kinematics

MD calc.

K_{Bz} in the A-frame is varied from –2.0 to 2.0 with the step size of 0.05 (unit is fm^{-1}).

K_{Bb} is varied from 0 to 2.0 with the step size of 0.05.

output files for the 1-dimensional MDs

The unit of 1dim-MD is μb/(MeV/c)

These lines have no meaning when IVAR=9

You must make these #s finite (15 is enough in usual cases).

MD of ^{11}B of ^{12}C(p,2p)^{11}B$_{g.s.}$@100 MeV/u in inv. kin.

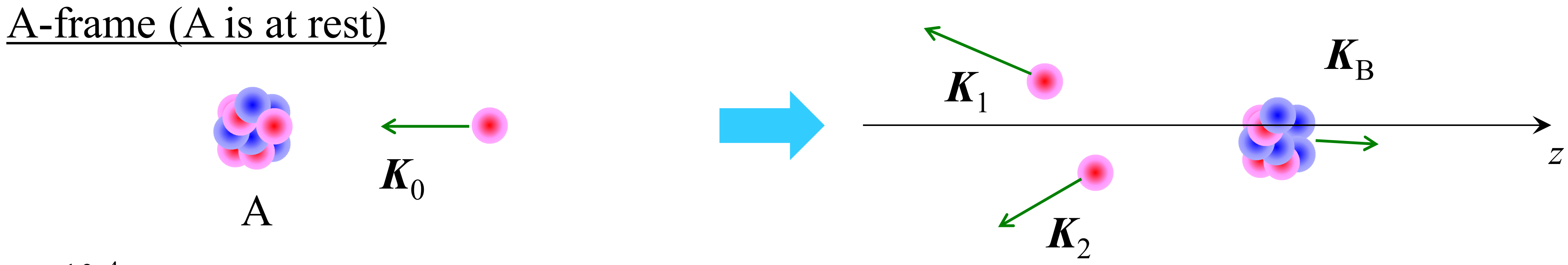

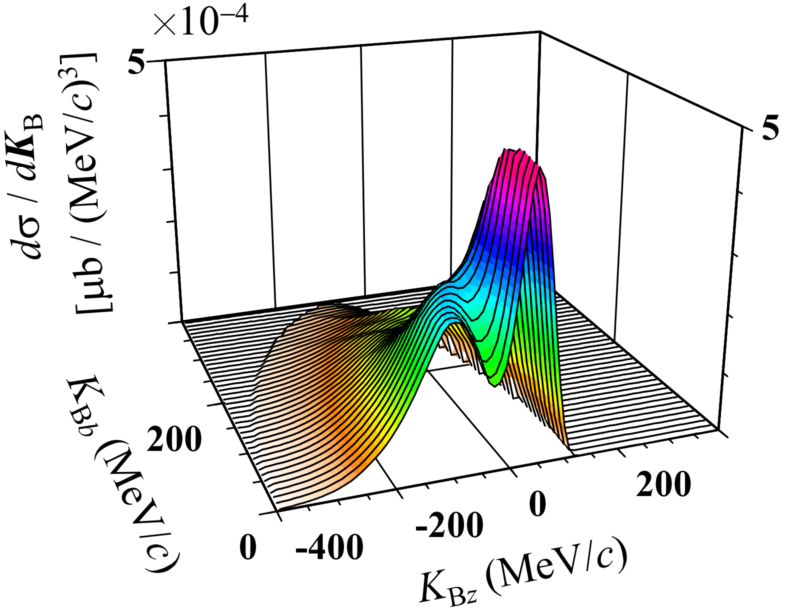

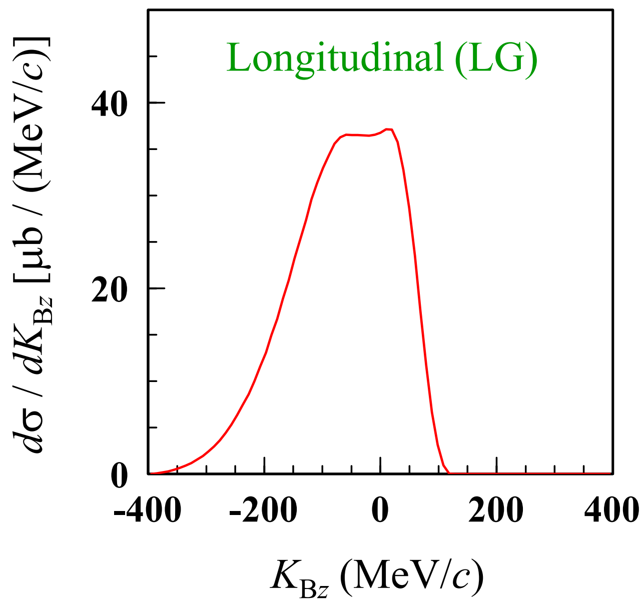

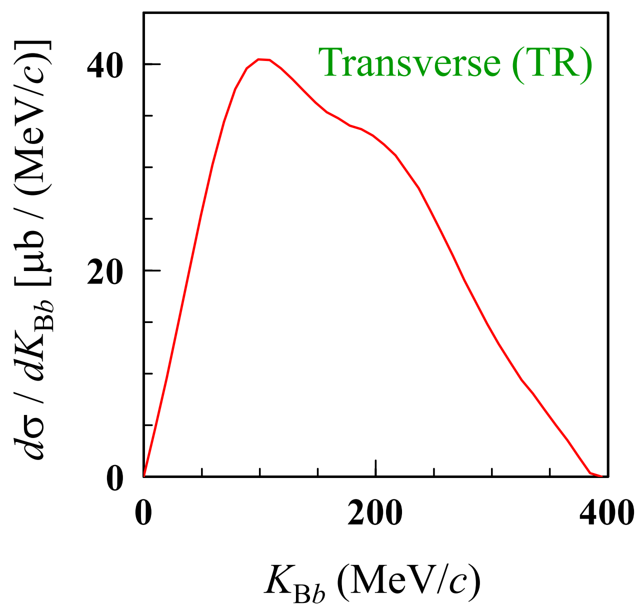

✓ The asymmetric LG-MD is due to the phase-volume & attractive distortion effects.

What is the phase volume (PV)?

- ✓ Answer: The size (volume) of the phase space (here, momentum space) that can satisfy the energy and momentum conservation. It depends on the choice of independent variables.
- ✓ Infinitesimal cross section defined in the *p*-A c.m. frame (the starting point)

$$d\sigma = C_0 \left|T\right|^2 \delta\left(\boldsymbol{K}'_{\mathrm{tot}} - \boldsymbol{K}_{\mathrm{tot}}\right) \delta\left(E'_{\mathrm{tot}} - E_{\mathrm{tot}}\right) d\boldsymbol{K}_1 d\boldsymbol{K}_2 d\boldsymbol{K}_{\mathrm{B}}$$

Lorentz invariance of the 4-dim. delta function and $d\boldsymbol{K}/E$ for each particle

Superscript A means the A-rest frame

$$d\sigma = C_0 \left|T\right|^2 \delta\left(\boldsymbol{K}'^{\mathrm{A}}_{\mathrm{tot}} - \boldsymbol{K}^{\mathrm{A}}_{\mathrm{tot}}\right) \delta\left(E'^{\mathrm{A}}_{\mathrm{tot}} - E^{\mathrm{A}}_{\mathrm{tot}}\right) \frac{E_1 E_2 E_{\mathrm{B}}}{E_1^{\mathrm{A}} E_2^{\mathrm{A}} E_{\mathrm{B}}^{\mathrm{A}}} d\boldsymbol{K}_1^{\mathrm{A}} d\boldsymbol{K}_2^{\mathrm{A}} d\boldsymbol{K}_{\mathrm{B}}^{\mathrm{A}}$$

- ✓ Let us decide to choose $\boldsymbol{K}_{\mathrm{B}}^{\mathrm{A}}$ and Ω_2^{A} as independent variables. Our aim is to calculate

$$\frac{d^2\sigma}{d\boldsymbol{K}_{\mathrm{B}}^{\mathrm{A}} d\Omega_2^{\mathrm{A}}}$$

Calculation of the PV

✓ We perform an integration over $\boldsymbol{K}_1^{\mathrm{A}}$. By the mom. cons. it is fixed at

momentum transfer to B

$$\boldsymbol{K}_1^{\mathrm{A}} = \boldsymbol{K}_0^{\mathrm{A}} - \boldsymbol{K}_{\mathrm{B}}^{\mathrm{A}} - \boldsymbol{K}_2^{\mathrm{A}} \equiv \boxed{\boldsymbol{q}_{\mathrm{B}}^{\mathrm{A}}} - \boldsymbol{K}_2^{\mathrm{A}}$$

✓ Infinitesimal cross section for which the mom. cons. is satisfied (in the A-rest frame)

$$d\sigma = C_0 \frac{E_1 E_2 E_{\mathrm{B}}}{E_1^{\mathrm{A}} E_2^{\mathrm{A}} E_{\mathrm{B}}^{\mathrm{A}}} |T|^2 \, \delta\left(E_{\mathrm{tot}}'^{\mathrm{A}} - E_{\mathrm{tot}}^{\mathrm{A}}\right) d\boldsymbol{K}_{\mathrm{B}}^{\mathrm{A}} \left(K_2^{\mathrm{A}}\right)^2 dK_2^{\mathrm{A}} d\Omega_2^{\mathrm{A}}$$

✓ PV

$$\rho \equiv \left(K_2^{\mathrm{A}}\right)^2 \int \delta\left(E_{\mathrm{tot}}'^{\mathrm{A}} - E_{\mathrm{tot}}^{\mathrm{A}}\right) dK_2^{\mathrm{A}} \equiv \left(K_2^{\mathrm{A}}\right)^2 \int \delta\left(f\left(K_2^{\mathrm{A}}\right)\right) dK_2^{\mathrm{A}}$$

$$f\left(K_2^{\mathrm{A}}\right) \equiv \sqrt{\left(m_1 c^2\right)^2 + \left(\hbar c\right)^2 \left(\left(q_{\mathrm{B}}^{\mathrm{A}}\right)^2 + \left(K_2^{\mathrm{A}}\right)^2 - 2 q_{\mathrm{B}}^{\mathrm{A}} K_2^{\mathrm{A}} \cos\theta_{2q_{\mathrm{B}}}^{\mathrm{A}}\right)} + \sqrt{\left(m_2 c^2\right)^2 + \left(\hbar c K_2^{\mathrm{A}}\right)^2}$$

$$+ \sqrt{\left(m_{\mathrm{B}} c^2\right)^2 + \left(\hbar c K_{\mathrm{B}}^{\mathrm{A}}\right)^2} - \sqrt{\left(m_0 c^2\right)^2 + \left(\hbar c K_0^{\mathrm{A}}\right)^2} - m_{\mathrm{A}} c^2$$

Calculation of the PV (Con't)

✓ One can perform the integration over K_2^{A} by using:

$$\delta\left(f\left(K_2^{\mathrm{A}}\right)\right) = \sum_i \left|\frac{\partial f}{\partial K_2^{\mathrm{A}}}\right|^{-1}_{\left(K_2^{\mathrm{A}}\right)_i} \delta\left(K_2^{\mathrm{A}} - \left(K_2^{\mathrm{A}}\right)_i\right), \quad f\left(\left(K_2^{\mathrm{A}}\right)_i\right) = 0$$

$$\frac{\partial\left(E'^{\mathrm{A}}_{\mathrm{tot}} - E^{\mathrm{A}}_{\mathrm{tot}}\right)}{\partial K_2^{\mathrm{A}}} = \frac{\hbar^2 c^2\left(K_2^{\mathrm{A}} - q_{\mathrm{B}}^{\mathrm{A}}\cos\theta^{\mathrm{A}}_{2q_{\mathrm{B}}}\right)}{E_1^{\mathrm{A}}} + \frac{\hbar^2 c^2 K_2^{\mathrm{A}}}{E_2^{\mathrm{A}}}$$

We implicitly assume that $\left(K_2^{\mathrm{A}}\right)_i$ satisfying the energy cons. is unique and is written as K_2^{A} for simplicity

$$\rho = \left(K_2^{\mathrm{A}}\right)^2\left[\frac{\hbar^2 c^2\left(K_2^{\mathrm{A}} - q_{\mathrm{B}}^{\mathrm{A}}\cos\theta^{\mathrm{A}}_{2q_{\mathrm{B}}}\right)}{E_1^{\mathrm{A}}} + \frac{\hbar^2 c^2 K_2^{\mathrm{A}}}{E_2^{\mathrm{A}}}\right]^{-1}$$

$$= \frac{E_2^{\mathrm{A}} K_2^{\mathrm{A}}}{\hbar^2 c^2}\left[1 + \frac{E_2^{\mathrm{A}}}{E_1^{\mathrm{A}}} + \frac{E_2^{\mathrm{A}}}{E_1^{\mathrm{A}}}\frac{\left(\boldsymbol{K}_{\mathrm{B}}^{\mathrm{A}} - \boldsymbol{K}_0^{\mathrm{A}}\right)\cdot\boldsymbol{K}_2^{\mathrm{A}}}{\left(K_2^{\mathrm{A}}\right)^2}\right]^{-1}$$

<u>Experimental condition</u>

$\boldsymbol{K}_0^{\mathrm{A}}$ and masses of all particles

<u>Independent variables</u>

$\boldsymbol{K}_{\mathrm{B}}^{\mathrm{A}}$ (thus $E_{\mathrm{B}}^{\mathrm{A}}$), Ω_2^{A}

<u>Fixed quantities</u>

$\boldsymbol{K}_1^{\mathrm{A}}$ (thus E_1^{A}), K_2^{A} (thus E_2^{A})

Calculation of MD in the A-rest frame

$$\frac{d^2\sigma}{d\boldsymbol{K}_{\mathrm{B}}^{\mathrm{A}} d\Omega_2^{\mathrm{A}}} = C_0 \frac{E_1 E_2 E_{\mathrm{B}}}{E_1^{\mathrm{A}} E_2^{\mathrm{A}} E_{\mathrm{B}}^{\mathrm{A}}} \boxed{\frac{E_2^{\mathrm{A}} K_2^{\mathrm{A}}}{\hbar^2 c^2} \left[1 + \frac{E_2^{\mathrm{A}}}{E_1^{\mathrm{A}}} + \frac{E_2^{\mathrm{A}}}{E_1^{\mathrm{A}}} \frac{\left(\boldsymbol{K}_{\mathrm{B}}^{\mathrm{A}} - \boldsymbol{K}_0^{\mathrm{A}}\right) \cdot \boldsymbol{K}_2^{\mathrm{A}}}{\left(K_2^{\mathrm{A}}\right)^2} \right]^{-1}} |T|^2$$

Phase Volume

$$\frac{d\sigma}{d\boldsymbol{K}_{\mathrm{B}}^{\mathrm{A}}} = \int \left(\frac{d^2\sigma}{d\boldsymbol{K}_{\mathrm{B}}^{\mathrm{A}} d\Omega_2^{\mathrm{A}}} \right) d\Omega_2^{\mathrm{A}}$$

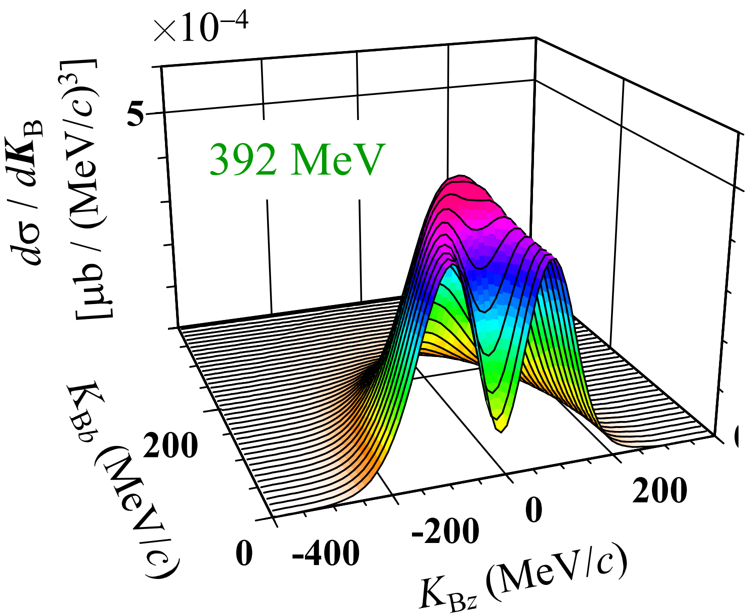

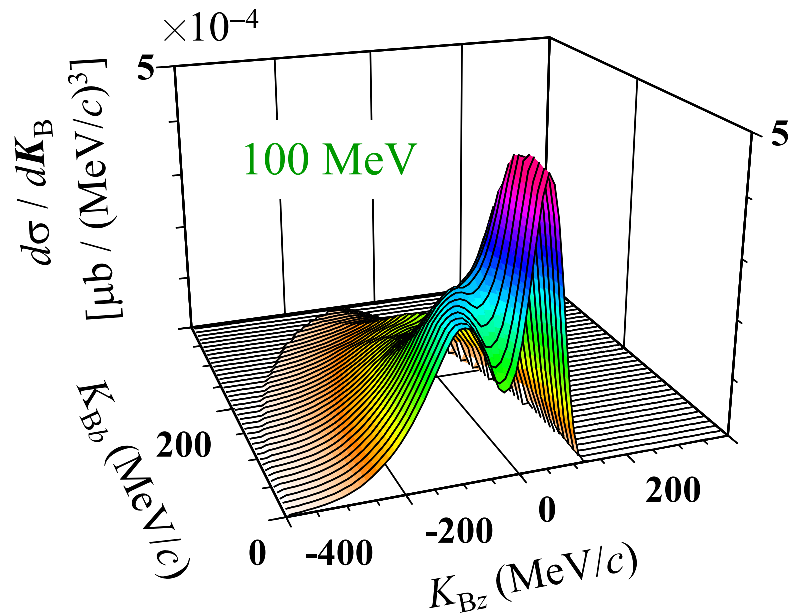

Role of the PV

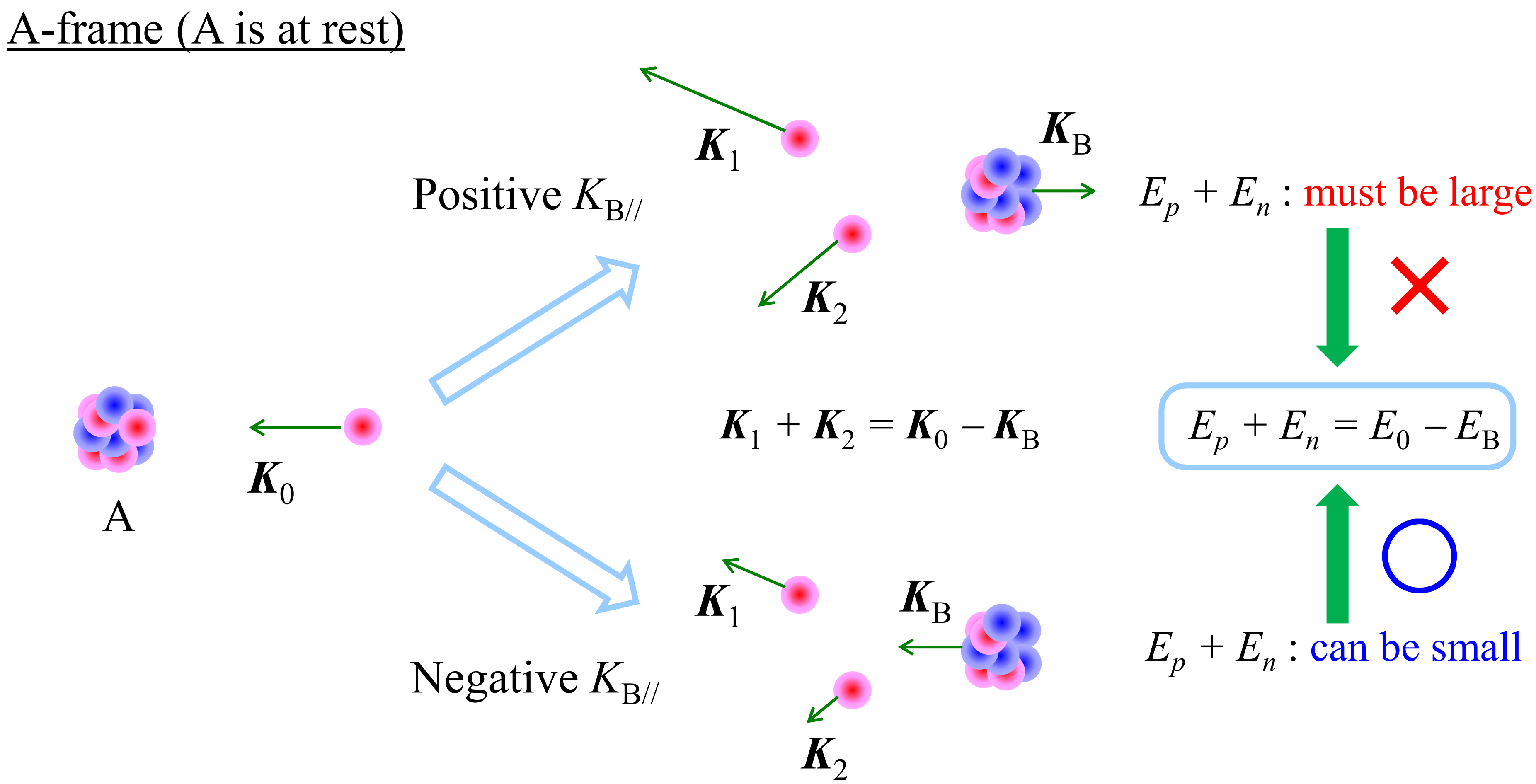

KO, K. Yoshida, K. Minomo, PRC 92, 034615 (2015).

PV effect on MD at 100 MeV (PWIA)

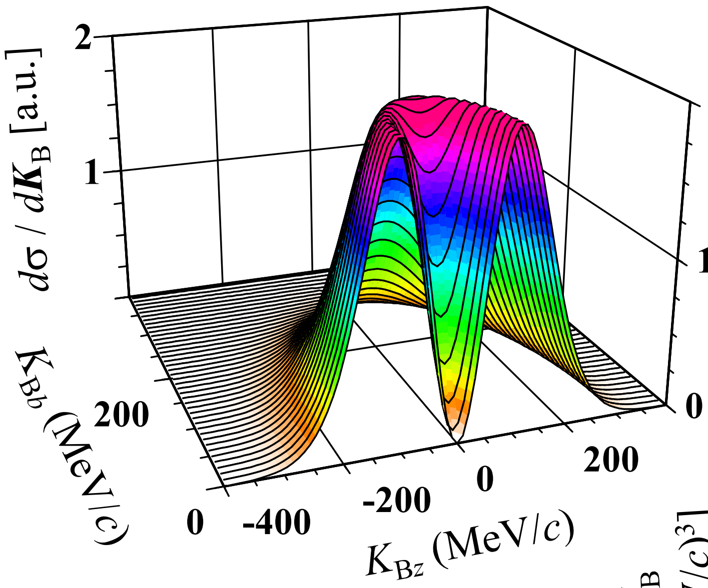

<u>$0p_{3/2}$ proton MD in ^{12}C</u>

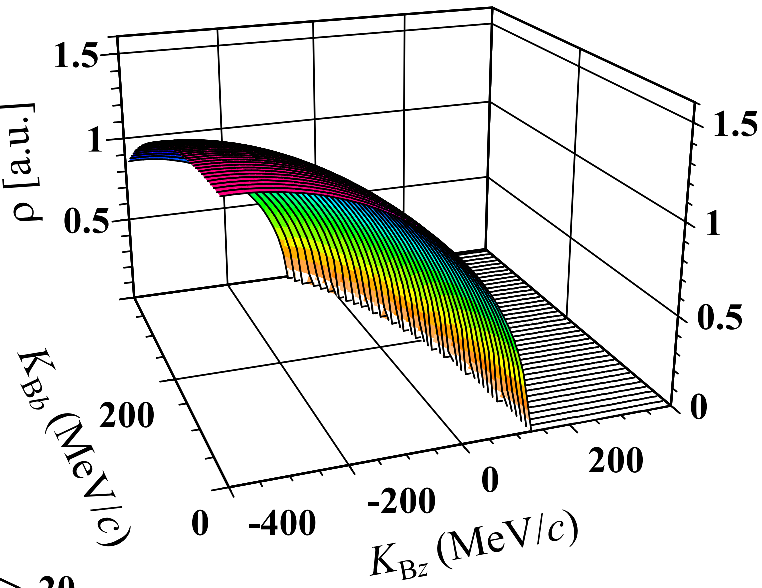

<u>Phase Volume</u>

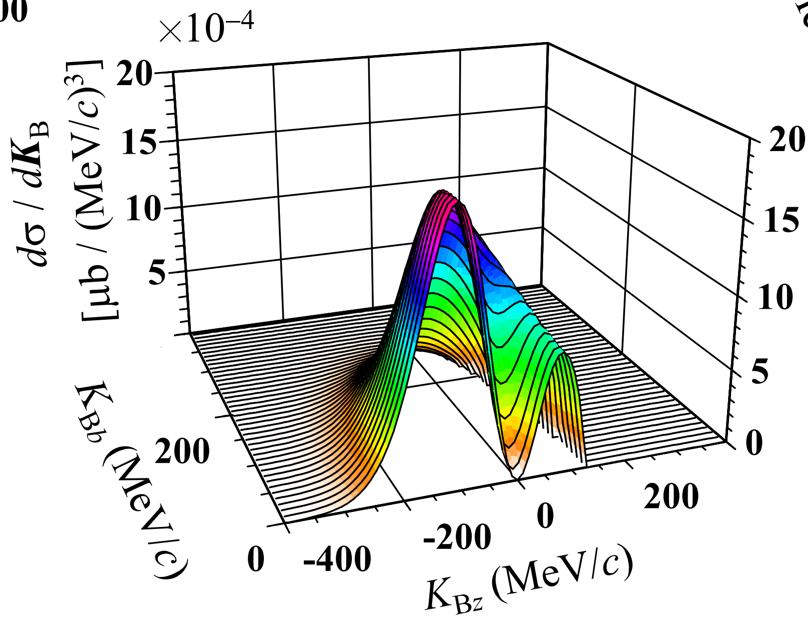

NOTE:
Energy dependence of the *NN* *t*-matrix is disregarded for a transparent interpretation (w/ IELM=0).

PV effect on LG-MD at 100 MeV (PWIA)

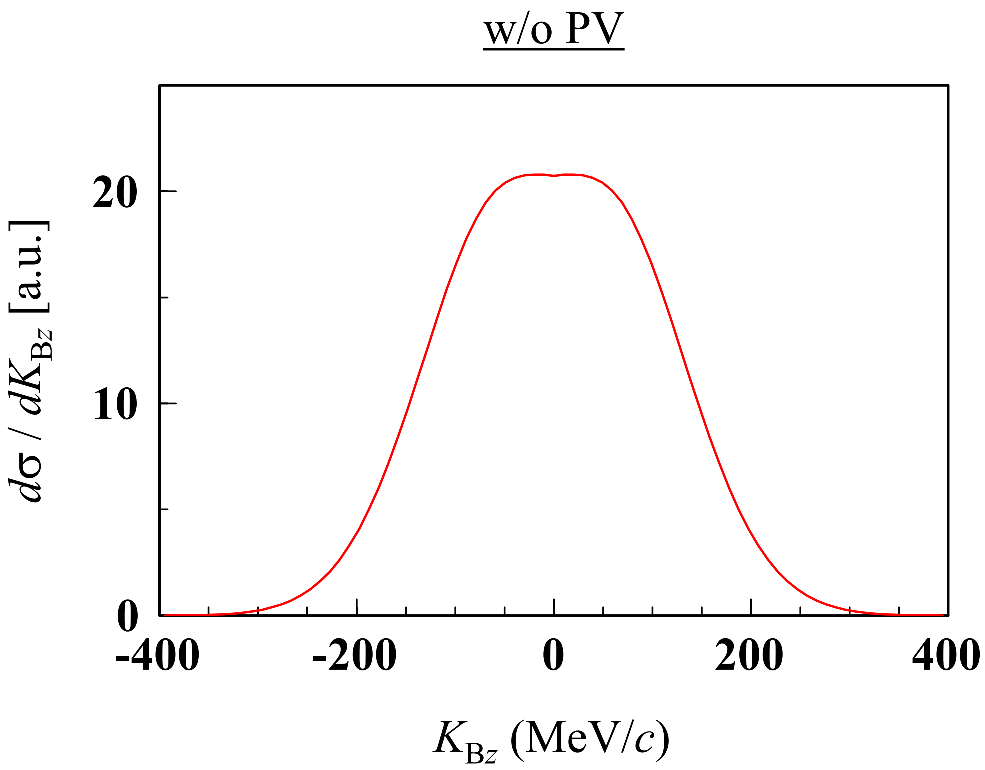

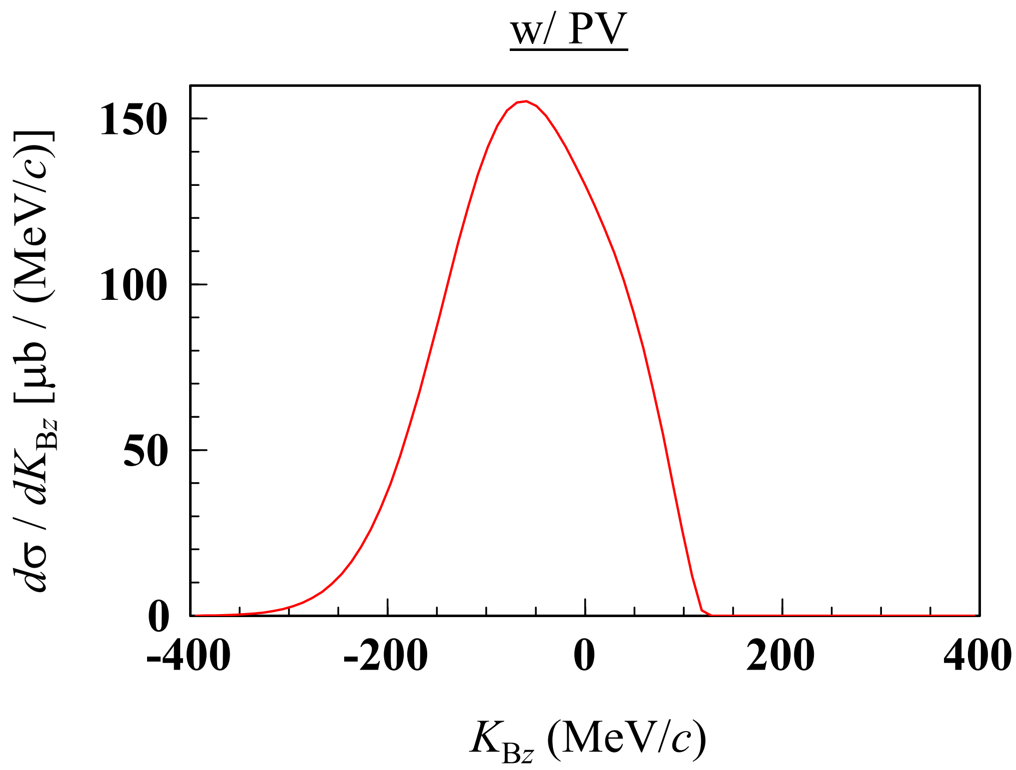

- ✓ The PV effect gives a cut on the high-mom side.
- ✓ This effect becomes large at low energies and/or for deeply bound nucleons.

KO, K. Yoshida, K. Minomo, PRC 92, 034615 (2015).

Attractive distortion effect

A-frame (A is at rest)

KO, K. Yoshida, K. Minomo, PRC 92, 034615 (2015).

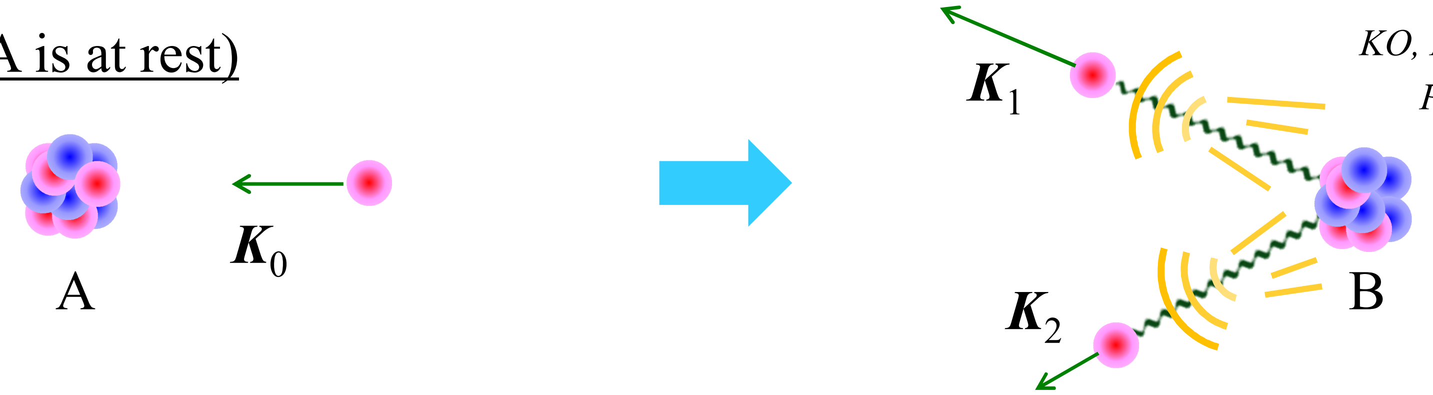

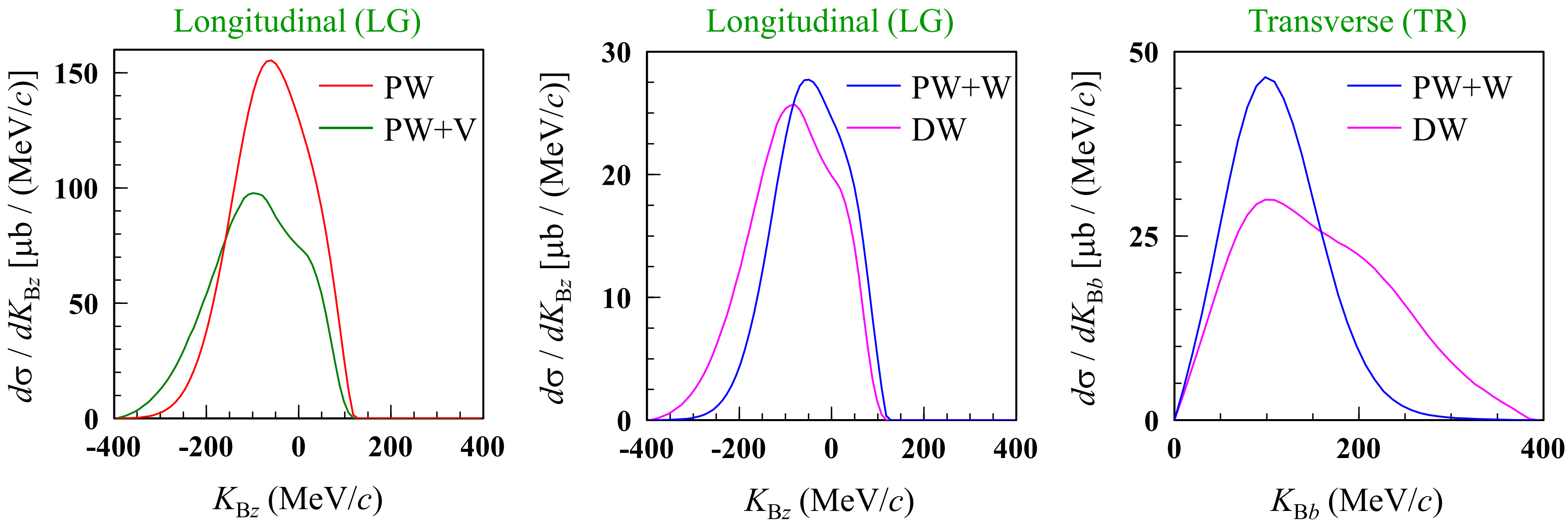

Input for checking the attractive distortion effect

sample4.cnt

```
  **** ppN control data ****
  10:unknown ::./tbl_12Cp2p11Bgs_MD100.dat
  11:old     ::./FLtbl_rede.dat
  12:old     ::./EDAD1p12C@100_e.dat
  13:old     ::./EDAD1p11B_e.dat
  14:unknown ::./LG_12Cp2p11Bgs_MD100.dat
  15:unknown ::./PX_12Cp2p11Bgs_MD100.dat
  16:unknown ::./TR_12Cp2p11Bgs_MD100.dat
  17:unknown ::./TL_12Cp2p11Bgs_MD100.dat
  06:unknown ::./12Cp2p11Bgs_MD100.outlist
 999:
---- INPUT ----
12C(p,2p)11B_gs@100MeV DWIA MD ielm=0
1000 0    2    0    1                                  LIMFS IONS IFRM IMIR ICAL
1.00 1.007825 6.0  12.00                               ZP AP ZA AA
1    100.0       0                                     IKIN ELAB ICTREIN
1    15.96       1.0  1.007825  0.85     1             ISH EBIND ZSP ASP BETASP ICTRM
1.5  1.0  1.77        0                                FJ FL SFAC NOD
0    1.35        1    0.65      1.35     1             IBMC RC ICTRC AOC RCL ICTRCL
0    8.2         1.35      1    0.65                   IBMS VOLS RS ICTRS AS
30   30   30                                           LMAX0 LMAX1 LMAX2
9    0    2.00   1    1                                IVAR IEX FKNCUT IXUNT KUNT
1    -2.0        2.0       0.05                        IVVAR VARMIN VARMAX DVAR
1    0.0         2.0       0.05                        IVTHX THXMIN THXMAX DTHX
0    0.0         40.0      10.0                        IVPHX PHXMIN PHXMAX DPHX
0    0.0         180.0     0.5                         IVTH2 TH2MIN TH2MAX DTH2
0    180.0       360.0     10.0                        IVPH2 PH2MIN PH2MAX DPH2
10   6    0      14   15   16   17                     KIB: TBL OUT TMD LG PX TR TL
0    11   1      0    1                                IELM KIBELM IONSH KINELM IELMEDG
15.0      0.1         30   30   40   15   15           RMAX DR NG24-B,TH,PH,K1,PH1Q
12   1.00 1.00 1.00 1.00 -0.85    0    1               0: IPOT FV FW FVS FWS BET MS EDG
13   1.00 1.00 1.00 1.00 -0.85    0    1               1: IPOT FV FW FVS FWS BET MS EDG
13   1.00 1.00 1.00 1.00 -0.85    0    1               2: IPOT FV FW FVS FWS BET MS EDG
```

Incident energy is 100 MeV (/u)

Distorted waves are calculated with orbital ang. mom. *L* up to 30.

A very simplified *NN* cross section is used by setting IELM=0

Now you need a *p*-^{12}C potential at 100 MeV, which can be downloaded from the web.

Change these values if you want to control real and imaginary parts of optical potentials

Attractive distortion effect

HW: Draw the figures below. Note that the DWIA calculations on the MD with the current setting take time; on RCNP HPCI (miho), it takes roughly two hours.

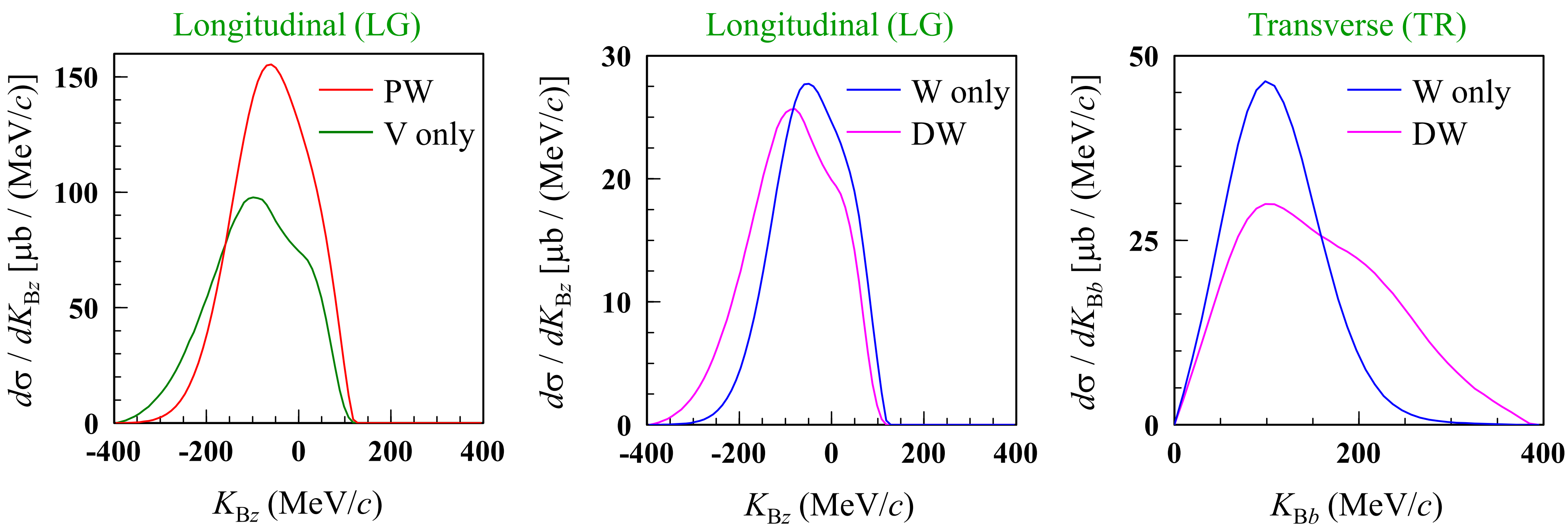

MD of EB in the Glauber model

K. Hencken, Bertsch, and Esbensen, PRC 54, 3043 (1996).

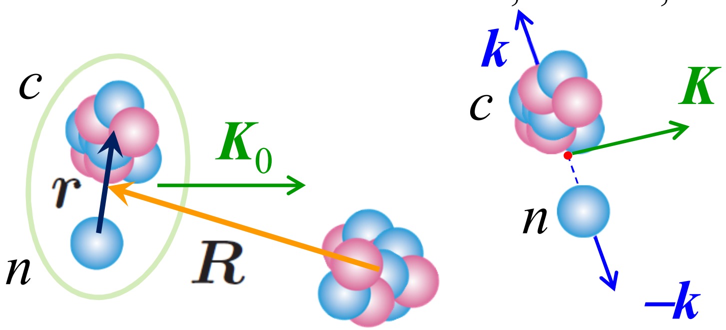

$$\boldsymbol{K} \approx \boldsymbol{K}_0 + K_\perp \boldsymbol{e}_\perp$$

(AD + forward scattering approximation)

$$\frac{d\sigma_{\rm diff}}{(d^2\vec{K}_\perp d^3\vec{k})} = \frac{1}{(2\pi)^5}\frac{1}{2L_0+1}\sum_{M_0}\left|\int d^3\vec{r}d^2\vec{R}_\perp e^{-i\vec{K}_\perp\cdot\vec{R}_\perp}\phi^*_{\vec{k}}(\vec{r})S_cS_n\phi_{0,M_0}(\vec{r})\right|^2.$$

- Taking a Jacobi representation results in the simplest form of the PV.
- small ω-q is assumed, with neglecting the E-conservation.

Integration over $\boldsymbol{K}_\perp$ in the whole region

$$\frac{d\sigma_{\rm diff}}{d^3\vec{k}} = \frac{1}{(2\pi)^3}\frac{1}{2L_0+1}\sum_{M_0}\int d^2\vec{R}_\perp\left|\int d^3\vec{r}\phi^*_{\vec{k}}(\vec{r})S_cS_n\phi_{0,M_0}(\vec{r})\right|^2.$$

- MD in the A-frame if the mom. of the c-n c.m. is 0.

Application of DWIA to SEASTAR data analysis

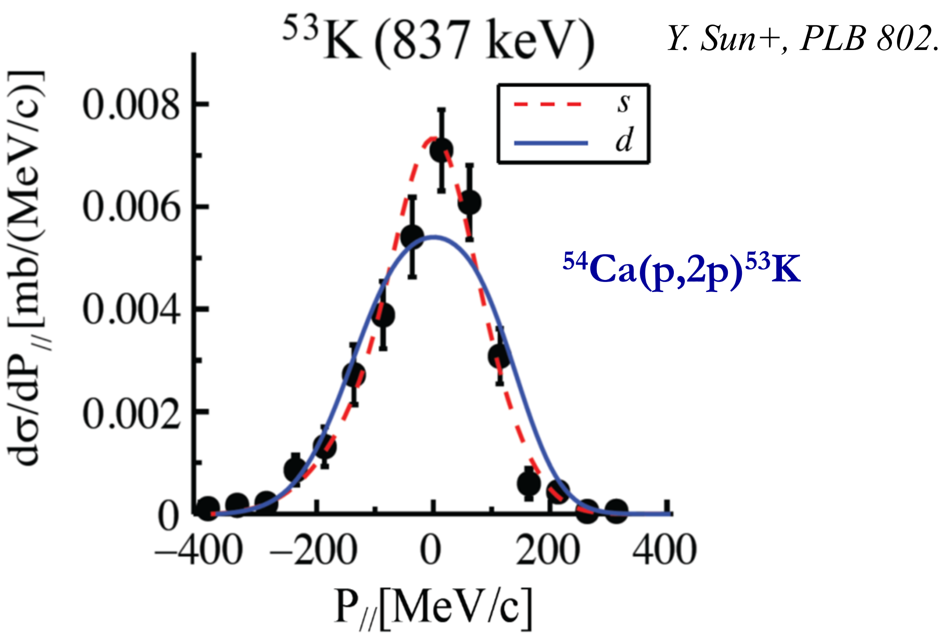

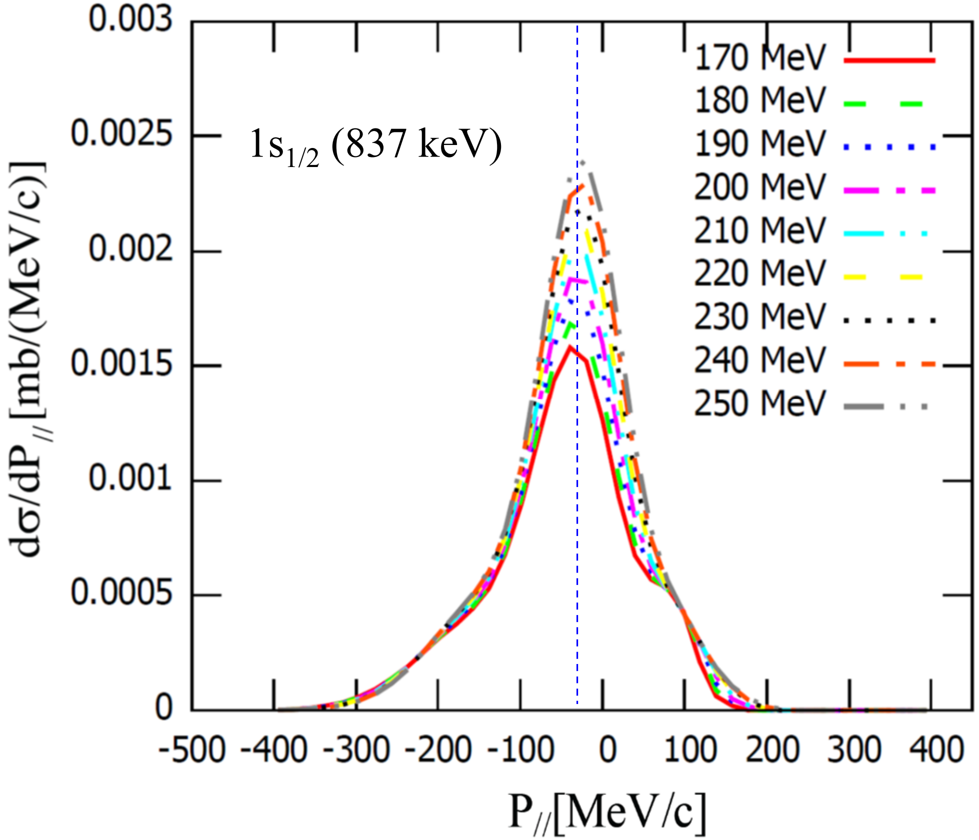

^{80}Zn(p,2p)^{79}Cu: L. Olivier+, PRL 119.

^{77}Cu(p,2p)^{76}Ni: Z. Elekes+, PRC 99.

^{79}Cu(p,2p)^{78}Ni: R. Taniuchi+, Nature 569.

^{54}Ca(p,pn)^{53}Ca: S. Chen+, PRL 123.

^{54,52}Ca(p,2p)^{53,51}K: Y. Sun+, PLB 802.

^{63}V(p,2p)^{62}Ti: M. L. Cortés+, PLB 800.

^{70,72,74}Ni(p,2p)^{69,71,73}Co: T. Lokotko+. PRC 101.

and more …

DWIA analysis of RIBF/RCNP data

S. Kawase+, PTEP 2018, 021D01 (2018).

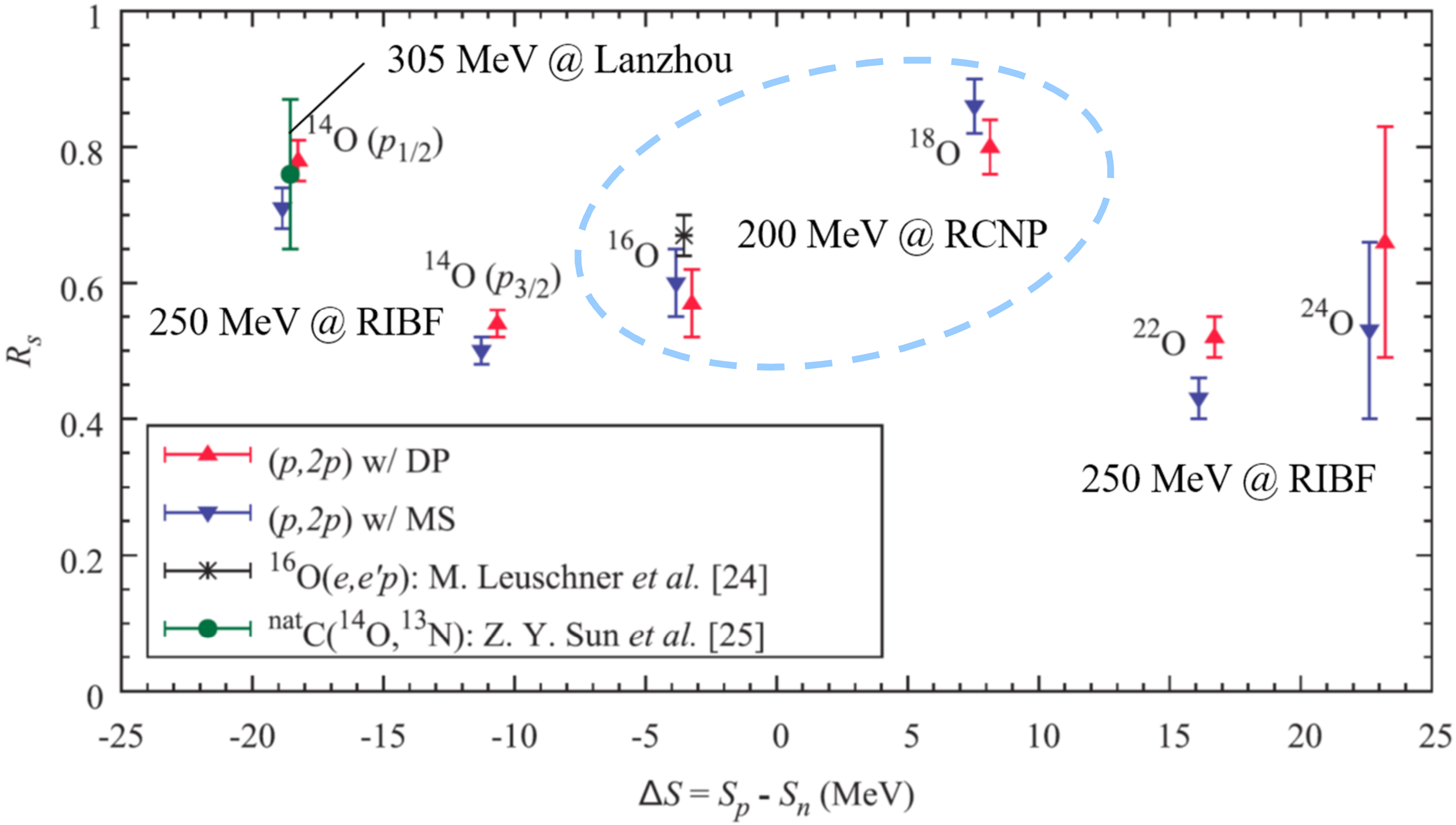

$$\sigma_{p2p} = \frac{1}{2}\int \left(\frac{d^3\sigma}{dE_1 d\Omega_1 d\Omega_2}\right) dE_1 d\Omega_1 d\Omega_2$$

with $T > 30$ MeV, 20 deg. $< \theta <$ 65 deg., and $|\phi| <$ 15 deg.

A puzzle

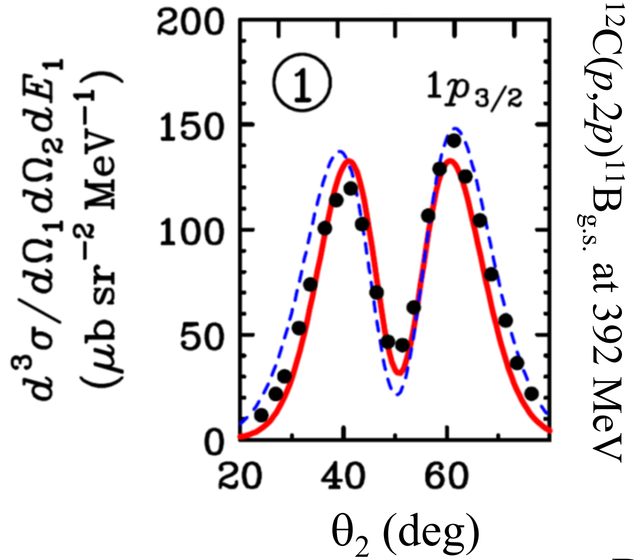

$$\sigma_{p2p} = \frac{1}{2}\int \left(\frac{d^3\sigma}{dE_1 d\Omega_1 d\Omega_2}\right) dE_1 d\Omega_1 d\Omega_2$$

DWIA triple-differential cross sections (TDX), are integrated over E_1, Ω_1, and Ω_2, and compared with the GSI data.

V. Panin+, PLB 753, 204 (2016).

Pikoe for the GSI data

	DWIA	local	w/o Moller	local + w/o Moller	PLB757 (GSI)	PPNP96 (RCNP)	(e,e'p)
$3/2^-$ g.s.	3.36	2.94	2.68	2.33	2.11	1.82(3)	1.72(11)
$1/2^-$ 2.13 MeV	0.34	0.31	0.27	0.25	0.26	0.30(2)	0.26(2)
$3/2^-$ 5.02 MeV	0.32	0.28	0.25	0.21	0.21	0.23(3)	0.20(2)

A puzzle

$$\sigma_{p2p} = \frac{1}{2} \int \left(\frac{d^3\sigma}{dE_1 d\Omega_1 d\Omega_2} \right) dE_1 d\Omega_1 d\Omega_2$$

DWIA triple-differential cross sections (TDX), are integrated over E_1, Ω_1, and Ω_2, and compared with the GSI data.

HW: Try to get these numbers.

V. Panin+, PLB 753, 204 (2016).

Pikoe for the GSI data

	DWIA	**local**	**w/o Moller**	**local + w/o Moller**	**PLB757 (GSI)**	**PPNP96 (RCNP)**	**(e,e'p)**
$3/2^-$ g.s.	3.36	2.94	2.68	2.33	2.11	1.82(3)	1.72(11)
$1/2^-$ 2.13 MeV	0.34	0.31	0.27	0.25	0.26	0.30(2)	0.26(2)
$3/2^-$ 5.02 MeV	0.32	0.28	0.25	0.21	0.21	0.23(3)	0.20(2)

Plan of this talk (2/2)

4) Some theoretical achievements (for future)

K. Yoshida, M. Goméz-Ramos, KO, and A. M. Moro, PRC 97, 024608 (2018).

4-1. Microscopic optical potential

4-2. Benchmark study on ^{15}C(p,pn) with DWIA, TC, and Faddeev,-AGS.

5) Divergence of the TDX in inverse kinematics

KO+, in preparation.

5-1. Two-value feature of the kinematics and divergence of PV

5-2. When occurs?

6) Some recent/ongoing KO reaction studies around RCNP/RIBF

6-1. ^2n correlation study via (p,pn)

6-2. α KO reactions

6-3. deuteron KO reactions

…

7) Summary

From phenomenology to microscopic theory

TABLE I. Optical-Model Parameters Neutrons

NUCLIDE	ENERGY	REAL POTENTIAL			VOL.IMAG. POTENTIAL			SURF.IMAG. POTENTIAL			SPIN-ORBIT POTENTIAL			ST	SR	FIT	NOTE	REF.
	(MEV)	V	R	A	W	RW	AW	WD	RD	AD	VSO	RSO	ASO					
AL	1.	40.	1.25*	0.65*				5.0G*	1.25*	0.98*	10.*	1.25*	0.65*	3520	1340	S3	15	GIL63
AL	1.5	47.4	1.25*	0.46				6.3G	1.25*	0.98*	10.*	1.25*	0.46	3204		S1	10	KOR68
AL	2.47	48.0	1.14	0.65				8.42	1.19	0.48*	8.0*	1.14	0.65	2530	1270	S2	2	HOL71
AL	3.00	47.9	1.13	0.72				7.35	1.08	0.48*	8.0*	1.13	0.72	2520	1250	S2	2	HOL71
AL	3.49	48.7	1.18	0.61				8.46	1.29	0.48*	8.0*	1.18	0.61	2360	1130	S1	2	HOL71
AL	4.00	49.1	1.20	0.62				7.99	1.26	0.48*	8.0*	1.20	0.62	2290	1090	S2	2	HOL71
AL	4.56	50.2	1.18	0.59				8.38	1.26	0.48*	8.0*	1.18	0.59	2060	1020	S1	2	HOL71
AL	6.09	47.8	1.20	0.67				8.23	1.23	0.48*	8.0*	1.20	0.67	1880	1070	S3	2	HOL71
AL	7.	45.5	1.25*	0.65*				9.5G	1.25*	0.98*	8.6	1.25*	0.65*			X3		BJO58
AL	7.05	49.1	1.20	0.68				7.90	1.20	0.48*	8.0*	1.20	0.68	1800	1040	S2	2	HOL71
AL	7.97	49.4	1.20	0.69				12.1	1.30	0.41	9.8	1.20	0.69			S1	2	BRA72

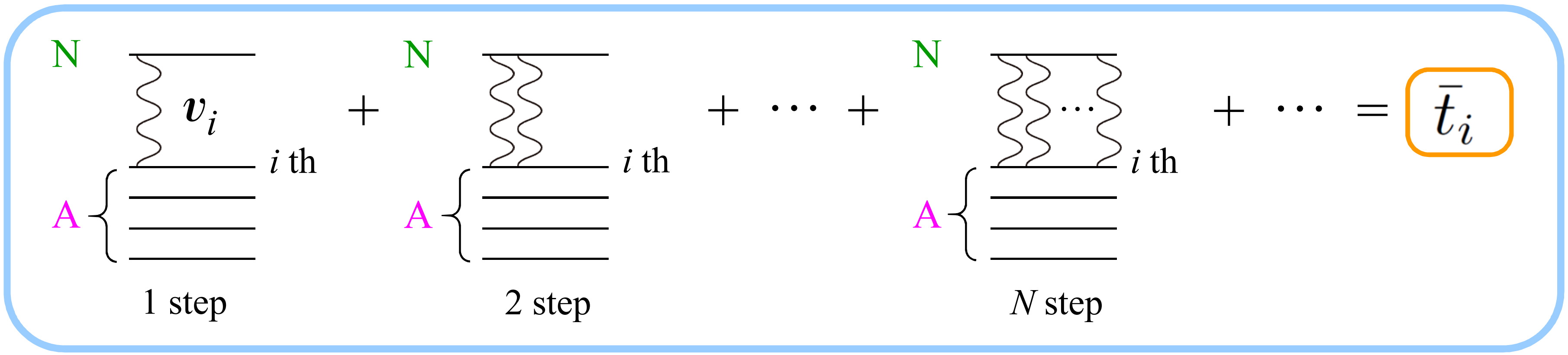

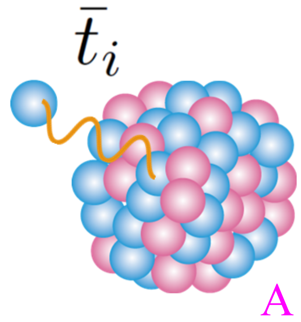

Multiple scattering theory (MST)

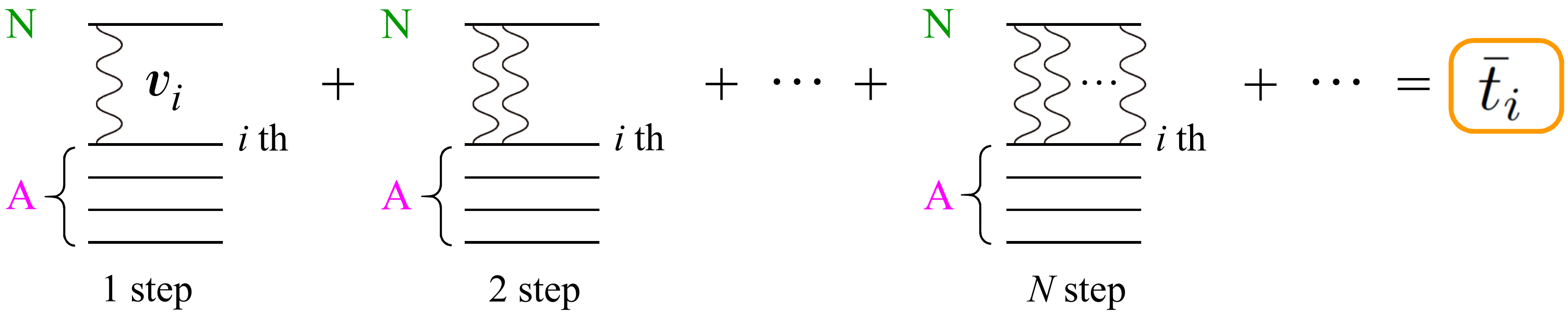

$$\left(T_{\mathrm{NA}} + \sum_i v_i + H_{\mathrm{A}} - E\right)\Psi = 0 \xrightarrow{\textit{Resummation}} \left(T_{\mathrm{NA}} + \sum_i \bar{t}_i + H_{\mathrm{A}} - E\right)\bar{\Psi} = 0$$

(for all boundary conditions) (for a specific b. c.)

$$\bar{t}_i = \frac{A-1}{A} t_i, \quad t_i = v_i + v_i G_0^{(+)} t_i$$

L. L. Foldy, Phys. Rev. ***67****, 107 (1945); K. M. Watson, Phys. Rev.* ***89****, 115 (1953).*

A. K. Kerman, H. McManus, and R. M. Thaler, Ann. Phys. (NY) ***8****, 551 (1959).*

Extension to nucleus-nucleus scattering $\longrightarrow$ *M. Yahiro, K. Minomo, KO, and M. Kawai, PTP* ***120****, 767 (2008).*

The folding model potential based on the MST

An “expectation value” of a nucleon-nucleon (*NN*) effective interaction

$t_i\left(|\boldsymbol{r}-\boldsymbol{r}_{\mathrm{T}}|\right)$ *NN* *t*-matrix (or *g*-matrix)

$$t_i = v_i + v_i G_0^{(+)} t_i$$

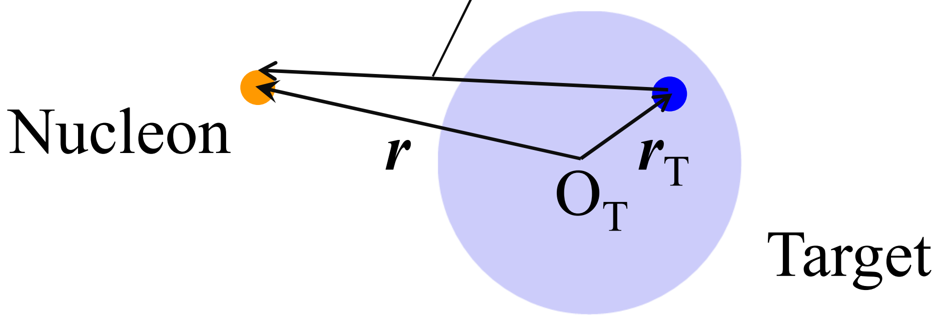

$$\boxed{U\left(\boldsymbol{r}\right) = \int v_{\mathrm{eff}}\left(|\boldsymbol{r}-\boldsymbol{r}_{\mathrm{T}}|\right)\rho_{\mathrm{T}}\left(\boldsymbol{r}_{\mathrm{T}}\right)d\boldsymbol{r}_{\mathrm{T}}}$$

one-body density

Microscopic description of nucleon-nucleus scattering

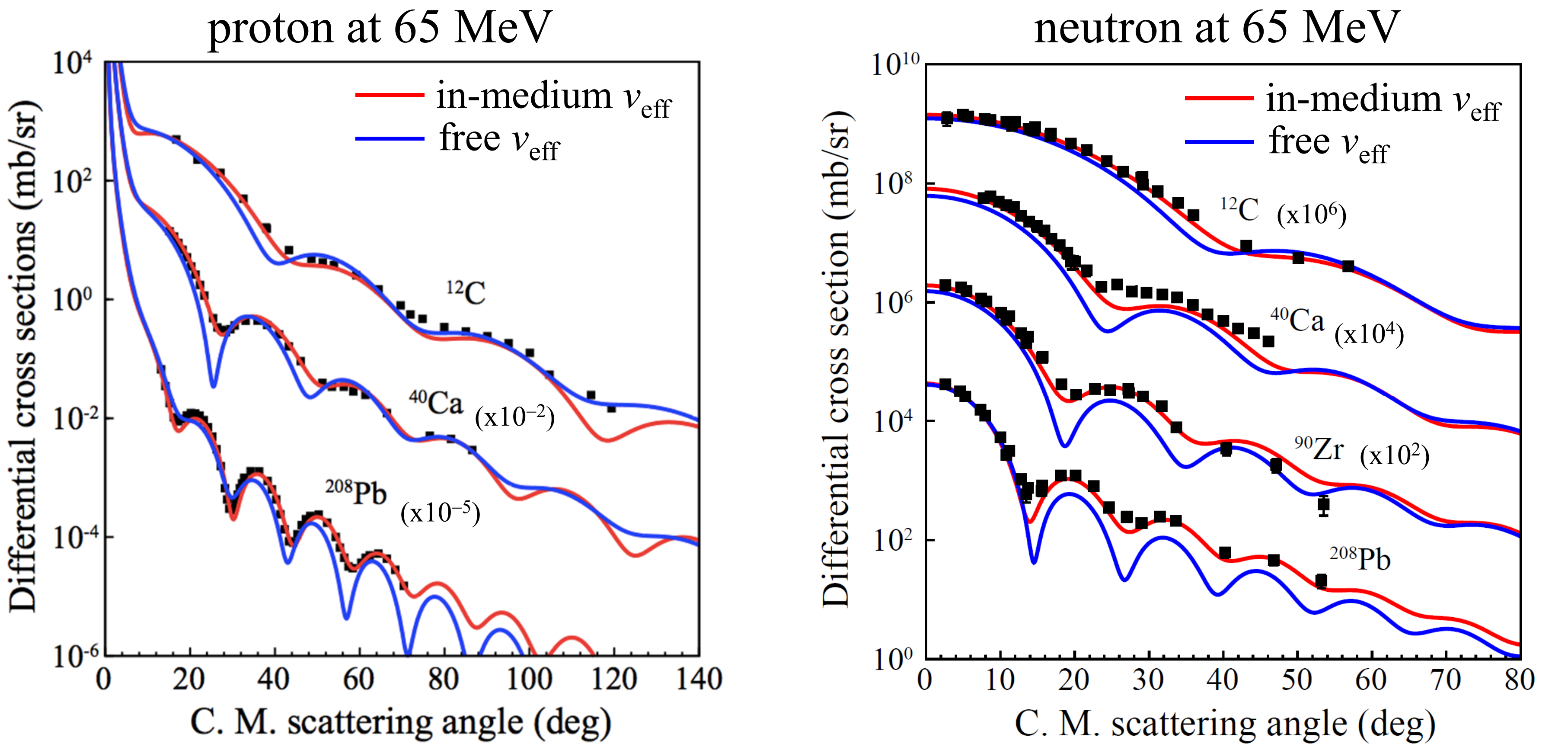

No free parameter ("prediction")

cf. K. Amos+, Adv. Nucl. Phys. ***25****, 275 (2000).*
T. Furumoto+, PRC ***78****, 044610 (2008).*
M. Toyokawa+, PRC ***92****, 024618 (2015).*

Benchmark with Transfer to the Continuum model

*K. Yoshida, M. Goméz-Ramos, KO, and A. M. Moro, PRC**97**, 024608 (2018).*

$^{15}C(p,pn)^{14}C_{g.s.}$ at 420 MeV/u

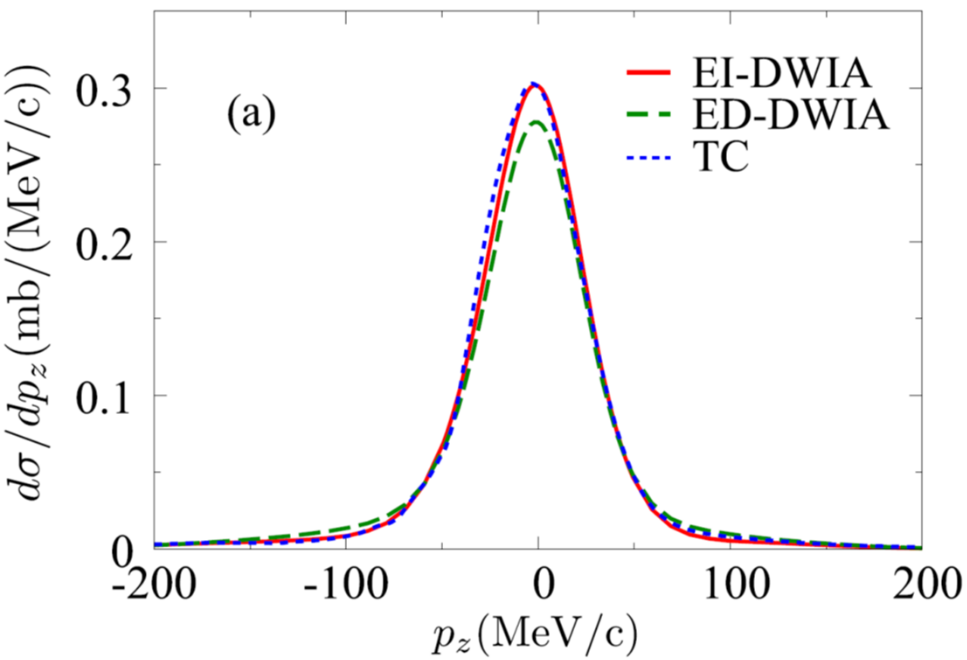

$^{15}C(p,pn)^{14}C_{g.s.}$ at 420 MeV/u

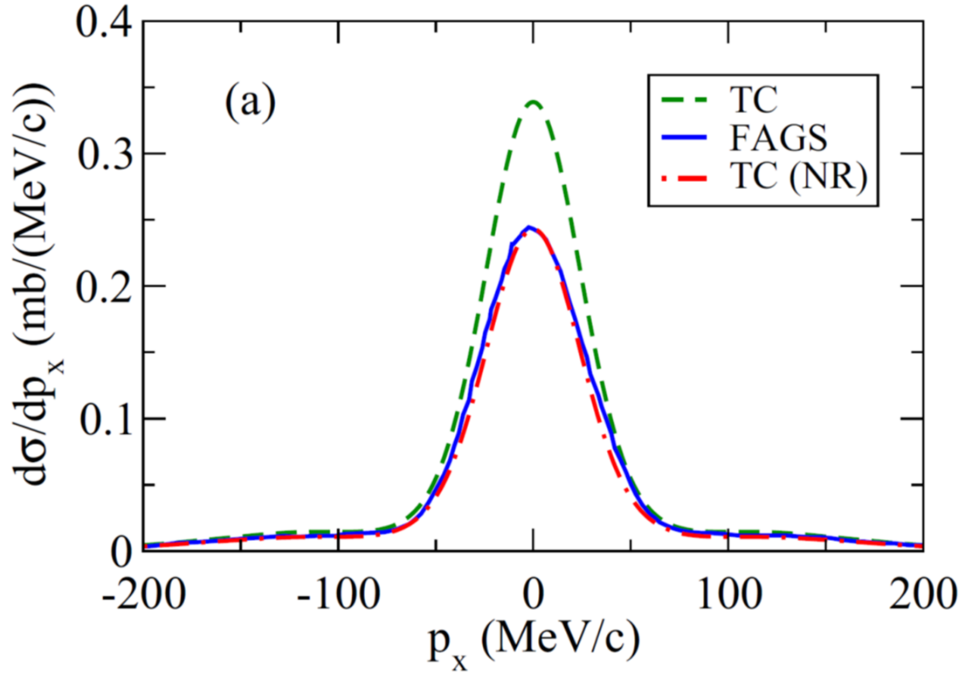

- ✓ TC justifies the impulse approximation (use of t_{NN}, with choosing *NN* kinematics according to the two asymptotic nucleon momenta and including the Møller factor)
- ✓ DWIA justifies fixing the optical potentials of outgoing nucleons at one energy.

DWIA vs. Faddeev-AGS

R. Crespo+, PRC77, 024601 (2008); PRC90, 044606 (2014).

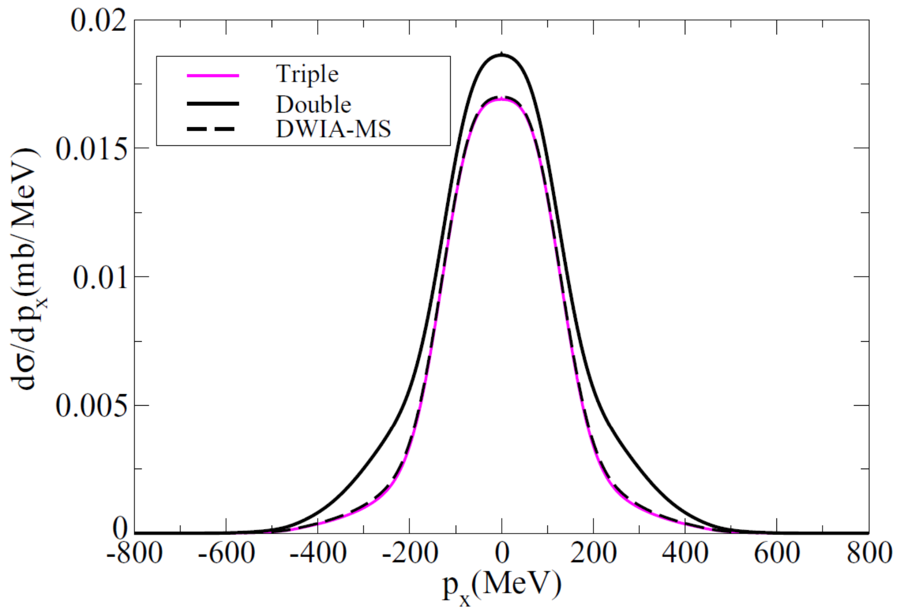

FIG. 8. (Color online) ^{11}B core transverse momentum distribution for the ^{12}C$(p,2p)^{11}$B reaction at 400 MeV/u The curves represent the observable calculated to second and third orders in the multiple scattering expansion using all the Faddeev-AGS terms and with a truncated series as in the DWIA reaction approach.

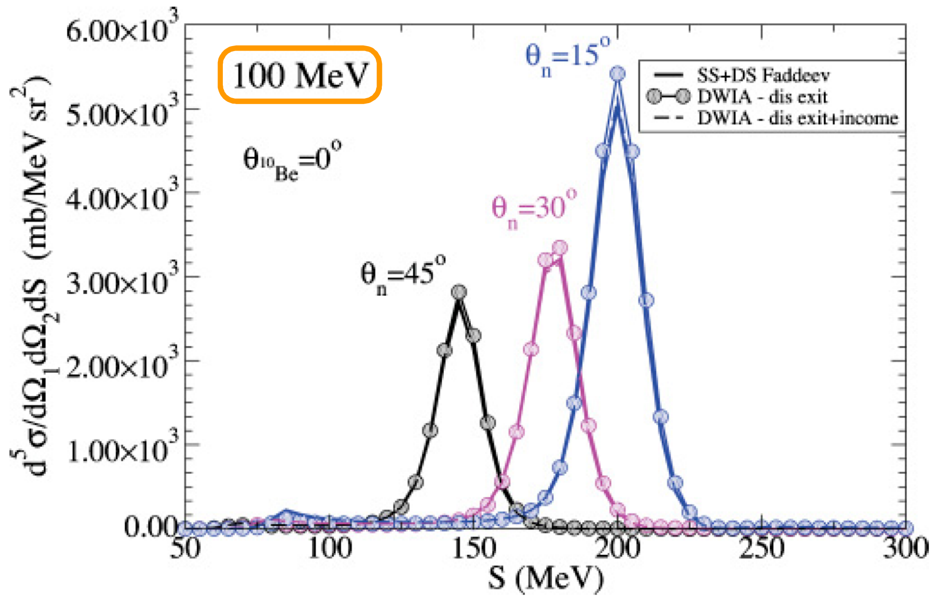

FIG. 15. (Color online) Cross section for the breakup ^{11}Be(p,pn) at 100 MeV.

Plan of this talk (2/2)

4) Some theoretical achievements (for future)

K. Yoshida, M. Goméz-Ramos, KO, and A. M. Moro, PRC 97, 024608 (2018).

4-1. Microscopic optical potential

4-2. Benchmark study on ^{15}C(p,pn) with DWIA, TC, and Faddeev,-AGS.

5) Divergence of the TDX in inverse kinematics

KO+, in preparation.

5-1. Two-value feature of the kinematics and divergence of PV

5-2. When occurs?

6) Some recent/ongoing KO reaction studies around RCNP/RIBF

6-1. ^2n correlation study via (p,pn)

6-2. α KO reactions

6-3. deuteron KO reactions

…

7) Summary

^{12}C(p,2p)^{11}B$_{\mathrm{g.s.}}$ at 392 MeV/u

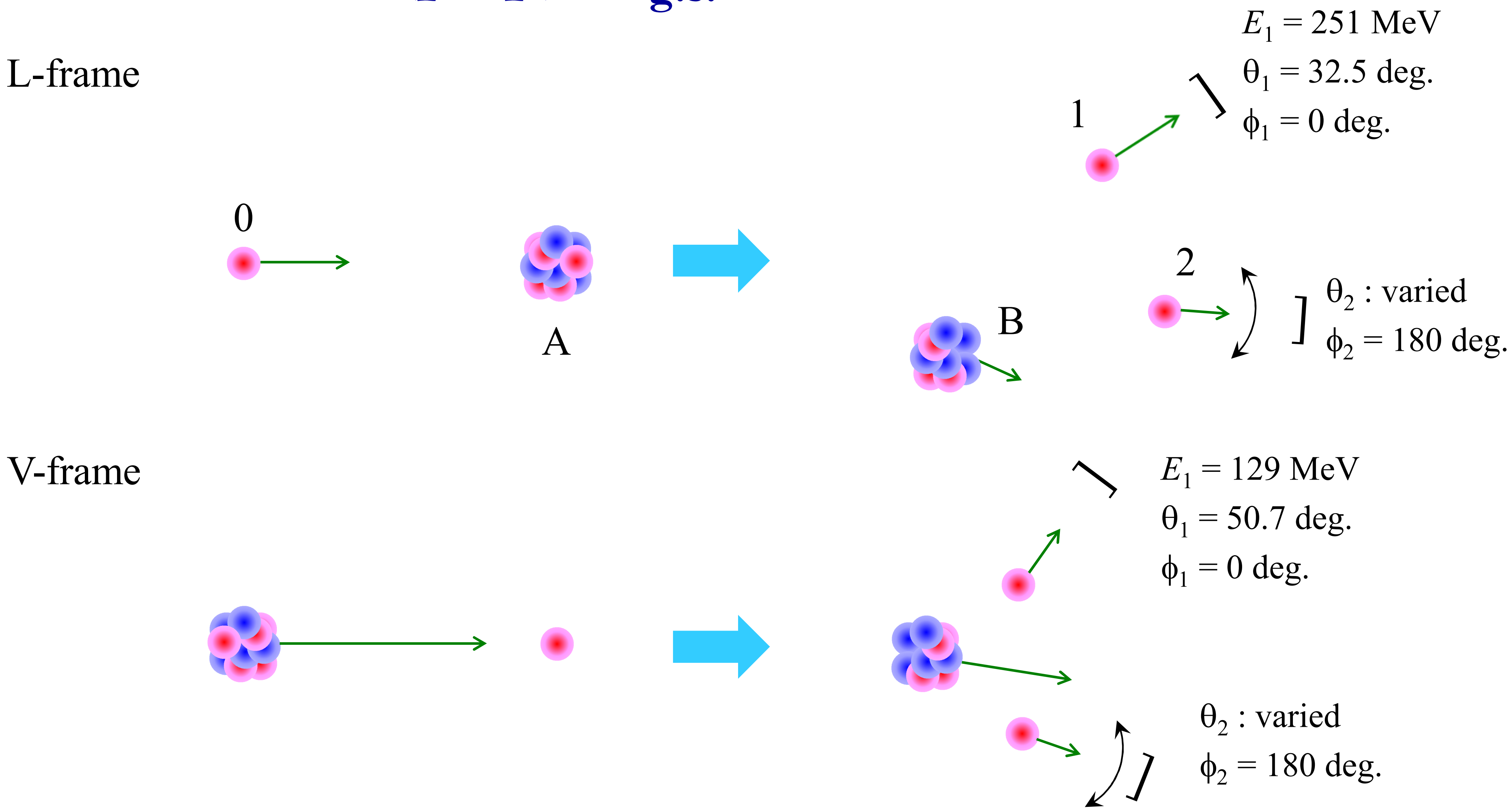

$^{12}C(p,2p)^{11}B_{g.s.}$ at 392 MeV/u (PWIA)

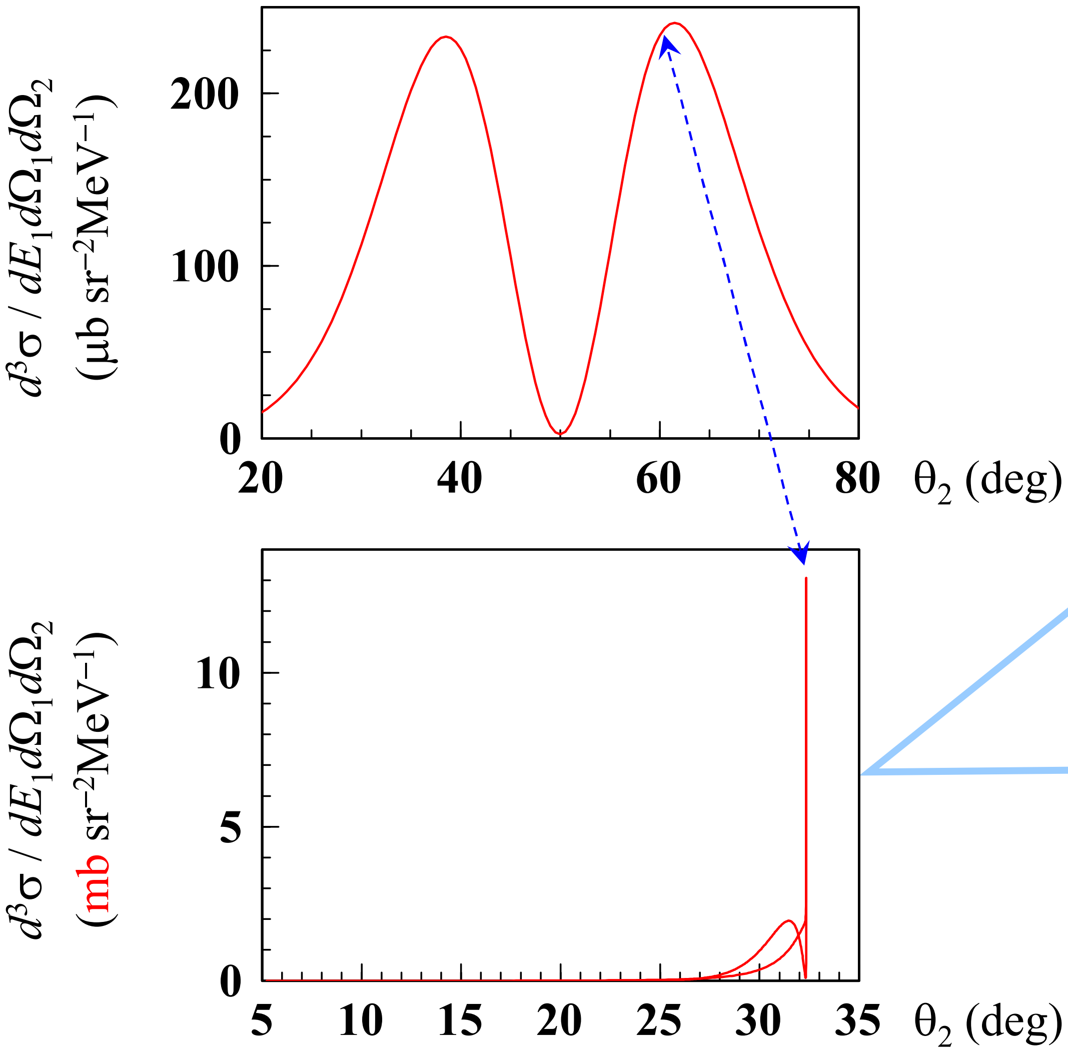

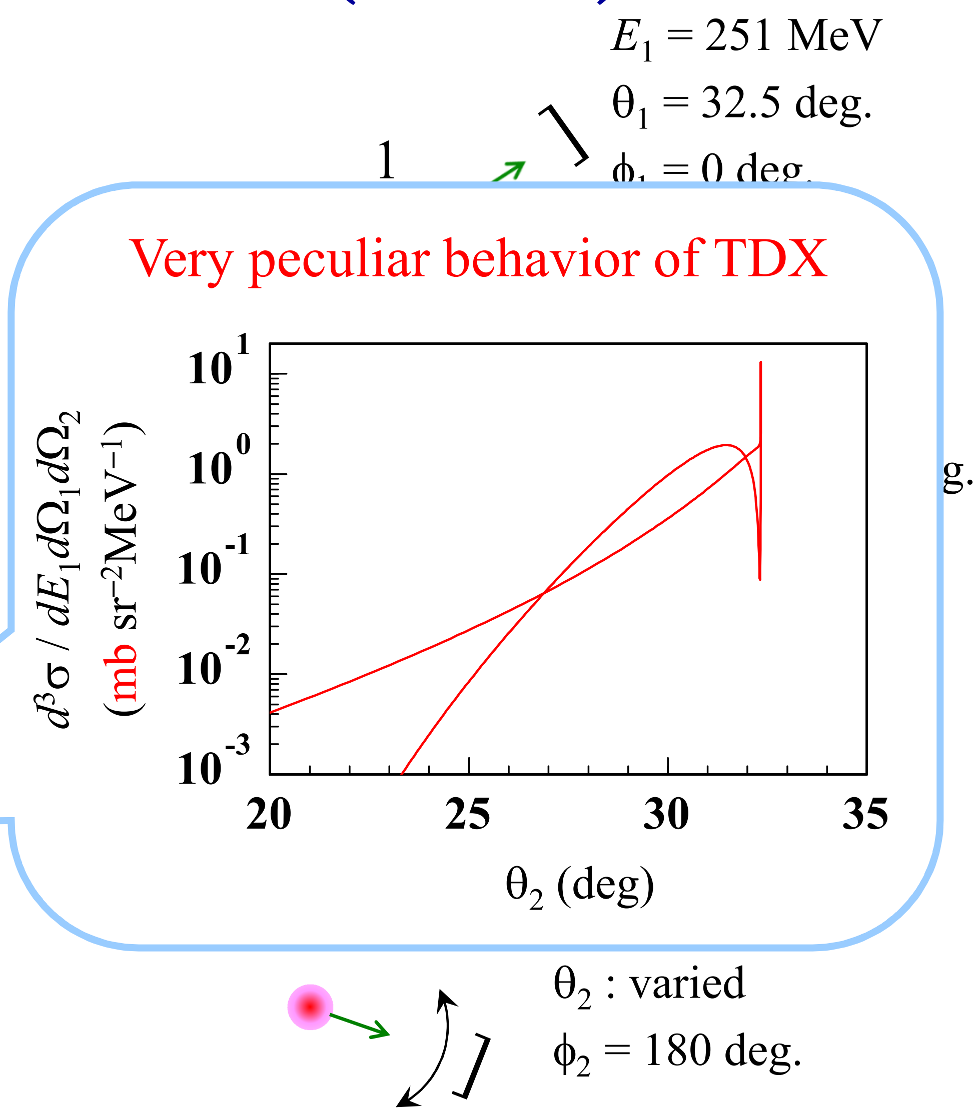

Input for TDX calc. of ^{12}C(p,2p) in inv. kin.

sample5.cnt

output in the V-frame

The direction of the z-axis is inverted.

When you investigate the correspondence between the forward and inverse kinematics, we recommend to use ICTREIN=1.

Usually it is better to use a smaller step size of θ in inverse kinematics.

```
  **** ppN control data ****
  10:unknown ::./tbl_12Cp2p11Bgs_set1_cs_PWi.dat
  11:old     ::./FLtbl_rede.dat
  06:unknown ::./12Cp2p11Bgs_set1_cs_PWi.outlist
 999:
---- INPUT ----
12C(p,2p)11B_gs@392MeV set1 PWIA cs inv
1000 0    2    1    1                             LIMFS IONS IFRM IMIR ICAL
1.00 1.007825  6.0  12.00                         ZP AP ZA AA
0    392.0     1                                  IKIN ELAB ICTREIN
1    15.96     1.0  1.007825  0.85     1          ISH EBIND ZSP ASP BETASP ICTRM
1.5  1.0  1.00      0                             FJ FL SFAC NOD
0    1.35      1    0.65      1.35     1          IBMC RC ICTRC AOC RCL ICTRCL
0    8.2       1.35      1    0.65                IBMS VOLS RS ICTRS AS
60   60   60                                      LMAX0 LMAX1 LMAX2
1    0    2.00 1    1                             IVAR IEX FKNCUT IXUNT KUNT
0    251.0     255.0     10.0                     IVVAR VARMIN VARMAX DVAR
0    32.5      180.0     10.0                     IVTHX THXMIN THXMAX DTHX
0    0.0       40.0      10.0                     IVPHX PHXMIN PHXMAX DPHX
1    0.0       180.0     0.25                     IVTH2 TH2MIN TH2MAX DTH2
0    180.0     360.0     10.0                     IVPH2 PH2MIN PH2MAX DPH2
10   6    0    0    0    0    0                   KIB: TBL OUT TMD LG PX TR TL
3    11   1    0    1                             IELM KIBELM IONSH KINELM IELMEDG
15.0      0.1       30   30   40   0    0         RMAX DR NG24-B,TH,PH,K1,PH1Q
0    1.00 1.00 1.00 1.00 -0.85     0    1         0: IPOT FV FW FVS FWS BET MS EDG
0    1.00 1.00 1.00 1.00 -0.85     0    1         1: IPOT FV FW FVS FWS BET MS EDG
0    1.00 1.00 1.00 1.00 -0.85     0    1         2: IPOT FV FW FVS FWS BET MS EDG
```

HW: You can directly control the kinetic variables in inverse kinematics measurement by putting IKIN=1, IFRM=0, and IMIR=0. Reproduce the result in the lower panel on the previous slide in that way.

$^{12}C(p,2p)^{11}B_{g.s.}$ at 392 MeV/u

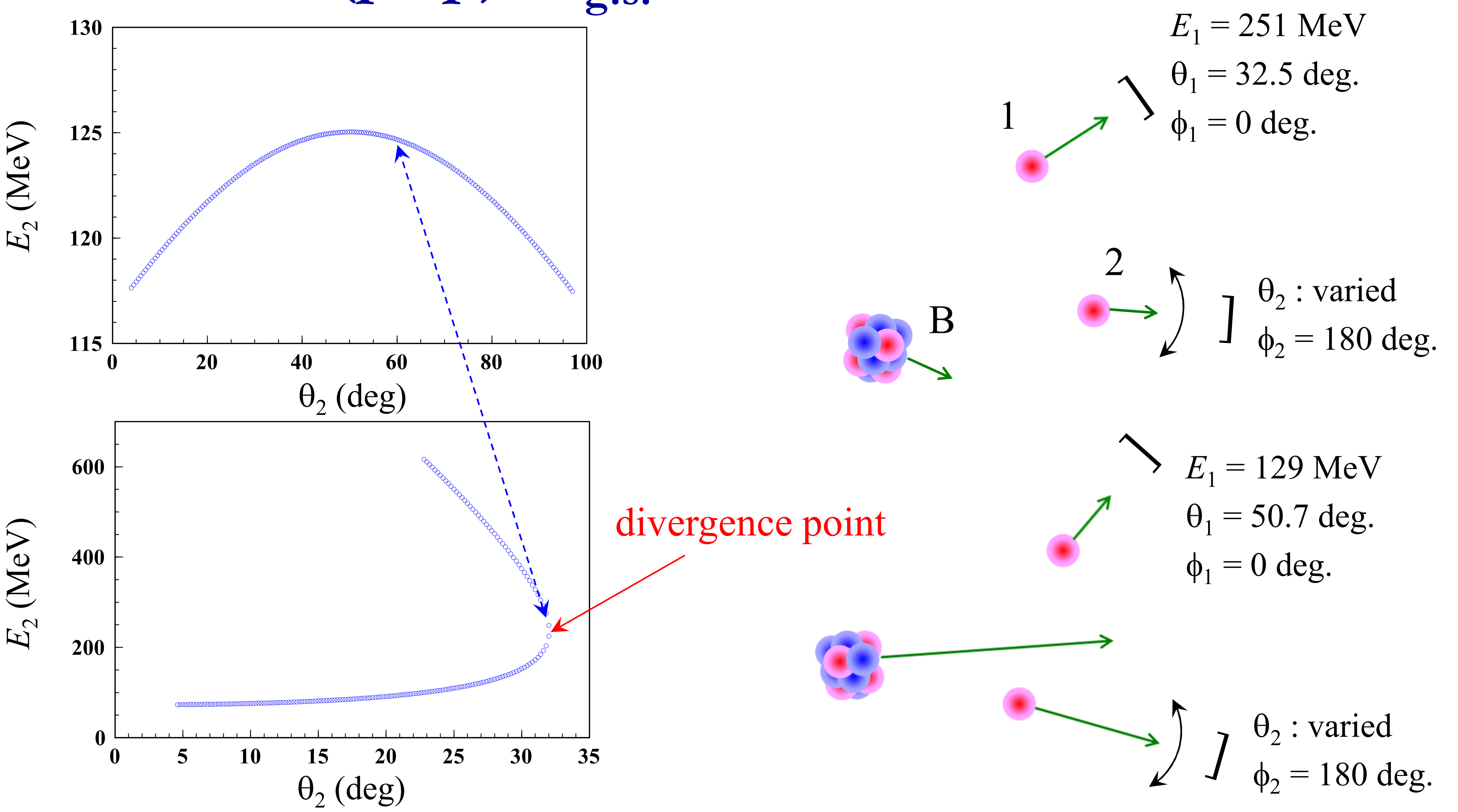

Plan of this talk (2/2)

4) Some theoretical achievements (for future)

K. Yoshida, M. Goméz-Ramos, KO, and A. M. Moro, PRC 97, 024608 (2018).

4-1. Microscopic optical potential

4-2. Benchmark study on ^{15}C(p,pn) with DWIA, TC, and Faddeev,-AGS.

5) Divergence of the TDX in inverse kinematics

KO+, in preparation.

5-1. Two-value feature of the kinematics and divergence of PV

5-2. When occurs?

6) Some recent/ongoing KO reaction studies around RCNP/RIBF

6-1. ^2n correlation study via (p,pn)

6-2. α KO reactions

6-3. deuteron KO reactions

…

7) Summary

$^{6}He(p,pn)$

Proving ^{2}n in ^{6}He via (p,pn) (in inverse kinematics)

Y. Kikuchi, KO, Y. Kubota, M. Sasano, and T. Uesaka, PTEP 2016, 103D03 (2016).

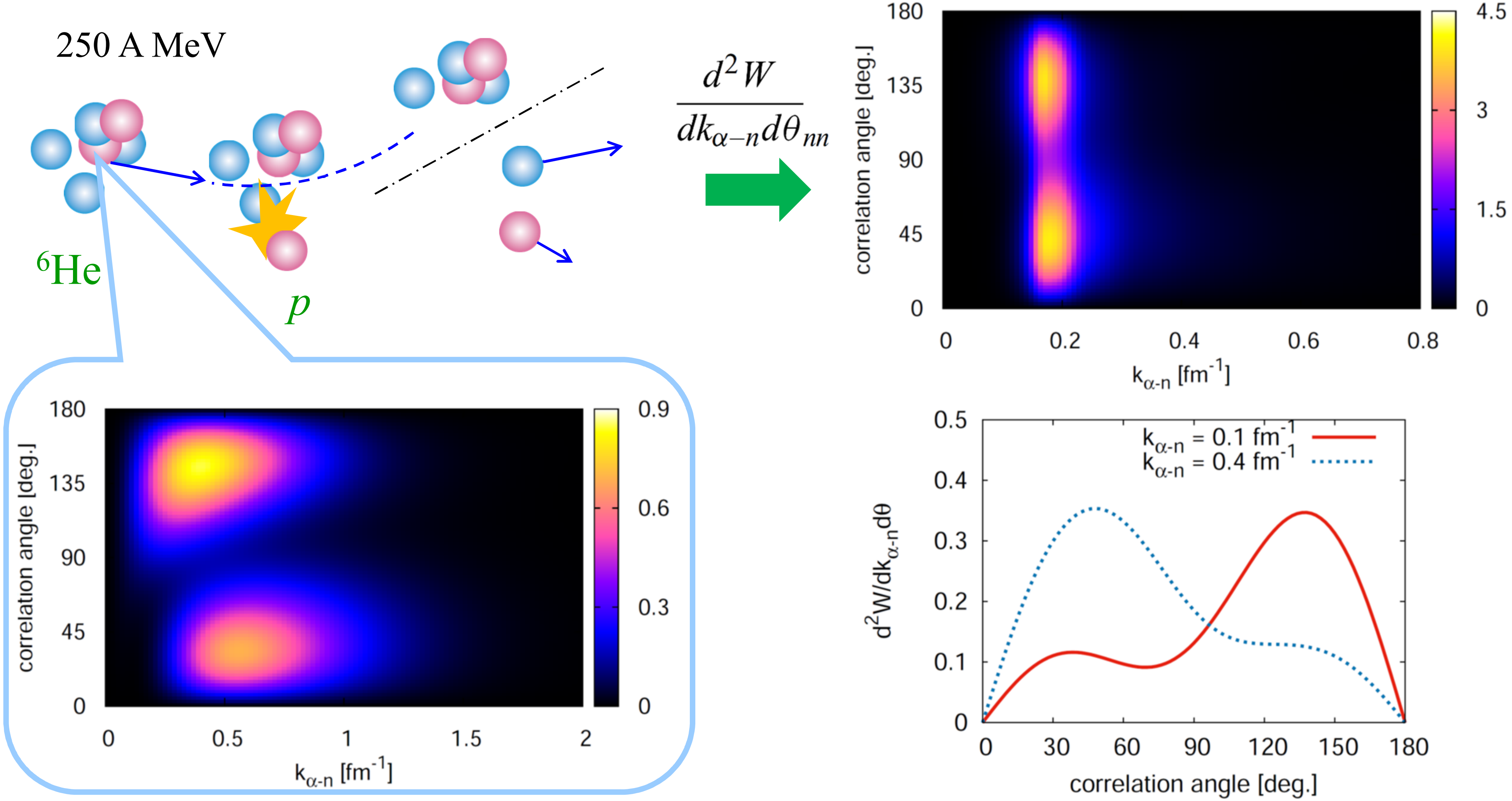

(p,pα)

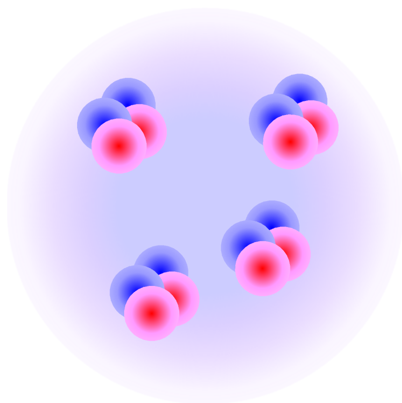

^{20}Ne(p,pα) at 101.5 MeV

K. Yoshida, Y. Chiba, M. Kimura, Y. Taniguchi, Y. Kanada-En'yo, and KO, PRC 100, 044601 (2019).

RWA obtained by AMD (20-body calculations)

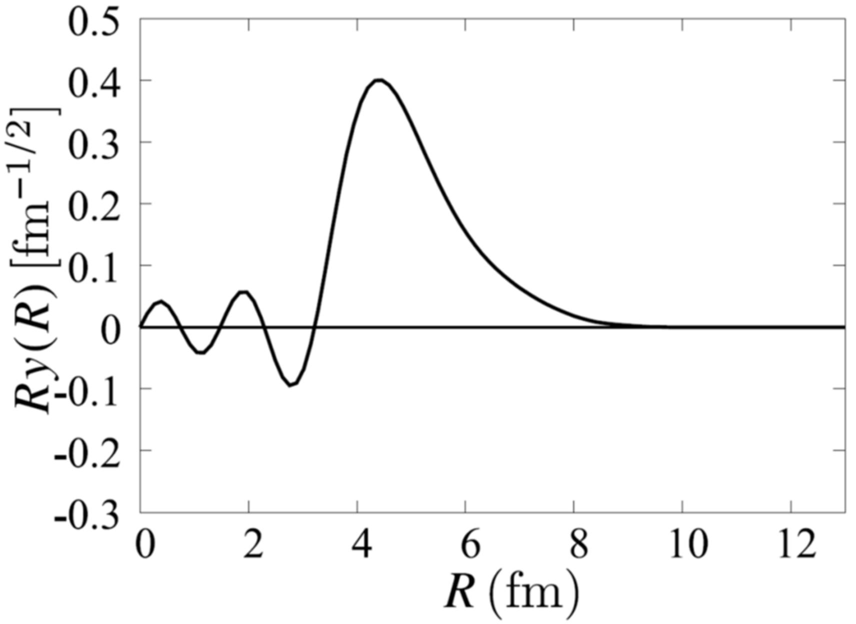

DWIA

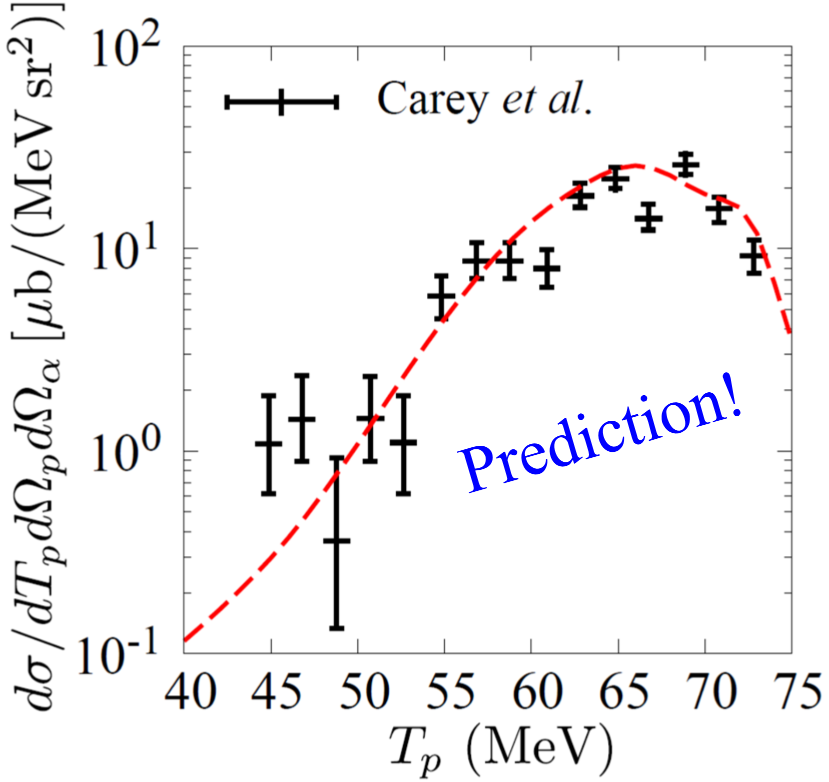

Other systems:

^{120}Sn(p,pα): K. Yoshida, K. Minomo, and KO, PRC 94, 044604 (2016).
^{10}Be(p,pα): M. Lyu, K. Yoshida, Y. Kanada-En'yo, and KO, PRC 97, 044612 (2018).
^{12}Be(p,pα): M. Lyu, K. Yoshida, Y. Kanada-En'yo, and KO, PRC 99, 064601 (2019).

(p,pd)

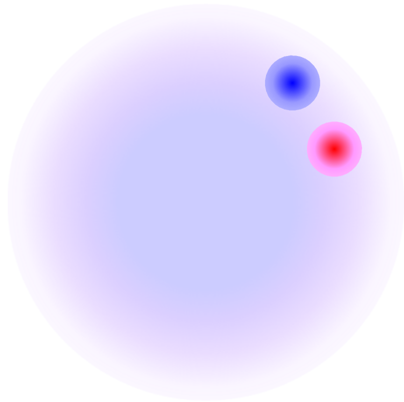

Experimental fact

*C. Samanta+, RRC **26**, 1379 (1982).*

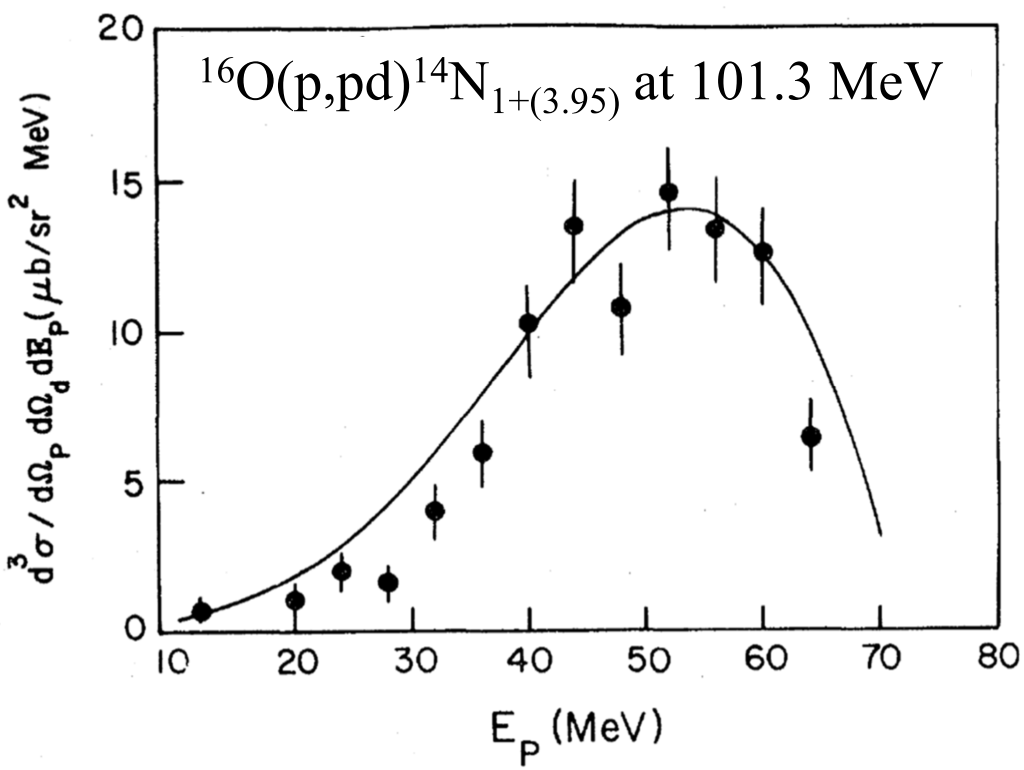

*C. Samanta+, RRC **34**, 1610 (1986).*

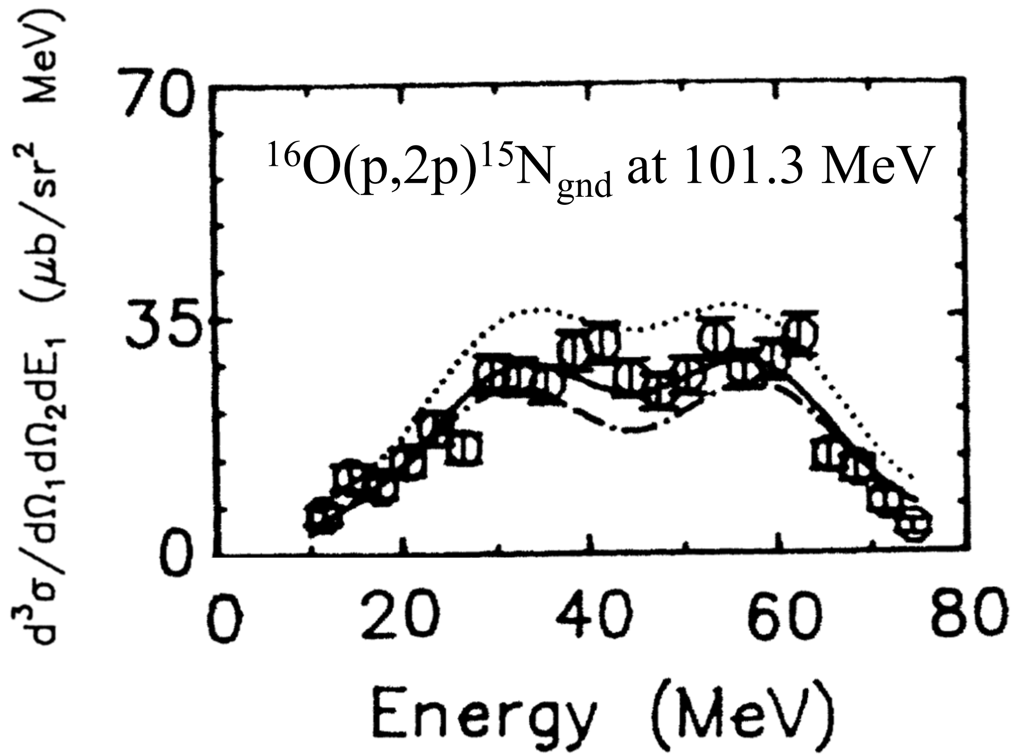

Remarks on pn knockout

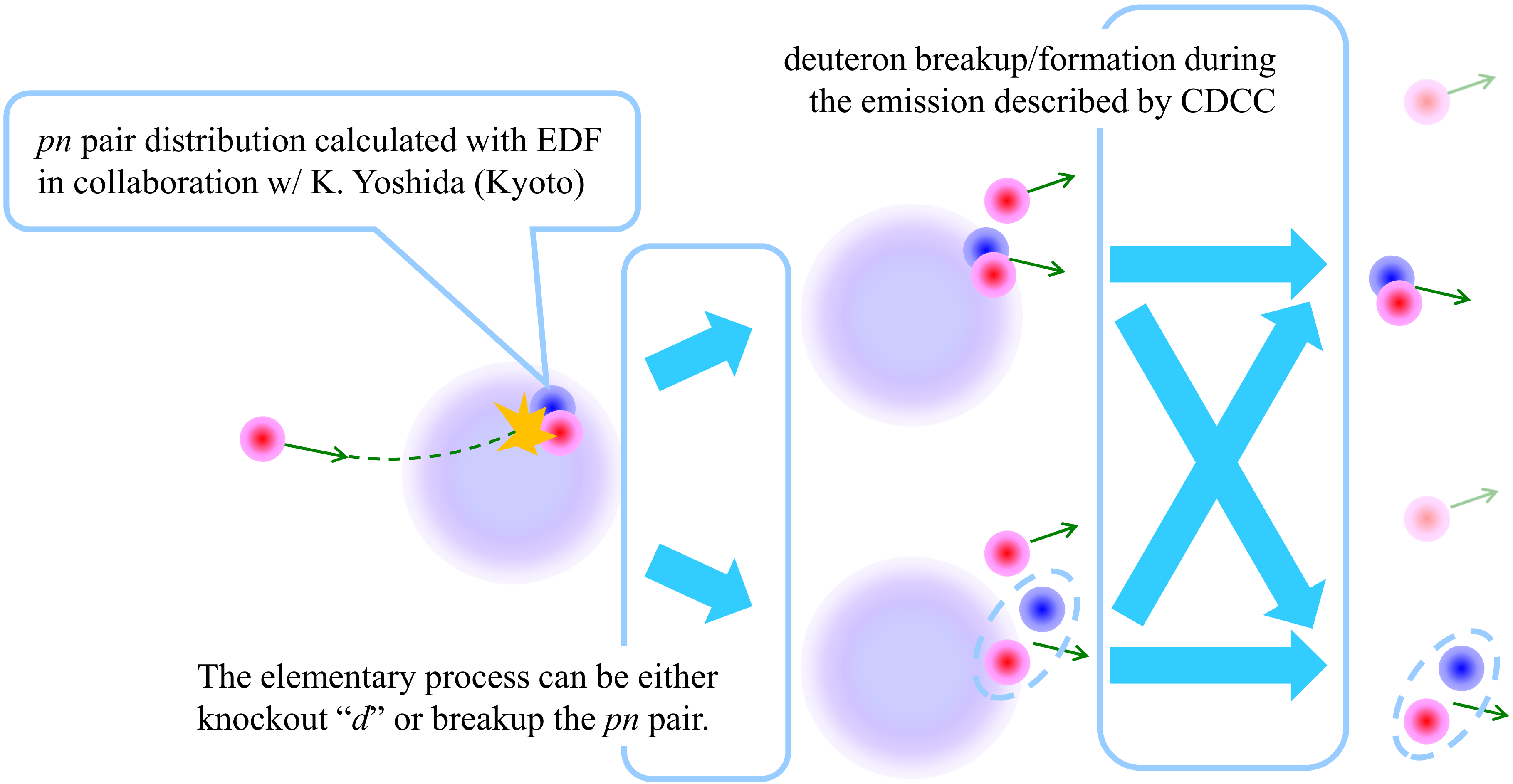

A pickup type of (p,pd) can also be considered (NP1912-SAMURAI53)

Pairing strength vs. TDX

Y. Chazono, K. Yoshida, K. Yoshida, and KO, arXiv:2007.06771

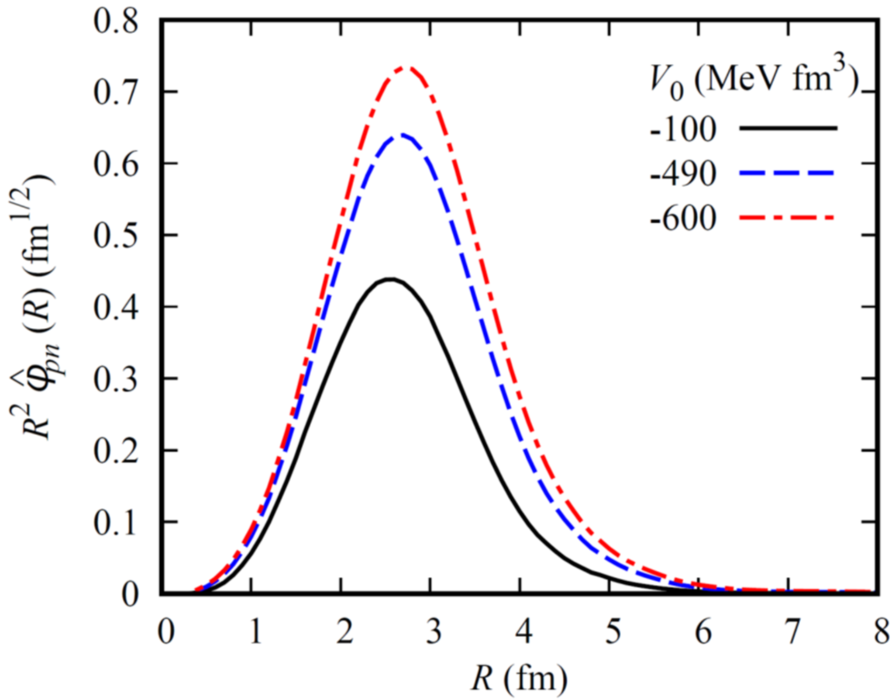

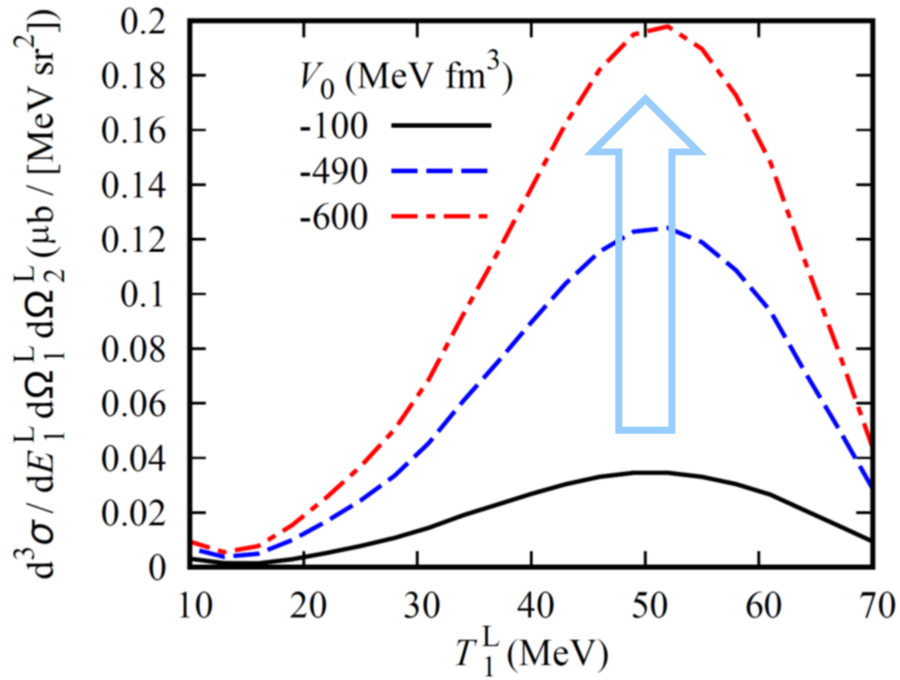

- The peak height of the TDX clearly reflects the *pn* pairing strength.
- The deuteron breakup is neglected.
- The elementary process is assumed to be the *pd* elastic scattering.

Breakup effect of the emitted deuteron

Y. Chazono, K. Yoshida, and KO, in preparation.

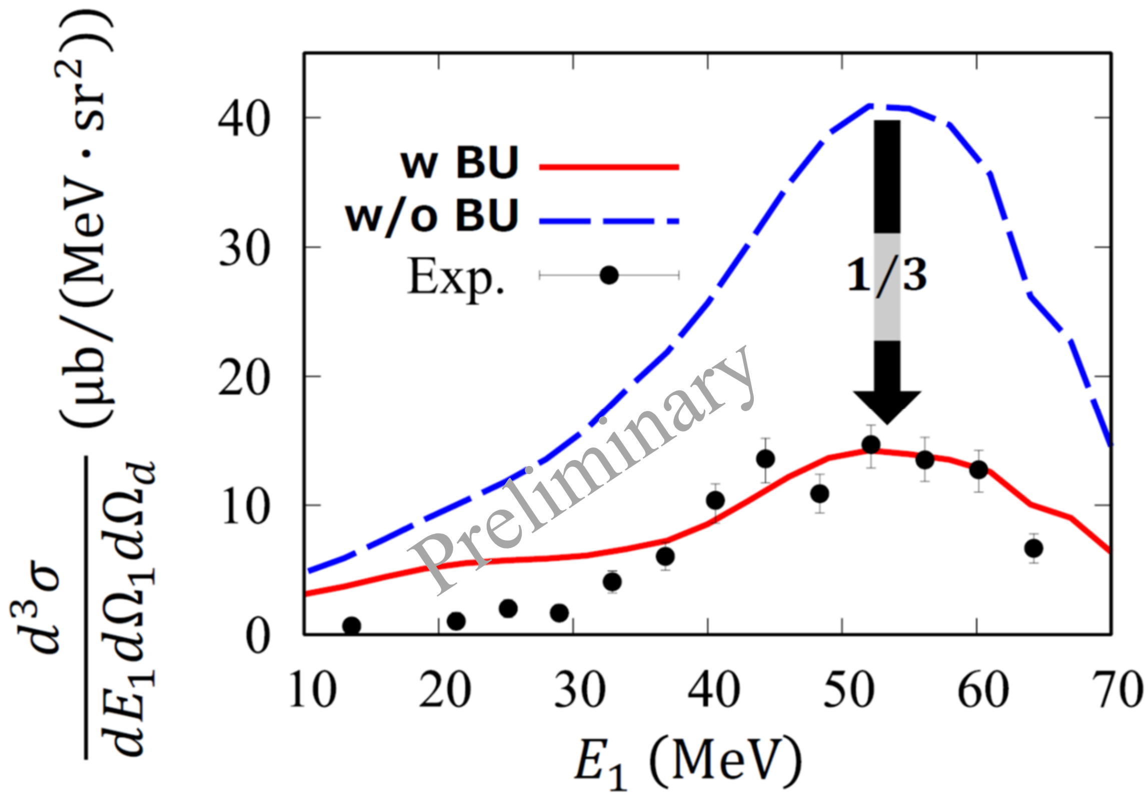

- The deuteron breakup effect is very large.
- A naïve *pn* single-particle wave function is adopted.
- The elementary process is assumed to be the *pd* elastic scattering.

^4n and ^7H

^{4}n and ^{7}H

Approved as an RCNP COREnet program
with Hiyama-san (Kyushu U / RIKEN)

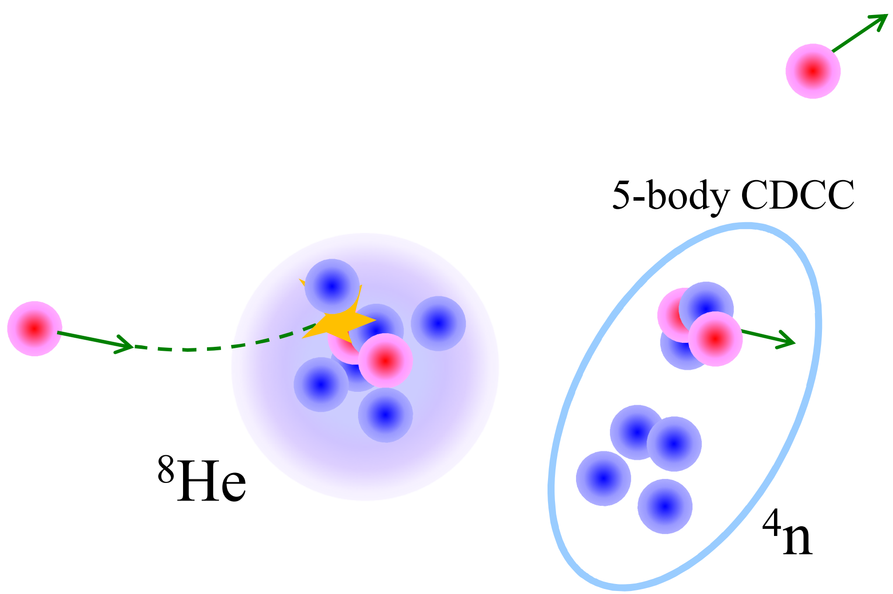

^{8}He(p,$p\alpha$): NP1406-SAMURAI 19

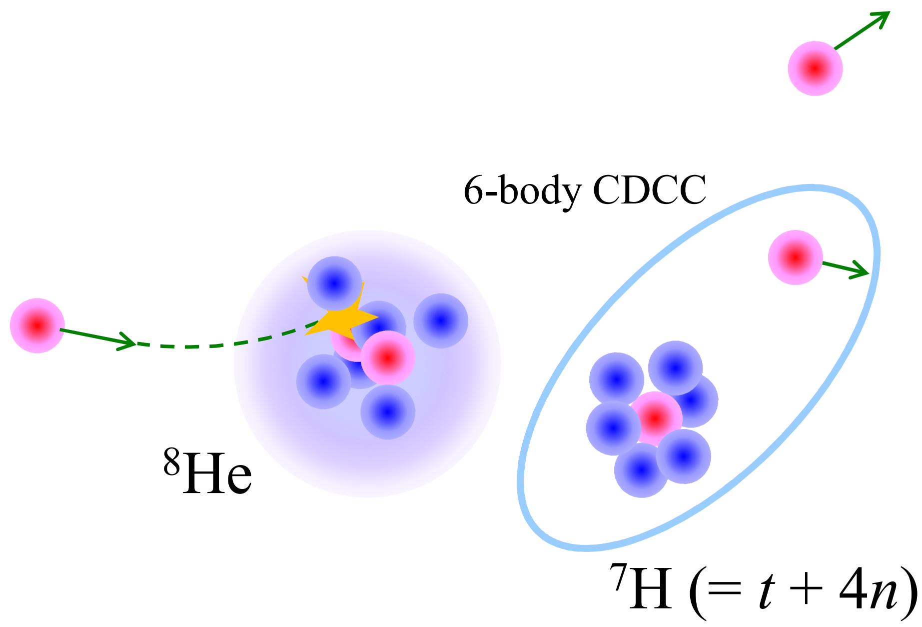

^{8}He(p,2p): NP1512-SAMURAI 34

Summary

1) (p,pN) is a powerful tool for investigating proton/neutron s.p. structure of stable and unstable nuclei. Determination of the S-factor is, however, not so trivial even for stable nuclei via kinematically complete measurement in forward kinematics.
2) Momentum distribution (MD) is a key observable in inverse kinematics. Its shape is asymmetric in general because of the asymmetry in the kinematics. The phase volume and attractive distortion effects are responsible for the asymmetric MD.
3) The triple differential cross section (TDX) diverges in some kinematical conditions in inverse kinematics. It happens when the solution to the energy conservation is a double root. Although an integrated cross section becomes finite, the TDX is significantly enhanced around the divergence point, which is nothing to do with the s.p. structure of nuclei.
4) ^{2}n correlation, α clustering, eff. polarization of residue, deuteron-like pn pair (and pn tensor correlation), ^{4}n, and ^{7}H are under investigation via knockout reactions.